Canonical correlation analysis methods for examining brain structure and behaviour

Grace Pigeau

Biological and Biomedical Engineering

McGill University, Montreal

September 10, 2022

A thesis submitted to McGill University in partial fulfillment of the requirements of the degree of Master's of Engineering

Table of Contents

Abstract

Canonical correlation analysis (CCA) is a multivariate technique designed to maximize the correlation between variable sets from two domains of measurement. CCA was first introduced in 1936, but it is more computationally expensive than other common analysis methods and as such has only become popular in recent years due to increases in computational power. One of the key advantages of CCA is that it can be used to evaluate two different sets of variables without assuming directionality or precedence. For example, with CCA it is possible to analyze a set of brain measurements derived from neuroimaging with respect to a set of behavioral measurements and identify sources of common variation. CCA is most likely to produce stable results when the number of observations (subjects in the case of neuroimaging) is greater than the number of features (from the imaging data and subject-specific variables) from both modalities. This is often not fulfilled in neuroscience, in which case CCA will produce results that are likely to be overfit to the dataset making them non-generalizable. As such, the variables typically undergo some form of data reduction and then are used as input for CCA. However, there are no current guidelines or recommendations for best practices regarding which data reduction technique to use or on the downstream effects of choosing different techniques on results and generalizability. The primary objective of this thesis is to design, test, and validate CCA techniques and the effect of different data reduction methods for neuroimaging studies. This project applies these techniques to study how risk factors for Alzheimer's disease (AD) may impact brain structure in individuals >40 years of age from the UK Biobank. Twelve AD-relevant modifiable risk factors have been identified which offer potential for disease prevention as well as opportunity for further investigation in the context of AD etiology and prevention. We use CCA to evaluate the relationship between these risk factors and cortical thickness -

a brain measure derived from magnetic resonance imaging. Four different methods of data reduction are applied and compared: single subject mean cortical thickness values derived from an anatomical parcellation, a spatially derived cortical surface atlas, principal component analysis, and independent component analysis. We found that these different data reduction methods revealed different relationships between brain areas and the risk factors. Additionally, we examined the impact of reducing the number of participants used for CCA. We found that the results using all reduction techniques were consistent even with fewer participants, however the significance became inflated as the sample size decreased.

Résumé

L’analyse des corrélations canoniques (ACC) est une technique statistique multivariée conçue pour maximiser la corrélation entre des ensembles de variables de deux types de mesure. L’ACC a été introduite pour la première fois en 1936, mais elle est plus coûteuse computationnellement que les autres méthodes d'analyse courantes et, en conséquence, n'est devenue populaire que ces dernières années en raison de l'augmentation de la puissance de calcul des ordinateurs. L'un des principaux avantages de l’ACC est qu'elle peut être utilisée pour évaluer deux ensembles différents de variables sans supposer de directionnalité ou de priorité. Par exemple, avec l’ACC, il est possible d'analyser un ensemble de mesures cérébrales dérivées de la neuroimagerie par rapport à un ensemble de mesures comportementales et d'identifier les sources de variation communes. L’ACC est plus susceptible de produire des résultats stables lorsque le nombre d'observations (participants dans le cas de la neuroimagerie) est supérieur au nombre de caractéristiques (à partir des données d'imagerie et des variables spécifiques au sujet) des deux modalités. Cette condition est rarement remplie en neurosciences, auquel cas l’ACC produira des résultats susceptibles d'être sur-ajustés à l’échantillon, ce qui les rendra non généralisables. Comme solution, plusieurs procèdent à une réduction de la dimensionnalité des variables, puis sont utilisées comme données d'entrée pour l’ACC. Cependant, il n'existe pas actuellement de lignes directrices ou de recommandations sur les meilleures pratiques concernant quelle technique de réduction des données à utiliser ou sur les effets en aval du choix de différentes techniques sur les résultats et la généralisabilité. L'objectif principal de cette thèse est de concevoir, tester et valider les techniques de l’ACC et l'effet de différentes méthodes de réduction de données pour les études de neuroimagerie. Ce projet applique ces techniques pour étudier comment les facteurs de risque de la maladie

d'Alzheimer (MA) peuvent avoir un impact sur la structure cérébrale chez les personnes de plus de 40 ans de la cohorte UK Biobank. Nous avons identifié douze facteurs de risque modifiables pertinents pour la MA qui offrent un potentiel de prévention de la maladie ainsi qu'une possibilité d'investigation plus approfondie dans le contexte de l'étiologie et de la prévention de la MA. Nous utilisons l'ACC pour évaluer la relation entre ces facteurs de risque et l'épaisseur corticale - une mesure cérébrale dérivée de l'imagerie par résonance magnétique. Quatre méthodes différentes de réduction des données sont appliquées et comparées: les valeurs d'épaisseur corticale moyennes d'un seul sujet dérivées d'une parcellation anatomique, un atlas de surface cortical dérivé spatialement, une analyse en composantes principales et une analyse en composantes indépendantes. Nous avons constaté que ces différentes méthodes de réduction des données révélaient des relations différentes entre les zones cérébrales et les facteurs de risque. De plus, nous avons examiné l'impact de la réduction du nombre de participants utilisés pour l'ACC. Nous avons constaté que les résultats utilisant toutes les techniques de réduction étaient cohérents même avec moins de participants, mais la signification statistique devenait gonflée à mesure que la taille de l'échantillon diminuait.

Acknowledgements

First and foremost, I would like to thank my supervisor Mallar Chakravarty for all of the support, guidance, and encouragement and for creating such an amazing lab environment despite the challenges of the past two years.

I would also like to thank all coworkers at the CoBrA Lab for all their assistance, motivation, and feedback. Even when we weren't able to meet in person, they made being a part of this lab a fun and truly rewarding experience. In particular, this project couldn't have been possible without Manuela Constantino who assisted in data management and quality assurance, and Gabriel Devenyi who helped with project design and troubleshooting.

I am also grateful to the Organization for Human Brain Mapping for funding a portion of my work and to the NeuroHub, UK Biobank, and Compute Canada teams for providing the resources necessary to make this all possible.

Finally, I'd like to thank my family, without whom I would not be where I am today. They were always incredible supportive, encouraging, and quick to step in with practical advice whenever I needed it.

Preface and Contributions

This thesis is original, unpublished, independent work by the author, Grace Pigeau. Quality control was performed by Grace Pigeau and Manuela Costatino. Dr. Gabriel Devenyi and Aurelie Bussy aided in initial processing and troubleshooting. Olivier Parent assisted with editing sections of the thesis. M. Mallar Chakravarty provided supervision, guidance, and assistance throughout the entirety of the project.

This research used the NeuroHub infrastructure and was undertaken thanks in part to funding from the Canada First Research Excellence Fund, awarded through the Healthy Brains, Healthy Lives initiative at McGill University. Additionally, this research was enabled in part by support provided by Calcul Québec and Compute Canada. This research has been conducted using the UK Biobank Resource under Application Number 45551.

List of Tables

List of Figures

List of Abbreviations

AD: Alzheimer's Disease

BEaST: brain extraction based on nonlocal segmentation technique

BET: brain extraction tool

CCA: canonical correlation analysis

CSF: cerebral spinal fluid

CT: cortical thickness

FOV: field-of-view

GM: grey matter

ICA: independent component analysis

MRI: magnetic resonance imaging

PCA: principal component analysis

T1w: T1-weighted

T2w: T2-weighted

TE: echo time

TR: repetition time

WM: white matter

Chapter 1: Background

Alzheimer's disease (AD) is the most common form of dementia and affects memory, thinking, behaviour, and judgement. AD is not a normal part of aging, and its symptoms eventually grow severe enough to interfere with daily living. First described in 1906 by Dr. Alois Alzheimer, AD is now at the forefront of biomedical research, which has shed light on its progression, effects, and biological underpinnings. Ongoing research has found that approximately 40% of overall AD-related risk is attributable to a combination of twelve factors which offer potential for disease prevention. However, much remains to be discovered about how AD diverges from the healthy aging process and the role these risk factors play. Technological and computational advances provide the opportunity for these discoveries. Magnetic resonance imaging (MRI) allows researchers to study complex changes in the brain, noninvasively. Advanced computational power allows for complex statistical analyses of increasingly large datasets. Nevertheless, as advances occur, it is important to ensure these tools are being used and interpreted with regard to proper scientific principles and practices. The remainder of this chapter discusses the current state of research surrounding aging, dementias, the impacts of these risk factors, and how one particularly promising methodology – canonical correlation analysis - is currently being used in neuroimaging research.

1.1 Aging and Alzheimer’s Disease

1.1.1 Aging

Aging is a complex and inevitable process associated with readily identifiable and characteristic changes in the brain’s appearance and function. Healthy aging is defined as the development and maintenance of functional ability that enables mental and physical wellbeing in late life. Healthy aging can occur even for those who experience neuroanatomical changes associated

with age. Unfortunately, many adults do not experience healthy aging and disease-free brains among older populations may be rare (Y. Hou et al., 2019). While brain volume decreases overall with age, the frontal lobe and hippocampus tend to shrink more than other areas (Wyss-Coray, 2016). The cerebral cortex also thins with age, often following a pattern similar to volume loss. Additionally, molecular studies have revealed that brain tissue from older individuals contains abnormal deposits of aggregated proteins associated with neurodegenerative diseases (Elobeid, Libard, Leino, Popova, & Alafuzoff, 2016).

Aging is the primary risk factor for most neurodegenerative diseases. Additionally, beyond being a risk factor, aging also increases the severity of disease. How and when dementia diverges from healthy aging remains poorly understood and is the focus of ongoing research (Irwin, Sexton, Daniel, Lawlor, & Naci, 2018; Mortamais et al., 2017; Ritchie, Ritchie, Jaffe, Skoog, & Scarmeas, 2015). Although aging is known to be the primary risk factor for neurodegenerative diseases, the exact mechanisms underlying this association have not yet been identified.

In this thesis, we examine participants aged 40 years and older who have no dementia diagnosis to see how risk factors for Alzheimer's disease may impact brain structure in cognitively healthy individuals. Like aging, the mechanisms underlying these risk factors are not fully understood, and how they interact with one another is unclear and only beginning to be studied.

1.1.2 Alzheimer's Disease

Dementia is a devastating family of neurodegenerative disorders which involves the deterioration of memory, thinking, behaviour, judgement, and activities of day-to-day living. Alzheimer's disease (AD) is the most common form of dementia, making up 60–70% of all cases. In 2019, approximately 50 million people were living with dementia worldwide and this number is

projected to reach 82 million by 2030 (World Health Organization, 2021). AD pathology is characterized by the accumulation of hyperphosphorylated tau protein – which form intracellular neurofibrillary tangles – and extracellular β-amyloid plaques in addition to extensive neuronal death (atrophy) and synaptic loss within the brain. Given the ever-increasing prevalence of AD due to ageing demographics around the world and no cures, dementia is likely to become a public health crisis (*Dementia: A STRATEGY FOR CANADA*, 2019; Livingston et al., 2020; Macklin, 2021). Furthermore, AD has a physical, psychological, social, and monetary impact not only on those diagnosed, but on their caregivers and families, and on healthcare systems as a whole (*Dementia: A STRATEGY FOR CANADA*, 2019; Livingston et al., 2020). People suffering from AD experience symptoms in many domains and often experience complex issues as the disease progresses such as problems with speech and memory, increasing confusion and disorientation, difficulty performing simple tasks, and changes in weight and mood. As such, interventions, support, and treatment must be provided in a context which considers the person as a whole and meets their medical, cognitive, and psychological needs alongside their environmental, cultural, and social needs. Unfortunately, this is not currently the case. Often those in pursuit of dementia care end up in acute hospital settings either due to limited knowledge of or lack of affordable services, and as such their needs go unmet (Martin, O'Connor, & Jackson, 2020). These acute hospital settings may not have the necessary skillsets or environments to provide the multi-dimensional care required. It is estimated that the combined health care system and out-of-pocket caregiver costs totaled $10.4 billion in Canada in 2016 (Alzheimer Society of Canada, 2016). This staggering figure is expected to rise substantially in the coming years.

There has been continued failure of drug trials to cure or modify disease progression. There are many possible causes for the continued

failure of drug trials. One is that trials are occurring too late in the disease process when irreversible neurodegeneration has already occurred in participants (Aisen, Vellas, & Hampel, 2013). Clinical symptoms may only emerge after decades of AD pathology progression. Therefore, a strong consensus is emerging which suggests that preventative measures and delaying symptom onset are particularly important to prevent disease progression (Barnes & Yaffe, 2011; Livingston et al., 2020). Another explanation for the lack of demonstrated drug efficacy could be due to heterogeneity within clinical AD populations. There are multiple subtypes of AD and an individual's risk and disease progression depends on a variety of factors including genetics, environment, and behaviour (S. Evans et al., 2019; Livingston et al., 2020). The following section describes these modifiable risk factors and the way in which they influence dementia onset progression in life-course order beginning with early life (<45 years), then progressing through midlife (45-65 years) and late-life (65+ years).

1.1.3 AD Lifestyle Risk Factors

Approximately 40% of overall AD-related disease risk is attributable to a combination of twelve potentially modifiable risk factors: education, hypertension, obesity, hearing loss, traumatic brain injury, alcohol misuse, smoking, depression, physical inactivity, social isolation, diabetes, and air pollution (Livingston et al., 2020). The 12 modifiable risk factors account for around 35% of the population attributable fraction of worldwide dementias. The population attributable fraction is the proportional reduction in population disease which would occur if a risk factor were eliminated or reduced to ideal levels. There is high potential for prevention, especially in low-income and middle-income countries where more dementias occur (Livingston et al., 2020). These risk factors span across all ages, suggesting it's never too early or late to make changes to help prevent dementia. Listed

below are the risk factors for each stage of life which can be influenced through modifying lifestyle and behaviour, impacting dementia prevalence and onset.

Early Life (< 45 yrs)

Only one modifiable risk factor has been identified before the age of 45 and that is amount of education received. Lower levels of educational attainment in early life are associated with increased dementia risk and has a high population attributable factor due to the lack of access to education worldwide. It has been theorized that education results in higher cognitive reserve and overall cognitive ability in early life, reaching a plateau in late adolescence (Kremen et al., 2019). Cognitive reserve enables flexible use of brain resources which allows people to maintain function despite brain pathology. However, separating the specific effects of education from the effect of cognitive activity and overall cognitive ability is challenging (Blacker & Weuve, 2018; Kremen et al., 2019). It is also difficult to separate the impact of educational attainment from the impacts of socioeconomic status (Mehta et al., 2022; J. D. Petersen et al., 2021; Russ et al., 2013).

Midlife (45-65 yrs)

Between the ages of 45 and 65, five modifiable risk factors have been identified. All of these have the potential to impact AD onset and progression before the neurodegeneration associated with aging begins. Of all the potentially modifiable risk factors identified in a well-known Lancet review of dementia, prevention, intervention, and care, hearing loss is the single largest preventable contributing factor to dementia worldwide (Livingston et al., 2020). Despite being included as a midlife factor, hearing loss continues to increase dementia risk in later life. A meta-analysis of 36 epidemiologic studies from 12 countries found an increased risk of dementia for each 10 dB of decline of hearing loss (Loughrey, Kelly, Kelley, Brennan, & Lawlor, 2018). Hearing was measured using audiometry at baseline and the long

follow-up times (9–17 years) make reverse causation unlikely. One theory is that hearing loss may result in cognitive decline due to decreased cognitive stimulation. However, studies suggest that using hearing aids can mitigate this risk (Amieva, Ouvrard, Meillon, Rullier, & Dartigues, 2018; Maharani et al., 2018; Ray, Popli, & Fell, 2018).

Another risk factor for AD is mild traumatic brain injury (TBI). TBI is defined as a concussion and severe traumatic brain injury is defined as skull fracture, oedema, or brain injury and bleeding. In both humans and mouse models, a single severe TBI is associated with widespread hyperphosphorylated tau pathology. One nationwide Danish cohort study of almost 3 million people over 50 years of age found dementia and AD risk increased for each incidence of TBI and was highest in the 6 months subsequent to the TBI (Fann et al., 2018). Likewise, a nationwide Swedish cohort study of over 3 million people of the same age range found increased dementia risk 1 year after TBI, and slightly increased risk up to 30 years after TBI. This study also found that more severe TBI and multiple TBIs increased the risk (Nordström & Nordström, 2018).

Additionally, alcohol misuse has been identified as a risk factor for dementia and cognitive impairment and heavy drinking can lead to brain changes. One French longitudinal study of over 32 million people who had been admitted to hospital found that those diagnosed with harmful alcohol use or alcohol dependence (as defined by the International Classification of Diseases) were at higher risk of developing dementia over a 5-year period (Schwarzinger et al., 2018). This relationship was especially prevalent when looking at those with earlier onset dementia (younger than 65 years), over half of whom had an alcohol use disorder. However, light to moderate alcohol consumption has been associated with a decreased risk of cognitive impairment and dementia. It can be particularly challenging to understand

these relationships due to the complex associations between alcohol and cultural, social, and other health-related factors.

Ongoing midlife hypertension is associated with increased risk of a late life dementia, however there's conflicting evidence for whether this trend continues into late life (Abell et al., 2018; McGrath et al., 2017). In one UK cohort study, a single measure of high systolic blood pressure (130 mm Hg or higher) between 50-60 years was associated with increased risk of dementia and persistent high systolic blood pressure, was associated with increased dementia risk even in those without cardiovascular disease (Abell et al., 2018). A separate study suggests a possible mechanism: hypertension starting at age 40 is associated with increased white matter hyperintensity volume and reduced total brain volume (Lane et al., 2019).

Despite being associated with hypertension, obesity has been identified as a separate risk factor in midlife. Obesity is linked to pre-diabetes and metabolic syndrome. One review of longitudinal studies with a total of almost 600,000 participants between 35-65 years found that obesity (BMI >30) is associated with late life dementia but being overweight (BMI 25-30) is not (Albanese et al., 2017). A separate meta-analysis of overweight and obese adults without dementia determined that losing at least 2 kg was associated with significant improvements in memory and attention with follow-up times from 8 weeks to 1 year (Veronese et al., 2017).

Later Life (>65 yrs)

Late life is often when targeted dementia interventions are considered and implemented. Ideally, strategies for preventing and delaying AD should take into account the late life risk factors described below. One risk factor which has been identified and is easily targetable for intervention is smoking.

Smoking in later life is associated with cognitive impairment and increased risk for all forms of dementia. This has been attributed to both the

link between smoking and cardiovascular health and the presence of neurotoxins in cigarette smoke (Durazzo, Mattsson, & Weiner, 2014; Swan & Lessov-Schlaggar, 2007). Exposure to second hand smoke is also a risk. One study found that second-hand smoke exposure was associated with increased memory deterioration in woman aged 55-64 years, and risk increased with exposure duration (Pan, Luo, & Roberts, 2018). Even at an older age reducing or stopping smoking can decrease the risk of developing dementia. A nationwide Korean cohort study found that among 50,000 men above the age of 60, stopping smoking for at least 4 years substantially reduced dementia risk for the next 8 years when compared to those who continued smoking (D. Choi, Choi, & Park, 2018).

Additionally, depression is both associated with increased dementia risk and is a symptom of the prodrome and early stages of dementia. It is important to note that depressive symptoms may result from dementia pathology years before clinical dementia onset, however this does not exclude depression from increasing dementia incidence through a variety of possible psychological or physiological mechanisms (Livingston et al., 2020). A meta-analysis of 32 studies with over 60,000 participants from high income countries found even a single depressive episode was a risk factor for dementia (Prince, Albanese, Guerchet, & Prina, 2014). In the UK Whitehall study of 10,189 people, which had follow-up times of 11-28 years, late life depression symptoms increased dementia risk but symptoms in midlife did not, even when those symptoms were chronic (Singh-Manoux et al., 2017). There is conflicting evidence as to whether antidepressant treatment may reduce dementia risk and most studies considering depression as a risk factor don't differentiate between treated and untreated depression (Livingston et al., 2020).

Similar to depression, a lack of physical activity can be both a consequence and risk factor of dementia. It can also result from prodromal

dementia. Inactivity is linked to both hypertension and obesity, and potentially poses a greater risk for those with cardiovascular morbidity. Two meta-analyses of longitudinal studies and systematic reviews found exercise was associated with reduced risk of dementia and may be protective against clinically diagnosed AD (Hersi et al., 2017; Livingston et al., 2017). The HUNT study of over 28,000 participants found that weekly moderate-to-vigorous physical activity (defined as breaking a sweat) lowered dementia risk over a 25-year period (Zotcheva et al., 2018). In contrast, the Whitehall study of over 10,000 participants found that at least 2.5 hours a week of moderate-to-vigorous physical activity was associated with reduced dementia risk over 10 years but was not protective after that period (Sabia et al., 2017).

Social contact is a protective factor for dementia and several studies have shown that social isolation increases the risk of dementia. Social contact is thought to enhance cognitive reserve and potentially encourage beneficial behaviours for dementia prevention. One meta-analysis of 51 longitudinal cohort studies examining social isolation and cognition included over 100,000 participants aged 50 years or older with follow-up times between 2 and 21 years (I. E. M. Evans, Martyr, Collins, Brayne, & Clare, 2019). This review found that one or both of high social activity and large social network was associated with improved late-life cognitive function. Both a UK longitudinal study and a Japanese longitudinal study, with over 10,000 participants each, found higher social contact to be associated with a reduction in dementia risk (Saito, Murata, Saito, Takeda, & Kondo, 2018; Sommerlad, Sabia, Singh-Manoux, Lewis, & Livingston, 2019). Despite sociocultural variation in the definition and perception of social isolation, findings of the protective effects of social contact are consistent across global studies and meta-analyses (I. E. M. Evans et al., 2019; Kelly et al., 2017).

Another risk factor for AD is diabetes. Diabetes is a metabolic disease which is characterised by insulin resistance and a high concentration of peripheral insulin. One meta-analyses of 14 cohort studies with over 2 million total subjects, found that dementia risk increased with duration and severity of type 2 diabetes mellitus (T2DM) (Chatterjee et al., 2016). It has been shown in both human and animal models that insulin plays a role in clearing amyloid from the brain. The peripheral insulin anomalies associated with diabetes may cause a decrease in brain insulin production, suggesting a possible mechanism by which diabetes impairs cognition (Luchsinger & Gustafson, 2009; Milene, Philippe, & Frédéric, 2015). Additionally, diabetes can result in inflammation and high blood glucose concentrations which could be a potential mechanism relating diabetes to increased AD risk (Yaffe, 2007). Furthermore, T2DM is intrinsically connected with other cardiovascular risk factors: hypertension and obesity.

Finally, exposure to air pollution in later life is another factor which can impact AD. Air pollution has long been associated with a variety of diseases and poor health outcomes. Animal models have been used to demonstrate particulate pollutants accelerating neurodegeneration via a multitude of processes. These processes include beta-amyloid deposition, amyloid precursor protein processing, and cerebrovascular and cardiovascular disease (Fonken et al., 2011; Power, Adar, Yanosky, & Weuve, 2016; Sirivelu, MohanKumar, Wagner, Harkema, & MohanKumar, 2006). One review of longitudinal studies investigating air pollutant exposure and incident dementia found that exposure to fine ambient particulate matter (PM), nitrogen dioxide (NO2), and carbon monoxide (CO) were all associated with increased dementia risk. PM and NO2 are often produced by traffic, and it can be difficult to separate their effects (Carey et al., 2018; Chen et al., 2017; Oudin et al., 2016). In addition, multiple studies have found additive

effects of different pollutants (Carey et al., 2018; Chen et al., 2017; Oudin et al., 2016; Oudin, Segersson, Adolfsson, & Forsberg, 2018).

1.2 Magnetic Resonance Imaging of AD

1.2.1 Magnetic Resonance Imaging

Magnetic Resonance Imaging (MRI) is a non-invasive technique that permits imaging of the soft tissue of the body. It uses non-ionizing radiation, which is safe for humans, and has no known negative side effects even after repeat exposures. Additionally, MRI allows for the collection of high-resolution, 3D images. As a result, MRI is a popular tool in neuroimaging both clinically and for research.

Within atomic nuclei, all protons and neutrons precess about their own axis. Atoms with an odd number of protons or neutrons thus possess an angular momentum, referred to as spin, which creates a microscopic magnetic moment. MRI takes advantage of the properties of nuclei with an odd number of protons. When placed in a strong magnetic field, they will exhibit a slight net magnetization in one direction. Of particular importance to MRI signal are hydrogen nuclei, each of which is a single proton, and are the most abundant source of protons in the body and the brain (McRobbie, Moore, Graves, & Prince, 2006). The spin of protons not exposed to any external magnetic field is random, resulting in a net magnetization of zero. In an MRI scanner, a homogenous magnetic field (B_0) is generated from the main magnet. When B_0 is applied, each proton will assume one of two possible spin states, either aligned with the direction of B_0 or aligned opposed to the direction of B_0. Spins precess at a characteristic frequency (Larmor frequency) which is proportional to B_0. A small fraction of protons will align parallel to B_0, resulting in a bulk magnetization M in the direction of B_0. The ratio of parallel to anti-parallel spins is governed by the Boltzmann equation.

MRI scanners also contain a radio frequency (RF) coil which generates a RF pulse tuned to the Larmor frequency (Currie, Hoggard, Craven, Hadjivassiliou, & Wilkinson, 2013; Lerch et al., 2017). This pulse is used to manipulate M in order to generate measurable MRI signal. Typically, B_0 is denoted as being in the z-axis. A perpendicular pulse (B_{xy}), tuned to the Larmor frequency, creates an M component in the xy plane. The "creation" of this transverse component was first observed in 1946 by Bloch and Purcell (Bloch, 1946; Purcell, Torrey, & Pound, 1946). When B_{xy} is removed, M precesses about the z-axis and eventually realigns with B_0. The creation of this magnetic flux results in a signal oscillating at the Larmor frequency which can be measured using Faraday induction.

The realignment of M with the net magnetization is referred to as relaxation. Two types of relaxation govern this process: spin-lattice (T1) relaxation and spin-spin (T2) relaxation (Currie et al., 2013; Lerch et al., 2017). In T1 relaxation, the protons exchange energy with their environment - referred to as a lattice - and slowly return to their original state, re-aligning with B_0 and restoring the longitudinal magnetisation. The T1 relaxation time refers to the time it takes for the magnetisation M_z to return to its equilibrium state of M_0. T1 is dependant on tissue type, resulting in differences in signal intensity which can be manipulated to provide contrast between tissue types in an MRI image. In T2 relaxation, or transverse relaxation, the protons interact with each other and lose coherence. Spins lose coherence when they are near each other and their frequency is altered. This alteration is temporary and will revert once spins move away from each other, however, consistent interactions lead to an accumulation of dephasing which reduces transverse magnetization. Additionally, inhomogeneities in B_0 are inevitable, such that spins in different locations will experience slightly different field strengths and thus have different precession frequencies. Similar to T1, T2 relaxation time is

dependent on tissue type due to the different tumbling properties of molecules.

After the removal of the RF pulse, the signal emitted by the proton relaxation is spatially localised using additional linear gradient magnetic fields (Currie et al., 2013; Lerch et al., 2017; McRobbie et al., 2006). These create a gradient of field strength in one dimension without changing the net magnetisation. At the same time as the RF pulse, a slice selection gradient is applied which alters the strength of B_0 in a chosen direction. This changes the Larmor frequency of the protons along the gradient. A certain section of the brain in two dimensions (slice) can then be excited by an RF pulse applied only to the protons within a specified frequency range. In another direction, a phase encoding gradient is applied which alters the phase of protons depending on their position along the gradient. This allows for differentiation in one direction due to the varying spin phases within the gradient without any change in the frequency of the protons. In the third direction, a frequency encoding gradient is applied. These gradients allow for the localization of MR signals in image reconstruction. The spatially localised signal is recorded in k-space: a raw data matrix in which data points represent specific spatial frequencies. Fourier transformations are then used to transform the k-space data into an MR image.

1.2.2 Structural MRI

There are multiple MR imaging types which utilize the method described above to measure different properties of the brain. The one relevant to this thesis is structural MRI. Structural MRI is commonly used in neuroimaging to obtain anatomical information which provides exceptional contrast between tissue types in the brain (Currie et al., 2013; Lerch et al., 2017; McRobbie et al., 2006). The main tissue contrast is between white and grey matter,

however structural MR images also contain finer details such as contrast between smaller regions and substructures in the brain.

The two primary types of structural MRI are T1-weighed (T1w) and T2-weighted (T2w) imaging. In a T1w image, the signal intensity in a given voxel is proportional to the tissue's T1 properties (Currie et al., 2013; Lerch et al., 2017; McRobbie et al., 2006). Similarly, in a T2w image, the signal intensity in a given voxel highlights differences in T2 properties of the tissue (Currie et al., 2013; Lerch et al., 2017; McRobbie et al., 2006).

Two properties of structural MRI are the repetition time (TR) which refers to the time between two RF pulses, and echo time (TE) which refers to the time between initial RF pulse and the readout of signal. The TR and TE are typically shorter in T1-weighted images than T2-weighted images in order to maximize the difference in signal obtained from different tissue types (Currie et al., 2013). The manipulation of MRI settings to differentiate brain regions and neuroanatomy enables important neuroanatomical work including the automated extraction of biological measurements of individual brain regions (Chakravarty et al., 2013; Lerch et al., 2017; Pipitone et al., 2014; Raznahan et al., 2014).

1.2.3 MR Image Processing

1.2.3.1 Image Registration

To fully utilize MR images and derive meaningful biological measurements, the images must be processed after acquisition. Spatial normalization is foundational to image processing for all MRI data. Spatial normalization, also known as image registration, is the process of spatially aligning two images via transformation into a common coordinate space (Collins, Neelin, Peters, & Evans, 1994; Friston et al., 1995; Maintz & Viergever, 1998; Oliveira & Tavares, 2014). Image registration enables point-to-point comparisons across images, facilitating comparison of MRI data across different subjects,

datasets, and studies (Collins et al., 1994; Friston et al., 1995; Maintz & Viergever, 1998; Oliveira & Tavares, 2014; Toga & Thompson, 2001). Registration can be described as either linear or nonlinear, both of which are essential to any MR image processing pipeline. In linear registration, images are mapped to one another using translations, rotations, scales, and shears. After a linear transformation is applied, parallel lines will always remain parallel to each other (Maintz & Viergever, 1998). In addition to linear registration, nonlinear registration methods can be used to account for localized spatial differences between images (Maintz & Viergever, 1998; Toga & Thompson, 2001). In nonlinear registration local differences in morphology are mapped to one another using spatially varying deformations. Unlike linear transformations which must be applied globally, nonlinear transformations may vary as a function of location.

1.2.3.2 Bias field correction

Magnetic field inhomogeneities, referred to as a bias field, occur because MRI scanners cannot achieve perfect uniformity when applying the main magnetic field and RF pulses. A bias field can lead to low-frequency spatial variations in image intensity which do not represent true neuroanatomical differences (Belaroussi, Milles, Carme, Zhu, & Benoit-Cattin, 2006; Deoni, 2011; Z. Hou, 2006). Bias field correction is essential to represent the underlying tissue using voxel intensity. Many methods for performing this correction exist and one of the most commonly used is the N4ITK algorithm, commonly referred to as N4 correction (Tustison et al., 2010). This method employs an iterative multiresolution approach based on b-spline fitting which assumes a simple parametric model and does not require any tissue classification.

1.2.3.3 Tissue Classification

Tissue classification is a prerequisite for many widely used MRI processing pipelines. Classification is performed by assigning a label to every voxel in

an MR image based on intensity. This is typically performed at a high level by differentiating grey matter (GM), white matter (WM), and cerebrospinal fluid (CSF).

The majority of tissue classification algorithms use T1w images, however some multi-contrast options exist which can enhance accuracy (U. S. Choi, Kawaguchi, Matsuoka, Kober, & Kida, 2019; Tohka, Zijdenbos, & Evans, 2004). One of the primary technical concerns with tissue classification is partial volume effects (PVE). PVE can occur because, due to the resolution of MRI voxels, each voxel may contain a distribution of tissues as opposed to a single tissue (U. S. Choi et al., 2019; Tohka et al., 2004). A number of methods exist to address the issue of PVE, the majority of which consider the intensity of a voxel as weighted sum of partial volume coefficients (Ahmed, Yamany, Mohamed, Farag, & Moriarty, 2002; Tohka et al., 2004; Van Leemput, Maes, Vandermeulen, & Suetens, 2003; Y. Zhang, Brady, & Smith, 2001). One commonly used method for tissue classification is the trimmed minimum covariant method (Tohka et al., 2004). Each voxel in this methodology is labelled based on its most dominant tissue type. Then, the morphological characteristics of the voxels are examined to determine which are susceptible to PVE. These voxels are removed, and ellipsoid estimators are used to find partial volume coefficients based on the remaining data. Another common method classifies voxels based on intensity with an added Markov random field component which considers voxels neighbours to improve performance (Y. Zhang et al., 2001). This method estimates partial volume coefficients using an expectation-maximization framework.

1.2.3.4 Brain Extraction

Non-brain tissues such as skull, fat, and neck can interfere with intensity-based image processing. As such, they are typically removed from MR images to aid in image registration and cortical surface reconstruction

(Eskildsen et al., 2012; Ségonne et al., 2004; van der Kouwe, Benner, Salat, & Fischl, 2008). Brain extraction involves the creation of a binary mask, typically referred to as a brain mask, which indicates all voxels belonging to GM, WM, or CSF. This mask can then be multiplied with the original MR images to remove non-brain tissue. Additionally, the brain mask itself can be used to extract brain volume measurements. Most brain extraction methods require only a T1w image for operation. Two common methods for brain extraction include the Brain Extraction Tool (BET) developed by Smith (Smith, 2002) and the Brain Extraction based on non-local Segmentation Technique (BEaST) tool developed by Eskildsen et al. (Eskildsen et al., 2012). The BEaST tool assigns each voxel a class by comparing the neighbouring voxels with data from a library of 80 previously labelled samples (Eskildsen et al., 2012). Alternatively, BET uses a deformable model that is able to match the surface of the brain (Smith, 2002). The first step in BET uses an image intensity histogram to identify the intensity thresholds of brain voxels. Next, the centre of gravity of the image is identified. The centre of gravity is then used as a starting point of a spherical mesh surface which is deformed until it fits the shape of the brain to a suitable degree (Smith, 2002).

1.2.4 Cortical Thickness

1.2.4.1 Interpreting Cortical Thickness

Cortical thickness (CT) and surface area (SA) are common metrics for examining neuroanatomy in MR images. Both measures reflect neurobiological processes and environmental influences (Rakic, 1988; Strike et al., 2019).

In the cerebral cortex, neurons are organized into columnar units (Mountcastle, 1997). Surface area reflects the number of these columns and cortical thickness reflects the number of cells within columns (Chenn &

Walsh, 2002) Cortical thickness is also affected by the amount and density of synapses as well as dendrite pruning and ramification (Huttenlocher, 1990; Schüz & Palm, 1989). Cortical thickness measures can be potentially confounded by the dura mater and blood vessels (Schüz & Palm, 1989).

Both cortical thickness and surface area can provide important information about neuroanatomical changes during aging in addition to information about neuroanatomical correlates of numerous neuropsychiatric conditions and diseases. For this thesis, I will focus on investigating cortical thickness, as it has been shown to vary throughout the healthy aging process in a regionally specific manner (Salat et al., 2004; Thambisetty et al., 2010) and changes in cortical thickness have been related to the effects of dementia (Avants, Cook, Ungar, Gee, & Grossman, 2010; Hartikainen et al., 2012; Hersi et al., 2017) and dementia risk factors (Apostolova et al., 2006; Armstrong et al., 2019; Ha et al., 2020; Karama et al., 2015; Mohamed, Nestor, Cumming, & Nasrallah, 2022; Verbaten, 2009; Vuorinen et al., 2013).

1.2.4.2 Measuring Cortical Thickness

Surface-based computational methods investigating the cerebral cortex aim to construct a mesh of vertices and connecting edges representing geometry of the cortical surface, from which morphological measures of each vertex can be analysed (Dale, Fischl, & Sereno, 1999; Fischl, Sereno, & Dale, 1999; Lerch & Evans, 2005). This process is challenging due to the highly complex and variable folding pattern of the cerebral cortex which makes it ill-suited for analysis in a volumetric space.

Initially, input images are linearly registered to a template space and segmented into GM, WM, and CSF. Surface meshes are then created to represent the GM-WM surface and pial (GM-CSF) surface. Two pipelines which are commonly used to perform surface-based analysis are CIVET (Ad-Dab'bagh et al., 2006; June et al., 2005a; Lerch & Evans, 2005; Zijdenbos,

Forghani, & Evans, 2002) and Freesurfer (Dale et al., 1999; Fischl et al., 1999). CIVET and Freesurfer both follow the same general preprocessing steps described above but differ in how they create the cortical surface meshes. The CIVET algorithm first estimates the GM-WM surface and then expands that surface to the area between GM and CSF in order to create the pial surface (June et al., 2005a). Conversely, the Freesurfer algorithm deforms a mesh to match the boundary of interest while optimising the greatest shift in image intensity (Dale et al., 1999; Fischl et al., 1999). Additionally, the CIVET cortical surface meshes permit direct vertex-to-vertex comparisons, due to its surface being topologically equivalent to a sphere, whereas Freesurfer surface meshes must be resampled to achieve this. In both pipelines, morphological measurements, - including CT and SA - can then be computed at each vertex of the modelled cortical surface. The CT value is calculated based on the length of the trajectory from the GM-WM surface to the pial surface.

1.2.5 Cortical Thickness and AD

In addition to providing information about the disease, MRI-derived patterns of cortical thickness changes have been used to track AD disease progression (Apostolova et al., 2007; Dickerson et al., 2009; Frisoni et al., 2009; Lerch et al., 2005; Prestia et al., 2010; Singh et al., 2006; Thompson et al., 2003) and distinguish AD subtypes (Murray et al., 2011; Noh et al., 2014; Park et al., 2017; B. Zhang, Lin, Liu, Shen, & Wu, 2022; B. Zhang, Lin, Wu, & Al-masqari, 2021). The AD cortical signature is approximately comprised of generally agreed upon regions: the medial temporal lobe, temporal pole, inferior temporal gyrus, supramarginal gyrus, superior parietal lobule, precuneus, middle frontal gyrus, and superior frontal gyrus (Ashraf, 2019; Busovaca et al., 2016; Huang, 2020). This neurodegeneration is a staged process which occurs throughout disease

progression, as seen in Figure 1.1. Early on, cortical atrophy is typically observed in the medial temporal lobe (hippocampal formations, parahippocampal gyrus, and entorhinal cortex) and moves on to the remainder of the cortex shortly after, progressing along a temporal-parietal-frontal trajectory, with the motor areas generally being unaffected until late AD progression (Ashraf, 2019; Huang, 2020; Y. Li et al., 2012). This progression correlates with the appearance of clinical symptoms and different cognitive profiles have markedly different patterns of neurodegeneration. Early stages of the disease – when degeneration is typically limited to the medial temporal lobe - are characterized by memory deficits. Progression from mild cognitive impairment (MCI) and mild AD is characterized by the appearance of non-memory related cognitive deficits including language and visio-spatial functions (Brooks & Loewenstein, 2010; R. C. Petersen, 2004). Finally, in the late stages of the disease, atrophy is seen in the sensorimotor and visual cortices, whose functions have been clinically observed to be relatively preserved until late stages of the disease. There is also research which has shown cortical atrophy closely recapitulating the patterns of Braak (neurofibrillary tangle) staging (Braak & Braak, 1996) and distinct patterns of neurofibrillary tangle deposition in early-stage Alzheimer's disease dementia versus late-stage Alzheimer's disease (Elobeid et al., 2016; Kovacs, 2018; Lowe et al., 2018; Okamura et al., 2014).

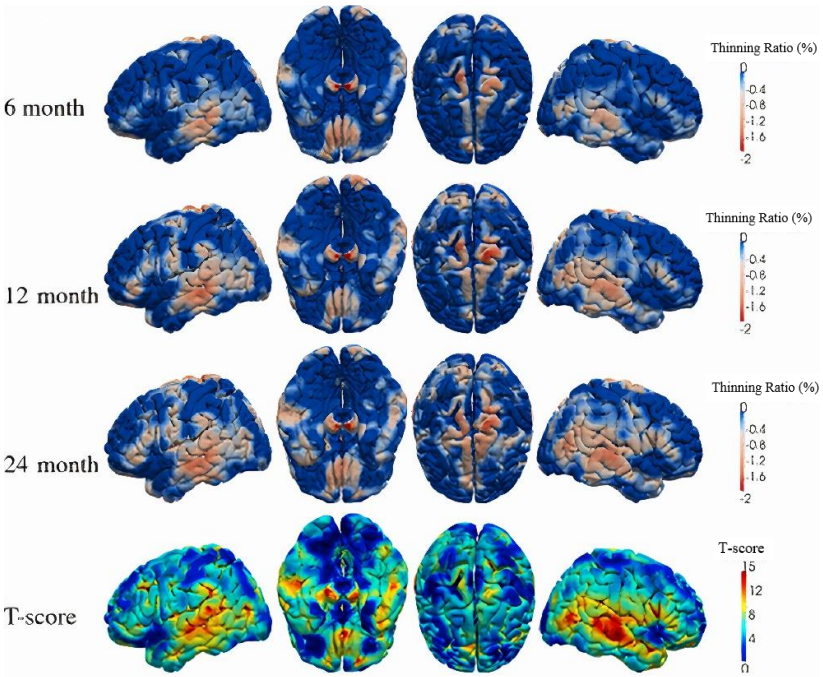

(a) NC

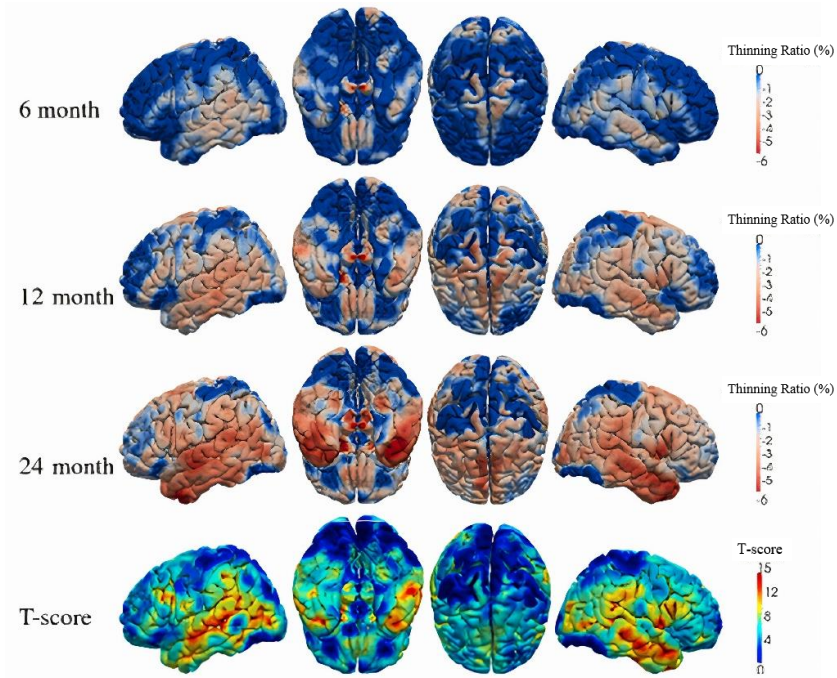

(d) AD

Figure 1.1. AD Cortical Thinning. Cortical thinning patterns in cognitively normal (NC) and Alzheimer's disease (AD) subjects. The fourth row shows the location where significant ($p < 0.05$) cortical thinning occurs. The Thinning Ratio is computed by comparing the CT at each follow-up time-point with CT at baseline. Subjects had an average baseline age of 74 yrs. Figure from Y. Li et al. (2012).

1.2.6 Cortical Thickness and Lifestyle Risk Factors

Work has been done to investigate the mechanisms behind each of the above risk factors, and this work has included investigations using MRI-derived CT as an outcome to measure brain atrophy.

One study investigating healthy older adults and adults with MCI from the ADNI dataset were categorized into those with high (>17 years) and low (<14 years) education (Pillai et al., 2012). Higher education was associated with thinner cortices in right lateral occipital and right middle temporal areas, but one-year atrophy rates in these areas did not significantly differ. Some studies found that higher education was associated with lower average CT (Apostolova et al., 2006; Jung et al., 2018); others found it was associated with higher average CT (Kim et al., 2015; Liu et al., 2012; Solé-Padullés et al., 2009). Multiple studies found that that the relationship between education and CT was dependant on brain area, age, and AD stage (Habeck, Gazes, Razlighi, & Stern, 2020; Steffener, 2021). These differences may be attributable to sample size, differing methodology, and interactions with age, sex, and other variables.

There is a well-established relationship between acquired hearing loss and the macroscopic structure of the auditory cortex (Eckert, Cute, Vaden, Kuchinsky, & Dubno, 2012; Neuschwander, Hänggi, Zekveld, & Meyer, 2019; Peelle, Troiani, Grossman, & Wingfield, 2011; Profant et al., 2014). However, this is unlikely to be a mechanism for increased dementia risk as dementia pathology typically manifests in multimodal cortices (Griffiths et al., 2020). A further association with dementia is suggested in a study which found that hearing loss in midlife is associated with late-life temporal lobe volume loss, in both the hippocampus and entorhinal cortex (Armstrong et al., 2019). Additionally, women with late-life hearing loss showed mild cortical thinning in the bilateral frontal, bilateral occipital, and right temporal areas compared to the normal hearing group (Ha et al., 2020).

One study of American veterans found that individuals with mild TBI and high genetic AD risk showed reduced CT in AD-vulnerable regions, suggesting that TBI may moderate the relationship between genetic risk and CT (Hayes et al., 2017). Similar studies have shown that subjects with mild to severe TBI have smaller average CT and reduced CT in AD-vulnerable regions compared to non-TBI subjects (Mohamed et al., 2022; Rostowsky & Irimia, 2021; M. L. Wang et al., 2017).

A systematic review concluded that a negative association was observed between the volume of alcohol consumed and overall brain volume and CT (Verbaten, 2009). The Whitehall study, which measured alcohol use every 5 years found that alcohol use, even at light or moderate levels, was associated with hippocampal atrophy (Topiwala et al., 2017).

Hypertension is associated with reduced brain volume (Gianaros, Greer, Ryan, & Jennings, 2006; Korf, Scheltens, Barkhof, & De Leeuw, 2005; Raz & Rodrigue, 2006) and cortical thinning (Gonzalez, Pacheco, Beason-Held, & Resnick, 2015; Leritz et al., 2011). Midlife hypertension can also predict regional cortical thinning in late life (Vuorinen et al., 2013) and may moderate the relationship between genetic risk and CT (Rast et al., 2018). A meta-analysis of hypertension and brain atrophy concluded that there are some inconsistencies between studies, however, most found consistent shrinking in the bilateral frontal gray matter and the hippocampus (Beauchet et al., 2013). A study looking at the combined effects of T2DM and hypertension found that patients with T2DM but not hypertension had reduced CT in the bilateral paracentral lobule and those who also had hypertension showed reductions in the left inferior parietal lobe, left posterior cingulate gyrus, and right precuneus (Shi et al., 2019).

One meta-analysis of 21 studies investigating links between BMI and CT found consistent negative associations between obesity-related variables and lower grey matter volume in areas including the medial prefrontal

cortex, bilateral cerebellum, and left temporal lobe. They also found brain volume decreased with BMI in all regions except the cerebellum (García-García et al., 2018). A separate meta-analysis published in the same year found negative associations between obesity-related variables and the bilateral frontal gyrus, left middle temporal cortex, left precentral gyrus, and the cerebellum. Additionally, they found positive associations between obesity and the left cuneus, left middle frontal gyrus, left inferior occipital gyrus, and corpus callosum (Herrmann, Tesar, Beier, Berg, & Warrings, 2019).

Cigarette smoking has been associated with reduced cortical volume in a few cortical regions, including some of those associated with AD such as the bilateral frontal cortex, bilateral precuneus, and right thalamus (Almeida et al., 2008; Brody et al., 2004; Gazdzinski et al., 2005). As well, a study done using the ADNI dataset found that cognitively healthy elderly subjects with a history of smoking had a significantly higher rate of atrophy over 2 years in multiple brain regions associated with the early stages of AD when compared with non-smokers (Durazzo et al., 2014). A study of 500 elderly subjects showed that the number of packs per day is negatively correlated with CT however, partial cortical recovery occurred within a year of quitting and complete cortical recovery occurred within a 25 year period after quitting (Karama et al., 2015).

Studies investigating links between depression and CT have had variable results. One meta-analysis summarized that some studies have reported increased regional CT in patients with major depressive disorder while others have reported decreased CT in separate and overlapping regions (Q. Li et al., 2019). A separate meta-analysis also highlighted potential differences in CT due to differences in medicated and unmedicated participants (Suh et al., 2019). A preliminary study with 50 participants was done to investigate the possibility of cigarette smoking as an explanation for

inconsistencies in the CT and depression literature (Zorlu et al., 2017). Cigarette smoking is highly prevalent in major depressive disorders and this study found similar cortical thinning to that seen in smokers without major depressive disorder, including decreased CT in the left temporal cortex, right insular cortex, and left pre-and postcentral gyrus.

Studies have found increased cortical thickness after the introduction of an aerobic fitness regime in elderly participants with cognitive decline and healthy controls (Bae et al., 2020; Reiter et al., 2015) but not AD and healthy controls (Frederiksen et al., 2018; Jonasson et al., 2017). These differences may be related to the fitness regime and its duration, follow-up times, and interactions with other factors. One such factor is education: a study of 1,842 cognitively healthy individuals found that a combination of increased education length and increased exercise level showed greater global and frontal mean CT than either factor alone (Lee et al., 2016). However, even within this study they note the prevalence of diabetes among low-exercise groups as a potential confounding factor.

Recently, work has been done to investigate the direct impact of social contact on cortical thickness. One study examining the effect of social network size in older adults found CT was not impacted by social network, marital status, number of children, number of other relatives, or number of friends (Sharifian et al., 2022). However, they did find that lower mean CT was associated with worse global cognition among individuals with smaller friend networks, but not among individuals with larger friend networks. Certain areas in the AD prodrome are important in regulating complex social interactions and are an important component of the social perception system so this may also have an effect (Rankin et al., 2006; Seo et al., 2010). Researchers have investigated signatures of loneliness in grey matter morphology, intrinsic functional coupling, and fiber tract microstructure (Spreng et al., 2020). They found that lonely individuals display stronger

functional communication in the default network, and greater microstructural integrity of its fornix pathway.

T2DM has a pronounced negative effect on grey matter in the temporal lobe and hippocampal region. As well, total CT, and mean CT for both hemispheres are consistently lower in those with T2DM (Brundel, Van Den Heuvel, De Bresser, Kappelle, & Biessels, 2010). One study compared three groups: one group of healthy controls and two groups with T2DM, one with MCI and one who was cognitively healthy (Brundel et al., 2010). Compared with the healthy controls, the cognitively healthy T2DM group showed significant reduction in the CT of the left posterior cingulate gyrus, right isthmus cingulate gyrus, middle temporal gyrus, paracentral lobule, and transverse temporal gyrus. However, CT alterations in the T2DM with MCI group were bidirectional when compared with the cognitively healthy group. The study found increased CT in the left parahippocampal gyrus and the right isthmus cingulate gyrus and decreased CT in the left pars triangularis and the right pars opercularis.

Investigations into the effects of late life exposure to air pollution are a relatively recent phenomenon. One 2020 study found that increased exposure to PM is associated with globally reduced thicknesses in the frontal, parietal, insular, and temporal lobes (Cho et al., 2020). This study also evaluated the interactive effects of education, diabetes, cardiovascular diseases, smoking, and alcohol consumption. A separate study from the same year also found that NO2 and PM exposure was associated with lower cortical thickness in brain regions known to be affected by AD (Crous-Bou et al., 2020).

Many of the studies mentioned above do not look exclusively at those with AD. Instead, they use a healthy population to investigate the neurological impacts of each risk factor. This work has shown that these risk factors have an effect on brain structure and function which can be seen in

healthy participants. Similarly, this thesis looks at healthy individuals who do not have Alzheimer's disease. Many people who have these risk factors do not go on to develop AD or any form of dementia. The reasoning behind why certain people who have one or more of these risk factors develop AD and others do not is unclear. Additionally, despite the many studies discussed above which have investigated the associations between CT and AD risk factors, there is a major limitation in the current research: the majority of this work focuses on one or a limited number of risk factors and doesn't examine the effect of all the risk factors as a whole. This has resulted in fragmented understanding of the impacts of and the mechanisms behind these risk factors. This thesis aims to address this gap using a multivariate technique which investigates relationships both between and within datasets. This technique is discussed in detail in the following section.

1.3 Canonical Correlation Analysis

1.3.1 Overview of Canonical Correlation Analysis

Canonical correlation analysis (CCA) is a multivariate method which is used to uncover joint multivariate effects. CCA was first introduced in 1936 (Hotelling, 1936), however, it is more computationally expensive than other common analysis methods and as such, has become popular in recent years due to increases in computational power. CCA re-expresses data into high-dimensional linear representations, referred to as canonical variates. Each canonical variate is computed from the weighted sum of the original variable as indicated by the canonical vector.

One of the key advantages of CCA is that it can be used to evaluate two different sets of variables, without assuming any form of directionality or precedence. For example, with CCA it is possible to simultaneously analyze a data matrix of brain measurements with respect to a second data matrix of behavioral measurements and identify sources of common variation.

Moreover, CCA allows the identification of patterns describing many-to-many relations between two variable sets. Another important property of CCA is that it can produce multiple modes (unique pairs of canonical variates), which describe unique patterns of variation in the input sets. Each CCA mode consists of one canonical variate associated with the left variable set and a second canonical variate associated with the right variable set. The first mode calculated using CCA describes the largest variation in the observed data. The next mode consists of the pair of latent dimensions whose variation between both sets is not accounted for by the first mode. As a result, all CCA modes are orthogonal, since every new mode is calculated from the remaining variation in the input sets.

1.3.2 Mathematical Notions

CCA is designed to maximize the correlation between variable sets from two domains of measurement. Given two variable sets X and Y from the same set of n observations suppose there are p variables in set X and q variables in set Y.

$$X = \begin{pmatrix} X_1 \\ X_2 \\ \vdots \\ X_p \end{pmatrix} \qquad Y = \begin{pmatrix} Y_1 \\ Y_2 \\ \vdots \\ Y_q \end{pmatrix}$$

The first CCA mode is defined as a set of linear combinations named U and V. U corresponds to a linear combination of the variables in X.

$$U = a^T X, a \in R^n$$

V corresponds to a linear combination of the variables in Y.

$$V = b^T Y, b \in R^n$$

Each member of U is paired with a member of V defining canonical variate pairs denoted as: $(\mathrm{U_i}, \mathrm{V_i})$. In this primer, a and b are referred to as the canonical vectors, U and V as the canonical variates, and each (U, V) pair as a mode.

$(\mathrm{U_1}, \mathrm{V_1})$ is the first canonical mode. The goal is to find linear combinations that maximize the correlations between the members of each canonical variate pair in a mode. This correlation can be expressed as:

$$\rho = corr(U, V) = corr(a^T X, b^T Y)$$

The canonical correlation for the i[th] canonical variate pair is simply the correlation between $\mathrm{U_i}$ and $\mathrm{V_i}$. This is the quantity to maximize:

$$\rho_i = \frac{cov(U_i, V_i)}{\sqrt{var(U_i) var(V_i)}}$$

This can be subdivided into its component equations. The variance of $\mathrm{U_i}$ and $\mathrm{V_i}$ can be computed using the following equations:

$$var(U_i) = \sum_{k=1}^{p} \sum_{l=1}^{p} a_{ik} a_{il} cov(X_k, X_l)$$

$$var(V_j) = \sum_{k=1}^{p} \sum_{l=1}^{q} b_{jk} b_{jl} cov(Y_k, Y_l)$$

The covariance between $\mathrm{U_i}$ and $\mathrm{V_i}$ is defined as:

$$cov(U_i, V_j) = \sum_{k=1}^{p} \sum_{l=1}^{q} a_{ik} b_{jl} cov(X_k, X_l)$$

First mode ($\mathbf{U_1}$,$\mathbf{V_1}$): The canonical vectors a_1 and b_1 are calculated to maximize the canonical correlation ρ_1 of the first canonical variate pair. This is subject to the constraint that the variances of both canonical variates are equal to one:

$$var(U_1) = var(V_1) = 1$$

Second mode (U_2,V_2): Similarly, the canonical vectors a_2 and b_2 are calculated to maximize the canonical correlation ρ_2 of the first canonical variate pair. Again, this is subject to the constraint that the variances of both canonical variates are equal to one. Additionally, the second canonical variate pair must be uncorrelated with the first canonical variate pair. The constraints can be expressed as:

$$var(U_2) = var(V_2) = 1,$$
$$cov(U_1, U_2) = cov(V_1, V_2) = 0, \qquad cov(U_1, V_2) = cov(U_2, V_1) = 0.$$

ith mode (U_i,V_i): The canonical vectors a_i and b_i are calculated to maximize the canonical correlation ρ_i of the first canonical variate pair. This process may be continued up to $min(p, q)$ times given the constraints:

$$var(U_i) = var(V_i) = 1,$$
$$cov(U_1, U_i) = cov(V_1, V_i) = 0, \qquad cov(U_1, V_i) = cov(U_i, V_1) = 0,$$
$$cov(U_2, U_i) = cov(V_2, V_i) = 0, \qquad cov(U_2, V_i) = cov(U_i, V_2) = 0,$$
$$\vdots \qquad\qquad \vdots$$
$$cov(U_{i-1}, U_i) = cov(V_{i-1}, V_i) = 0, \quad cov(U_{i-1}, V_i) = cov(U_i, V_{i-1}) = 0,$$

This can also be expressed as a change of basis. Let $\sum_{XY}$ be the cross-covaraiance matrix $cov(X, Y)$ for any pair of random variables X and Y. A solution denoting the canonical correlation coefficient ρ of the canonical variates can be expressed as follows:

$$\rho = \frac{a^T \sum_{XY} b}{\sqrt{a^T \sum_{XX} a}\sqrt{b^T \sum_{YY} b}}$$

A change of basis can then be defined:

$$c = \sum\nolimits_{XX}^{1/2} a$$
$$d = \sum\nolimits_{YY}^{1/2} b$$
$$\rho = \frac{c^T \sum_{XX}^{-1/2} \sum_{XY} \sum_{YY}^{-1/2} d}{\sqrt{c^T c}\sqrt{d^T d}}$$

The canonical variates can thus also be expressed as:

$$U = c^T \sum\nolimits_{XX}^{-1/2} X = a^T X$$

$$V = d^T \sum\nolimits_{YY}^{-1/2} Y = b^T Y$$

An alternative understanding of CCA is it provides the best way to rotate the two original variable sets (X and Y) from their original measurement spaces to new spaces in a way that maximizes their linear correlation. The canonical vectors (a and b) define a transformation from the original measurement coordinate system to the new latent space and the canonical variates (U and V) encode the embedding of each data point in that new space. For detailed mathematical proof, see *A Tutorial on Canonical Correlation Methods* (Uurtio et al., 2017).

1.3.3 Use in Neuroscience

Often in neuroscience, a single measure is selected from multiple modalities and a one-to-one univariate association is analyzed. To ensure these results are statistically meaningful, multiple comparisons correction is performed. These one-to-one associations are limited as they overlook possible multivariate joint relationships among multiple measures. They are also limited because highly correlated noise in brain imaging data can decrease the sensitivity and effectiveness of mass-univariate voxel-wise analysis and it's possible for different multiple correction methods to lead to different statistically meaningful results (Cremers, Wager, & Yarkoni, 2017; Marek et al., 2022; Zhuang et al., 2017). In contrast, multivariate analyses do not require multiple correction steps and are able to find covarying associations between multiple modalities. They also often can reduce dimensionality, removing unnecessary information and noise and improving interpretability of data.

CCA produces stable results when the number of observations is greater than the number of features from both modalities, and some previous work suggests that there must be at least three times the number of observations. This is often not fulfilled in neuroscience as brain voxels are considered individual features. In this case CCA will still produce results, however, the results are likely to be overfitted and unstable. As such, data reduction techniques are typically applied before CCA. Principal component analysis (PCA) is the most commonly used data reduction technique and must be applied to the two datasets separately. Other techniques include independent component analysis (ICA), features selection based on statistical dispersion (e.g., mean or median absolute deviation), and traditional brain atlases.

Multiple studies of cognitively normal, healthy subjects have used CCA to investigate healthy aging and the relationship between imaging-derived features and non-imaging measurements (Irimia & Van Horn, 2013; Kuo, Kutch, & Fisher, 2019; Tsvetanov et al., 2016; Zarnani et al., 2019). Other studies have used CCA to determine these relationships in dementia and AD (Brier et al., 2016; Liao et al., 2010; McCrory & Ford, 1991; Zhu et al., 2016).

One study done by Smith et al. investigated the relationship between behavioral and demographic measures and functional connectomes using CCA (Smith et al., 2015a). Group-ICA was performed on the brain imaging data and then the resulting parcels and demographic data were further reduced using PCA. They identified one strong "positive-negative" mode of population co-variation linking positive personal qualities, cognitive ability, and intrinsic brain connectivity. Similarly, a Danish prospective study used CCA to identify markers of healthy aging by examining the relationship between structural brain-imaging derived measures and cognitive ability, health, lifestyle, and demographic factors (Zarnani et al., 2019). They

separately reduced the dimensionality of each dataset using PCA and determined significance of the resulting modes using permutation testing. They also found a single "positive-negative" mode of population co-variation linking higher cognitive performance, positive early-life social factors, and mental health to a larger brain volume of several brain structures, overall volume, and microstructural properties of some white matter tracts.

Other studies have investigated the links between imaging-derived features and cognition socio-behavioural correlates of psychotic disorders. The majority of these have chosen to use atlases to parcellate their data as opposed to matrix-based reduction techniques. Often regions of interest (ROIs) are selected from the atlases to further reduce the input size. For example, one study examining imaging variables and speech fluency in children with autism chose to focus on two language/speech-motor ROIs (Chenausky, Kernbach, Norton, & Schlaug, 2017). Another study examining patterns of cognitive deficits and functional network connectivity in patients with schizophrenia and healthy controls created resting-state network templates based on the probabilistic ROIs from the BrainMap activation database and a resting-state fMRI dataset (Adhikari et al., 2019).

Despite atlases and matrix factorizing methods being the most popular, other studies have chosen to use different parcellation methods. For example, a 2019 study used CCA to relate variation in insular cortex to clinical symptoms of schizophrenia in schizophrenic and healthy control individuals (Tian, Zalesky, Bousman, Everall, & Pantelis, 2019). The fMRI data used in this study was parcellated based on cluster analysis: insula voxels were grouped according to similarity in connectional profiles.

1.4 Matrix Decomposition

Within neuroimaging, techniques such as principal component analysis (PCA) and independent component analysis (ICA) are common choices for

dimensionality reduction (Arbabshirani, Plis, Sui, & Calhoun, 2017; Mwangi, Tian, & Soares, 2014; H. T. Wang et al., 2020). Typically, these matrix decomposition techniques are applied in an exploratory, data-driven fashion to identify dominant modes of variance in a single dataset (Hansen et al., 1999). One of the strengths of these decomposition methods is that they can produce a simplified description of the original dataset by re-expressing the variables using few dimensional representations. This reduction is often beneficial for human interpretation in addition to computational and statistical usability. Figure 1.2 provides visual intuition for the differences between PCA and ICA.

1.4.1 Principal Component Analysis

Principal Component Analysis (PCA) performs an orthogonal linear transformation which projects a dataset to a new coordinate system such that the greatest variance of the data is defined on the first coordinate (first principal component), the second greatest variance on the second coordinate, and so on. In other words, PCA extracts a set of latent dimensions as a linear approximation of the main components of variation inherent in a dataset. These components of variation are not always directly observable in the original dataset. CCA can be thought of as an extension of PCA which maximizes the linear correspondence between two sets of variables. Whereas PCA defines a new orthogonal coordinate system that optimally describes variance in a single dataset, CCA defines coordinate systems that optimally describe the cross-covariance between two datasets.

1.4.2 Independent Components Analysis

Analogous to PCA and CCA, independent component analysis (ICA) extracts dimensions of hidden variation from high-dimensional variable sets. ICA performs a transformation which projects a dataset to a maximally

independent set such that all components are statistically independent and non-gaussian. To rephrase, ICA extracts a set of additive latent dimensions which underlie the original dataset. ICA can be considered as an extension of PCA, however, whereas PCA optimizes the covariance matrix (second-order statistics) of the data, while ICA optimizes higher-order statistics such as kurtosis. This results in PCA identifying uncorrelated components and ICA identifying independent components. Additionally, the components of ICA are not naturally ordered. All ICA vectors have equal importance whereas different PCA vectors explain different amounts of variance within the data based on eigenvalues.

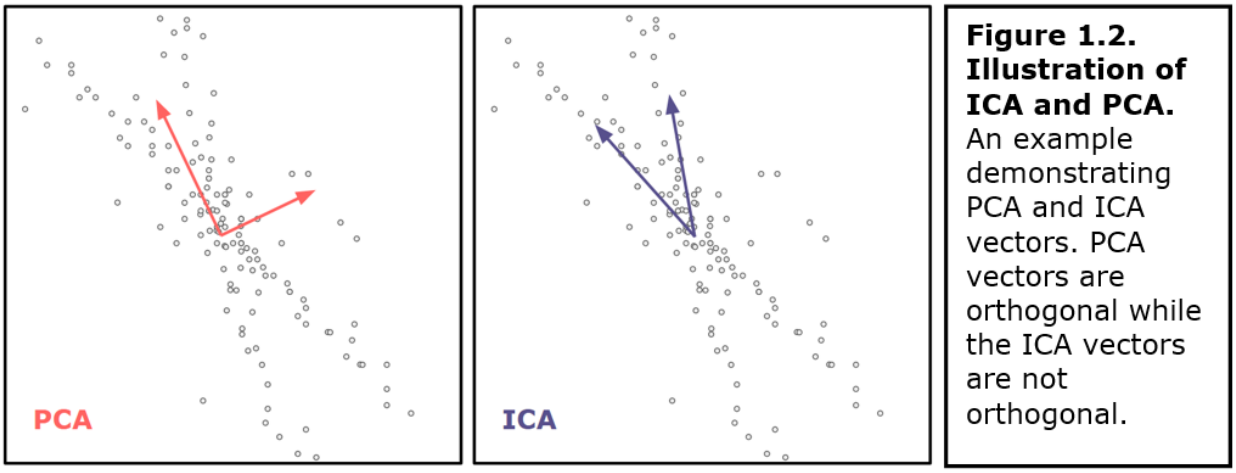

Figure 1.2. Illustration of ICA and PCA. An example demonstrating PCA and ICA vectors. PCA vectors are orthogonal while the ICA vectors are not orthogonal.

Chapter 2: Research Statement

The primary objective of this thesis is to examine the effect of different data reduction methods for neuroimaging studies in the context of CCA. This is done in the context of investigating how risk factors for AD may impact brain structure in individuals. Properly understanding the risk factors which contribute to AD will require an investigation into how they interact with each other as well as their relationship with neurodegeneration. Attempts thus far have been unable to uncover the reasoning behind why certain people who have these risk factors develop AD and others do not. These studies have been limited by small sample sizes and restricted scope which considers only one or a few risk factors at a time. In this work, I address these limitations by using CCA, a jointly multivariate approach to investigate relationships within a set of risk factor related measures and between this set and measures of cortical thickness. I analysed a population of 25,043 adults aged 40 years and older using 52 behavioural measures chosen to be representative of the 12 known AD risk factors and cortical thickness values parcellated into regions of interest using 4 separate parcellation methods.

This project design simultaneously addresses the methodological limitations of CCA. In spite of the increasing use of CCA in neuroimaging studies, particularly those investigating relationships between human brain and behaviours, little investigation has been done to investigate the impacts of data processing decisions in the CCA pipeline. Using a large, state-of-the-art dataset, I am sufficiently equipped to investigate the effects of parcellation methods and dataset size on interpretability of CCA results in a neuroimaging context. I do so by performing permutation testing and random subsampling in order to compare the effects on the correlation values measured between behaviours and CT as well the effects on the contribution of individual variables.

Chapter 3: Materials and Methods

Canonical correlation analysis (CCA) was run on behavioural and cortical thickness values from over 25,000 participants. These participants were aged 40–69 years at recruitment and all data is available through the UK Biobank, a large-scale biomedical database. Behavioural variables were chosen from this database to correspond with Alzheimer's disease (AD) risk factors. Cortical thickness (CT) values were derived using an automated image-processing pipeline. Dimensionality reduction of the CT values for each participant was performed using four different methods: principal component analysis, independent component analysis, spectral clustering, and anatomical parcellation. The reduced CT dimensions were then used as input into CCA along with the behavioural variables. The effect of each reduction technique, as well as the overall significance and loadings for the resulting canonical modes were examined. Additionally, random subsamples of the population were selected and used as input into CCA, in order to examine the effects of sample size on the significance and loading of canonical modes. The details of these steps are explained below.

3.1. Participants and Imaging

3.1.1 UK Biobank Overview

Data used in this project was obtained from the UK Biobank, a representative population-based prospective study with 500,000 participants from the United Kingdom (Sudlow et al., 2015). The primary goal of the UK Biobank is understanding the determinants of common life-threatening and disabling conditions via collection of extensive phenotypic and genotypic detail about its participants, including data from questionnaires, physical measures, sample assays, accelerometry, multimodal imaging, genotyping, and longitudinal follow-up. The UK Biobank began data collection in 2006. All

participants were aged 40–69 years at recruitment. The 500,000 participants were first assessed between 2006 and 2010. The assessment visit consisted of a self-completed touch-screen questionnaire, brief computer-assisted interview, and physical and cognitive testing. A subset of 100,000 participants was selected for follow-up data collection at a later date from physical activity monitors and multi-modal imaging, including brain MRI. The participant demographics after participant selection and quality control can be seen in Table 3.1. Ethnicity was recorded by the participant as white (W), black (b), Asian (A), Chinese (C), mixed (M), or other (O). The Townsend Deprivation Index is a measure of material deprivation, where a higher score represents a higher level of deprivation. This index is an aggregate of measures of unemployment, car ownership, home ownership, and household overcrowding.

Table 3.1. Participant Demographics. Participant demographic breakdown after quality control. These demographic measures are recorded during the first visit. Sex was recorded as male (M) or female (F). Ethnicity was self reported as white (W), black (B), Asian (A), Chinese (C), mixed (M), or other (O).

Participants	**Age**	**Sex**	**Deprivation Index**	**Ethnicity**
25043	*Mean:* 64 *Stdev*: 7.3 *Min:* 44 *Max:* 82	*M:* 12576 *F:* 12467	*Mean:* -1.29 *Stdev*: 3.09 *Min:* -6.25 *Max:* 11	*W:* 23408 *B:* 90 *A*: 552 *C:* 71 *M:* 761 *O:* 161

3.1.2 Behavioural Data Collection

The participants were assessed in 22 centres throughout the UK, chosen to cover a variety of different settings and provide socioeconomic and ethnic heterogeneity and urban–rural mix. The UK Biobank baseline questions were chosen to allow a wide assessment of health-related outcomes to be conducted in the whole cohort. The questionnaire was administered in two parts during the assessment center visit: a touchscreen self-completed questionnaire followed by a computer-assisted personal interview.

3.1.2.1 Cognitive Measures

A selection of cognitive and educational attainment measures are shown in Table 3.2. Five cognitive tests were included in the UK Biobank study during the touch-screen assessment: the Numeric Memory Test, Fluid Intelligence Test, Reaction Time Test, Visual Memory Test, and Prospective Memory Test.

The Numeric Memory Test consisted of showing a two-digit number to participants and asking them to recall it. The number of digits was then increased by one until the participant made an error, or they reached the maximum of twelve digits. The test of Fluid Intelligence consisted of thirteen logic/reasoning-type questions and a two-minute time limit where each question was worth one point. The Reaction Time Test consisted of a timed test of symbol matching. The Visual Memory Test required participants to memorize the positions of six card pairs, and then match them from memory. A higher score indicates more errors were made. The Prospective Memory Test asked to engage in a specific behaviour later in the assessment and then recorded whether they did so or not.

Table 3.2. Participant Cognitive Measures. Participant cognitive measures after quality control.

	Mean (Standard Deviation)
Age Completed Full-Time Education	17 (2.69)
Numeric Memory Score	6.70 (1.34)
Fluid Intelligence Score	5.99 (2.16)
Median Reaction Time (ms)	546 (130)
Visual Memory Errors	3 (3)
Prospective Memory Test	Pass: 23515, Fail: 1528

3.1.3 Imaging Data Collection

The full neuroimaging protocol is provided as part of the UK Biobank Brain Imaging Documentation (Smith, Alfaro-Almagro, & Miller, n.d.). The MR images were acquired at three separate sites with standardized equipment: Siemens Skyra 3T running VD13A SP4 with a standard Siemens 32-channel RF receive head coil. All released data used in this project was collected from three identical centers dedicated to UK Biobank imaging. The imaging protocol included T1-weighted 3D MPRAGE structural imaging with the following parameters: straight sagittal orientation, TR=3.15 ms, TE=1.37 ms, TI=880 ms, field of view (FOV) = 208x256x256 matrix, resolution = 1x1x1 mm, in-plane acceleration iPAT = 2, acquisition time of 5 minutes. These are the main neuroimaging focus for this thesis. The FOV for the T1 and T2 images was automatically determined based on Siemens' auto-align software, which aligns a scout scan to an atlas. All images acquired by the UK Biobank were defaced for subject anonymity before being released.

3.2 Data Processing

3.2.1 Image Processing

3.2.1.1 UKBB Preprocessing

In addition to releasing the raw, defaced T1w structural images, the UKKB also releases processed imaging data, quality control metrics, and T1-derived outputs. After defacing, the full FoV raw T1 image is cropped to reduce the amount of non-brain tissue (primarily tissues below the brain and blank space above the head) using BET (Smith, 2002). Gradient distortion correction is performed using FMRIB's Linear Image Registration Tool (Jenkinson, Bannister, Brady, & Smith, 2002; Jenkinson & Smith, 2001) in conjunction with the MNI ICBM152 non-linear 6th generation symmetric Average Brain Stereotaxic Registration Model (Grabner et al., 2006). This data is then nonlinearly warped to MNI152 space using FMRIB's Nonlinear Image Registration Tool (Andersson, Jenkinson, & Smith, 2007a, 2007b). Finally, brain-extraction is then performed by back-transforming a standard-space brain mask into the space of the T1 and applying it to the image. Next, FAST: FMRIB's Automated Segmentation tool (Y. Zhang et al., 2001) is used to perform tissue-type segmentation. FAST estimates probabilistic segmentations for grey matter, white matter, and cerebrospinal fluid. This step also estimates intensity bias and is used to generate a fully bias-field-corrected version of the brain-extracted T1.

There are multiple quality assurance steps performed throughout the image processing pipeline. A fully automated Quality Control Tool is used to identify images with problems either in their acquisition or in later processing for example: measures of asymmetry and subcortical structure normalised intensities (Alfaro-Almagro et al., 2018). The Quality Control Tool consists of three types of classifiers developed to classify issues that may be found in T1 images. The selected classifiers all exhibited satisfactory classification individually and using multiple classifiers compensates for

possible overfitting of individual classifiers (Alfaro-Almagro et al., 2018). The full set of image analysis pipeline scripts is available at www.fmrib.ox.ac.uk/ukbiobank/.

3.2.1.2 CIVET

The preprocessed T1-weighted images were processed by CIVET (version 2.1.1; Montreal Neurological Institute; Zijdenbos et al., 2002) using the NeuroHub infrastructure (Sherif et al., 2014) to estimate CT. CIVET is a fully automated image-processing pipeline for extracting cortical, morphometric, and volumetric data from MR images (Zijdenbos, Forghani, & Evans, 2002). Briefly, the image processing steps of CIVET are: linear registration to the MNI ICBM 152 average (Collins et al., 1994), non-uniformity correction (Sled, Zijdenbos, & Evans, 1998), brain extraction (Smith, 2002), tissue classification into white matter (WM), gray matter (GM) and cerebrospinal fluid (CSF) using priors derived from nonlinear registration and accounting for partial volume effects (Tohka et al., 2004), WM and pial surface extraction and registration (June et al., 2005b; Kabani, Le Goualher, Macdonald, & Evans, 2001; MacDonald, Kabani, Avis, & Evans, 2000), and estimation of cortical thickness at 81,924 vertices across the cortical mid-surface (Lerch & Evans, 2005). The CT values are calculated based on the length of the trajectory from the GM-WM surface to the pial surface, then blurred using a 30 mm geodesic surface kernel. The blurred values are used as input into the data reduction techniques described in Chapter 3.2.3.

3.2.1.3 Quality Control

In addition to the CT values, CIVET automatically creates figures showing the GM and WM classifications as well as boundary delineations for quality control. Quality control was performed on all CIVET outputs to control for accuracy of the surface definition and the GM and WM classifications. Outputs were given a score of 0 (fail), 0.5 (warn), or 1 (pass); see Figure 3.1 for examples. A passing score of 1 is given for outputs with accurate

classification and boundaries and no visible errors. A score of 0.5 is given for outputs which have minimal misclassification of GM or WM or slight errors in segmentation. This rating is given when these errors are minimal and localised to one or few parts of the cortex. A failing score of 0 is given for outputs with significant errors or numerous small errors. Data was excluded after quality control, and only outputs with a score of 1 were included in the analysis. The limited MR image slices shown in the automatically generated CIVET figures must be taken into account when assessing the accuracy of the ratings. The full quality control guidelines are made available by the CoBrA Lab at https://github.com/CoBrALab/documentation/wiki/CIVET-Quality-Control-Guidelines.

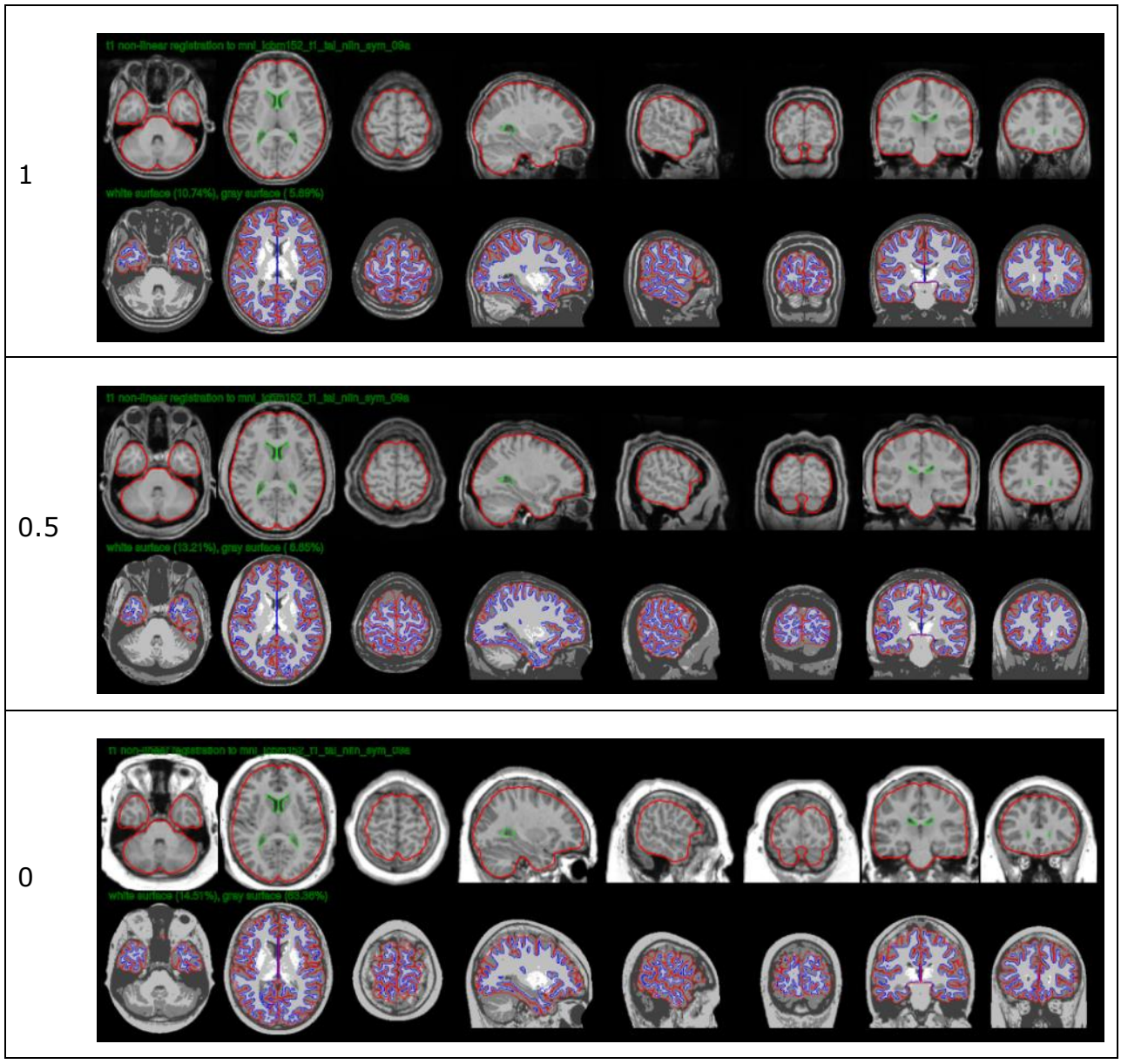

Figure 3.1. CIVET Quality Control Examples. Examples of QC scores for CIVET outputs. Scores are either 0 (fail), 0.5 (warn), or 1 (pass).

3.2.2 Reducing Behavioural Variables

A subset of the epidemiological and cognitive variables was selected to be representative measures of the twelve potentially modifiable risk factors. Behavioural variables were excluded if more than 10% of the population had missing values. This resulted in the exclusion of 11 variables, however each AD risk factor had at least one representative variable which was not

excluded. Since blood pressure could be taken either manually or automatically, these columns were combined. The 52 chosen variables are listed in Table 3.3 (see https://biobank.ndph.ox.ac.uk/showcase/ for detailed descriptions of these measures). Participants who were missing more than 10% (5) of these variables were not included in the study.

Table 3.3. UKBB Variable Descriptions. Table containing the codes for each behavioural variable used in the thesis, the UKBB Data Field Description, and the corresponding risk factor associated with the variable.

CODE	DESCRIPTION	CATEGORY
845	Age completed full time education	Education
864	Number of days/week walked 10+ minutes	Physical Activity
874	Duration of walks	Physical Activity
884	Number of days/week of moderate physical activity 10+ minutes	Physical Activity
894	Duration of moderate activity	Physical Activity
904	Number of days/week of vigorous physical activity 10+ minutes	Physical Activity
914	Duration of vigorous activity	Physical Activity
943	Frequency of stair climbing in last 4 weeks	Physical Activity
971	Frequency of walking for pleasure in last 4 weeks	Physical Activity
981	Duration walking for pleasure	Physical Activity
991	Frequency of strenuous sports in last 4 weeks	Physical Activity
1001	Duration of strenuous sports	Physical Activity
1011	Frequency of light DIY in last 4 weeks	Physical Activity
1021	Duration of light DIY	Physical Activity
1031	Frequency of friend/family visits	Social Support

1239	Current tobacco smoking	Smoking
1249	Past tobacco smoking	Smoking
1259	Smoking/smokers in household	Smoking
1269	Exposure to tobacco smoke at home	Smoking
1279	Exposure to tobacco smoke outside home	Smoking
1558	Alcohol intake frequency.	Alcohol
2050	Frequency of depressed mood in last 2 weeks	Mental health
2110	Able to confide	Social Support
2247	Hearing difficulty/problems	Hearing
2443	Diabetes diagnosed by doctor	Diabetes
2624	Frequency of heavy DIY in last 4 weeks	Physical Activity
2634	Duration of heavy DIY	Physical Activity
2966	Age high blood pressure diagnosed	Medical Conditions
3456	Number of cigarettes currently smoked daily (current cigarette smokers)	Smoking
3637	Frequency of other exercises in last 4 weeks	Physical Activity
3647	Duration of other exercises	Physical Activity
4537	Work/job satisfaction	Mental health
4548	Health satisfaction	Mental health

4559	Family relationship satisfaction	Mental health
4570	Friendships satisfaction	Mental health
4792	Cochlear implant	Hearing
4803	Tinnitus	Hearing
6160	Leisure/social activities	Social Support
20116	Smoking status	Smoking
20123	Single episode of probable major depression	Mental Health
20124	Probable recurrent major depression (moderate)	Mental Health
20125	Probable recurrent major depression (severe)	Mental Health
20126	Bipolar and major depression status	Mental Health
23104	Body mass index (BMI)	BMI
94	Diastolic blood pressure, manual reading	Blood Pressure
4079	Diastolic blood pressure, automated reading	Blood Pressure

3.2.3 Dimensionality Reduction

3.2.3.1 Preprocessing

Quality control was performed on all the images according to the procedures outlined in the previous section, Chapter 3.1.4.3. CT values for all participants were retrieved from NeuroHub using the CBrain portal (Sherif et al., 2014). Data decomposition was performed on these CT values using four different methods: the Automated Anatomical Labeling (AAL) atlas, a custom cortical surface atlas grouped via spatial proximity, and two matrix

decomposition methods: principal component analysis (PCA) and independent component analysis (ICA). The resulting brain parcellations from these methods are described in detail below. Each of these parcellation methods was propagated to all participants to obtain CT samples per region of interest. Vertex-wise CIVET outputs contain CT estimates at 40,962 vertices for each hemisphere of the brain. However, a portion of the vertices along the midline often contain unreliable estimates. These invalid vertices were removed using a mask, resulting in 38,561 vertices for each hemisphere.

Unlike CCA which is scale-invariant, the PCA and ICA dimension-reduction steps performed prior to CCA are influenced by the relative scaling of each variable. Thus, the vertex-wise CT values were normalised using z-scoring by vertex over all subjects. The effects of sex were regressed out of the values. When CCA was run with sex included, it dominated the first mode of correlation and overshadowed all other relationships.

3.2.3.2 Principal Component Analysis

PCA, as described in detail in section 1.4.1, is a form of matrix decomposition which reduces the original data to new variables which are orthogonal linear functions of those in the original dataset. Each principal component corresponds to the direction with the greatest variance in data. The top 600 principal components (PCs) were selected as they accounted for over 80% of the explained variance in cortical thickness.

3.2.3.3 Independent Component Analysis

ICA, as described in detail in section 1.4.2, performs matrix decomposition similar to PCA, removing correlations between components. However, unlike PCA, ICA also removes higher order dependence, and the vectors are not orthogonal. The ICA approach used included a pre-whitening step: the data were first transformed using PCA, which leads to a diagonal covariance matrix, and then each dimension was normalized such that the covariance

matrix is equal to the identity matrix. All independent components (ICs) are equally important, and 600 components were selected for consistency with PCA.

3.2.3.4 AAL Atlas

The anatomical labeling atlas (AAL) is a popular brain atlas, and has been widely employed to identify kinds of psychological disorders in recent years (Long et al., 2018). The AAL atlas is derived from a spatially normalized single-subject high-resolution T1 volume provided by the Montreal Neurological Institute. The parcellations can be seen in Figure 3.2. The AAL template was originally defined on the MNI single brain Colin27 brain (Tzourio-Mazoyer et al., 2002) and registered to the ICBM surface model (Lyttelton, Boucher, Robbins, & Evans, 2007). The AAL atlas used, partitions the whole cerebral cortex into 90 regions (without cerebellum) which can be seen in Figure 3.2. There is a slight asymmetry in the AAL which corresponds to the natural asymmetry of typical brains. For this thesis, an asymmetric AAL labeling package specific to the resampled surfaces generated from the CIVET pipeline was used.

3.2.3.5 Spatial Clustering

To contrast the anatomical atlas, a spatially derived brain atlas was created without considering neuroanatomical boundaries using spectral clustering; see Figure 3.2. Spectral clustering allows for the creation of parcels with a similar number of vertices, which is beneficial as it allows for unbiased sampling of vertices to estimate cortical thickness (Bhagwat, Pipitone, Voineskos, & Chakravarty, 2019). Spectral clustering uses graph connectivity to identify data points (vertices) connected or immediately next to each other. The verticees are then mapped to a low-dimensional space that can be easily segregated to form clusters. An affinity matrix, degree matrix, and Laplacian matrix can be derived from the graph. Information from the eigenvalues of these matrices is used to create the clusters based

on distance between the verticees. Spectral clustering is flexible and makes no assumptions about the form of the clusters.

The implementation of spectral clustering for this thesis was done in Python using scikit learn (version 1.1.1; Pedregosa et al., 2011). This implementation performs a low-dimension embedding of the affinity matrix followed by clustering. The affinity matrix is constructed using a radial basis function (RBF) kernel and the cluster labels are assigned using k-means clustering. A single brain mesh is taken as input and each brain vertex is assigned to a discrete parcel. The parcellation is then propagated to each individual subject. In order to ensure consistency with the AAL atlas, 90 brain parcels were created.

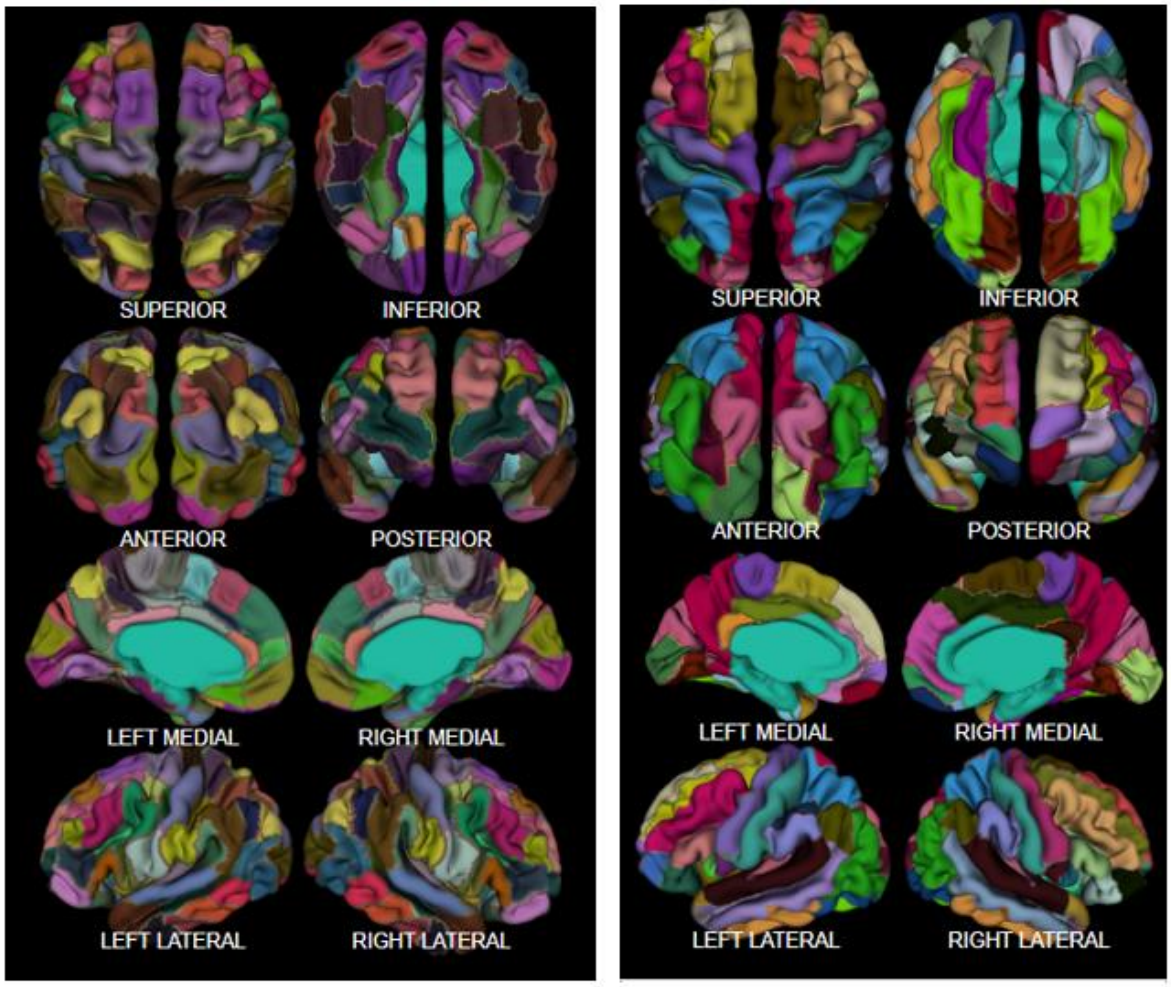

Figure 3.2. Brain Parcellation Visualizations. Left: Spectral clustering parcellations visualized on a brain, showing 90 unique areas across both hemispheres. Right: AAL parcellations visualized on a brain, showing 90 unique areas across both hemispheres.

3.3 Statistical Analysis

3.3.1 Canonical Correlation

CCA was performed to simultaneously co-analyse the matrix of brain variables along with the matrix of behavioural variables. These two matrices contained the data for all 25,043 participants. Each resulting mode identifies a linear combination that relates behavioural variables and CT components. This analysis was implemented in Python using scikit-learn (version 1.1.1; Pedregosa et al., 2011). The default values of 500 maximum iterations of the power method and a tolerance of 1e-06 for the convergence criteria were used.

For this thesis, CCA was used to estimate 52 modes - the minimum size of the two input matrices. The first solution found by CCA represents the most strongly correlated mode. The canonical correlation for each mode (variate pair) was calculated. Canonical correlation between two canonical variates is a primary performance measure for CCA. This measure quantifies the linear correspondence between the two variable sets based on the Pearson's correlation between their canonical variates. In other words, it measures how much the two variable sets can be brought near each other in the embedding space and can be thought of as a metric of successful joint information reduction.

The traditional approach to interpreting canonical correlation analyses involves examining the magnitude and sign of the canonical weight assigned to each variable in its canonical variate. However, the use of canonical weights for interpretation or contribution of a variable is subject to criticism. A small weight may be interpreted as insignificant due its corresponding variable being irrelevant to the overall relationship, or that it has been partialed out of the relationship due to a high degree of multicollinearity. This is the same issue faced regarding the interpretation of beta weights in regression techniques. Furthermore, canonical weights are subject to

considerable instability across samples. These limitations suggest caution in using standardized canonical weights to interpret the results of a canonical analysis (Dattalo, 2014; Lambert & Durand, 1975). Consequently, canonical loadings have been increasingly used as a basis for interpretation. Canonical loadings measure the linear correlation between an original variable and the canonical variate or the set it belongs to. This measure reflects the variance that the observed variable shares with the canonical variate. Intuitively, the larger the magnitude of loading, the more important it is in deriving the canonical variate. In this analysis, canonical loadings were considered to avoid the limitations inherent in canonical weights and to ensure comparisons across different runs of CCA were accurately measured.

3.3.2 Permutation Testing

Permutation testing is an increasingly popular statistical tool for creating sampling distributions as a means of generating a null distribution by resampling. The data was shuffled by assigning different outcome variables to each set of observed variables without replacement.

In this case, a permutation testing procedure was used to create a null distribution of canonical variate pairs. The behavioural data matrix was kept constant, while the rows of the cortical thickness matrix were shuffled so as to break the linkage between participants CT variables and their behavioural variables. The canonical variates resulting from these re-aligned datasets then serve as the null distribution against which the real correlations are compared. For each parcellation method, 5,000 permutations were created and input into CCA.

3.3.3 Random Sampling

In order to evaluate the effects of participant sample size on the results, CCA was performed on randomly selected subsets of the data. Unlike permutation testing which includes all participants, random sampling includes only a subset of the participants and can be used to demonstrate consistency of results across reduced sample sizes. A random sample was taken of 75% (18,782 participants) of the participants – without replacement - and CCA was performed in an identical manner to the complete participant analyses. This was repeated 100 times. The individual brain and behavioural loadings and the order of the variables within the variates were compared across the repetitions. The first mode was also compared with the first mode found using all participants. This was done for all parcellation methods.

Additionally, CCA was run with random samples of 50% (12,521 participants), 25% (6,260 participants), and 10% (2,504 participants) of the data. This procedure was performed using the same procedure as running CCA for the full list of participants with all modes of parcellation. The canonical correlation for the first mode was calculated with the reduced sample size. This analysis was also repeated 100 times and averaged for comparison with the first mode from CCA performed on all participants.

Chapter 4: Results

4.1 Canonical Correlates

All four parcellation methods resulted in first modes with similar loading patterns. The behavioural variables with the strongest positive and negative loadings are consistent between the four methods, however the values of the loadings are not. Likewise, similar loading patterns emerge in certain brain areas for all four methods, but the values differ. These similarities are examined in more detail for the first modes in chapter 4.2. The resulting modes calculated using all parcellation methods were not statistically significant. As such, the relationships found between CT and behavioural variables can not be concluded to have any specific effect. F-approximations of Wilks' Lambda are used as the test statistic. The first p-value is calculated including all canonical correlation coefficients, the second p-value is calculated including all except the first coefficients, the third p-value is calculated by excluding the first two coefficients etc., allowing assessment of the statistical significance of each individual correlation coefficient. The canonical correlation for the first mode of CCA using the PCA and ICA matrices is similar (PCA: cc=0.801, p-val=0.067; ICA: cc=.800, p-val=0.066), while the canonical correlation for the first mode using the spectrally clustered matrix as input was lower (cc=0.733, p-val=0.23), and the canonical correlation for the first mode using the AAL matrix as input was the lowest (cc=0.669, p-val=0.36). The correlation values for all modes are shown in Figure 4.1.

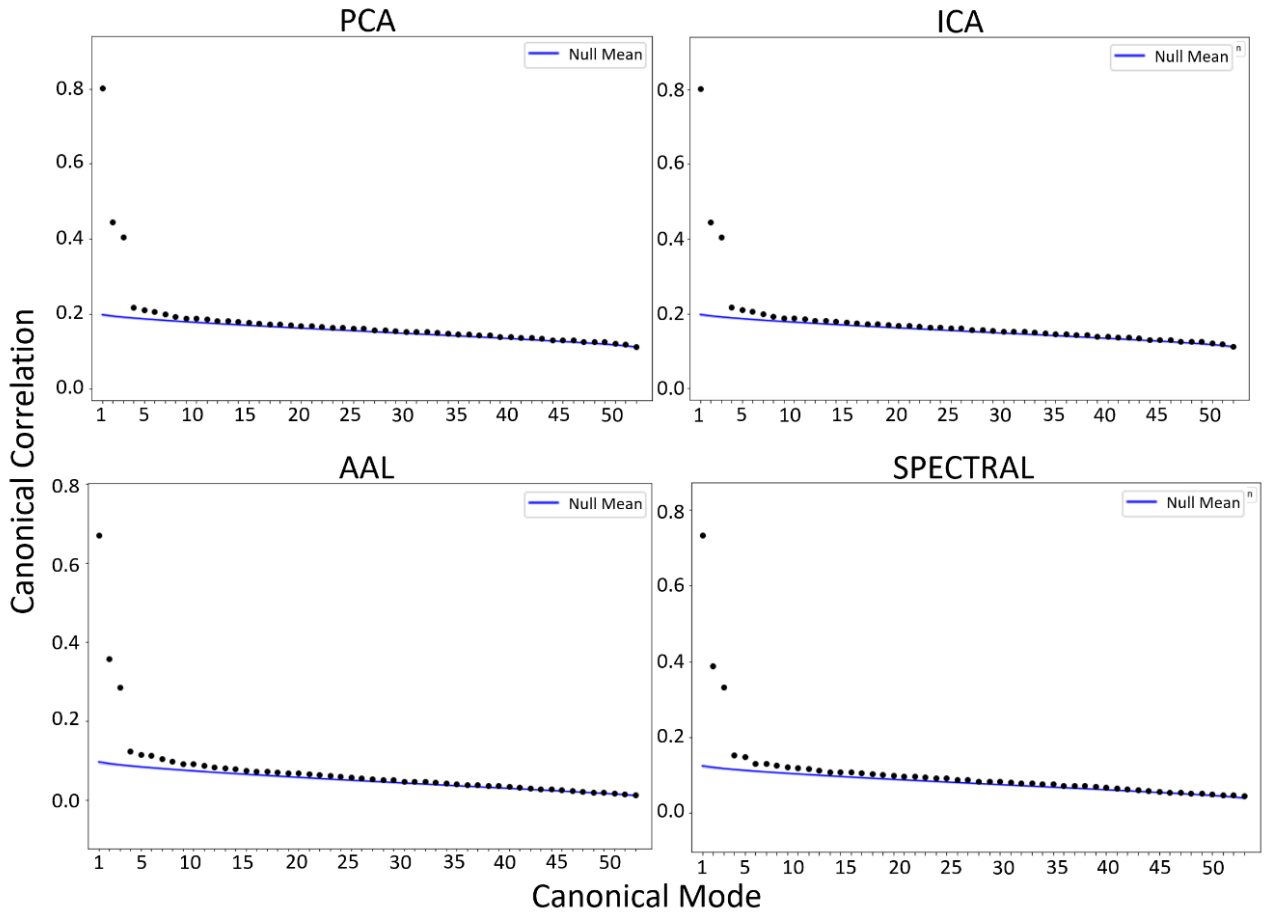

Figure 4.1. Canonical Correlates of All Modes. The canonical correlation of all 52 modes is plotted for each set of inputs. The blue line shows the mean of the null distribution of the same measures, estimated via permutation testing.

4.2 First Canonical Mode

The first canonical mode represents the most significant mode of population co-variation, for which individual subjects' strength of involvement with this mode is highly similar for both a subset of the brain regions and a subset of the behavioural variables. Permutation testing using null distributions accounts for the fact that the first modes are expected to have higher correlations, and the nulls show that this is a small effect.

4.2.1 Comparing Parcellation Methods

The Hamming distance measures similarity by comparing the changes in the number of positions between the two lists of ordered behavioural variables. The normalized Hamming distance is the ratio of the Hamming distance to the length of the lists being compared, with a measure of 0 representing two identical lists. This can be used to compare the variable ordering, without taking into account the strength of the loadings. The table of normalized Hamming distances for each parcellation methodology can be seen in Table 4.1. The loadings calculated using PCs and ICs are the most similar and both are equally dissimilar from the loadings found using AAL parcellations. Additionally, the distance between the ordered behavioural loadings was calculated for reduced lists. Table 4.2 shows the normalized Hamming distance between the top 5 positive loaded variables and bottom 5 negative loaded variables. When taking into account only the variables with the strongest loadings, the normalized Hamming distance is always lower (the lists are more similar). The lists of behavioural loadings can be seen with text size according to their loadings in Figure 4.2. The behavioural variables being input remain the same, and thus the changes in their loadings reflect the changes in the relationships uncovered using CCA based on the parcellation method.

Table 4.1. Hamming Distance of Loadings. The normalized Hamming distance between the behavioural variables based on the canonical variate loading from CCA performed using each parcellation method (specified along the axis) as input.

	PCA	ICA	Spectral	AAL
PCA	0	0.19	0.67	0.71
ICA	0.19	0	0.69	0.71
Spectral	0.67	0.69	0	0.54
AAL	0.71	0.71	0.54	0

Table 4.2. Hamming Distance of Top Loadings. The normalized Hamming distance between the top and bottom five behavioural variables based on the canonical variate loading from CCA performed using each parcellation method (specified along the axis) as input.

	PCA	ICA	Spectral	AAL
PCA	0	0	0.3	0.3
ICA	0	0	0.3	0.3
Spectral	0.3	0.3	0	0
AAL	0.3	0.3	0	0

In addition to the normalized Hamming distance, which looks at the relative loadings within the first canonical variates; the correlation between the behavioural loadings themselves can be calculated. The correlations between the behavioural variable loadings calculated using CCA with all four parcellation methods can be seen in Table 4.3. The correlation values are all high, with the strongest correlations between ICA and PCA and the lowest correlations between ICA and spectral clustering. These correlations measure the strength of the linear relationship between the variate loadings. Large correlations suggest that the loadings are relatively stable across all implementations of CCA (Lambert & Durand, 1975).

Table 4.3. Correlation of Loadings. The correlation between the behavioural variables based on the canonical variate loadings from CCA performed using each parcellation method (specified along the axis) as input.

	PCA	ICA	Spectral	AAL
PCA	1	0.99998	0.99909	0.99844
ICA	0.99998	1	0.99908	0.99847
Spectral	0.99909	0.99908	1	0.99919
AAL	0.99844	0.99847	0.99919	1

4.2.2 Loading Values

The strongest loading for the spectral clustered results is on a parcel which is composed of bilateral areas from the inferior frontal gyrus, opercular part; precental gyrus; rolandic operculum; superior temporal gyrus; and temporal pole of the superior temporal gyrus (loading: -0.858) and can be seen in Figure 4.2 (bottom right). The strongest loadings for the AAL parcellated results occur bilaterally for the precentral gyrus (loading: -0.900), closely followed by the superior temporal gyrus (loading: -0.890), and postcentral gyrus (loading: -0.849) and can be seen alongside the behavioural loadings in Figure 4.2 (bottom left). The three principal components with the strongest absolute loadings are shown in Figure 4.3. The fifth principal components had the highest absolute loading (loading: -0.437), closely followed by the second (loading: 0.320), and third components (loading: -0.334). Of these three components, the fifth shows the most bilateral differences which can be seen clearly in Figure 4.3. All three of these components have strong absolute loadings along the precentral gyrus and the temporal pole of the superior temporal gyrus. Component 2 has a progression of positive to negative loadings anteriorly to posteriorly throughout the cortex excepting the areas mentioned previously. Component 3 has the inverse progression with positive loadings posteriorly transitioning to negative values anteriorly. Additionally, the combined weight of the top

5% of the loadings is shown in Figure 4.2 (top left). This was calculated to visualize the cumulative effect of the canonical loadings because visualizing the weight effects on all 600 components is intuitively challenging. This combined weighting results in a distinct bilateral, negatively weighted area along the postcentral gyrus. The most positively weighted areas are bilaterally spread across the inferior temporal gyrus, temporal pole of the superior temporal gyrus, and superior frontal gyrus. The three independent components with the largest absolute loadings are shown in Figure 4.4. The 492^{th} independent components has the highest absolute loading (loading: -0.140), closely followed by the 249^{th} (loading: -0.124), and 279^{th} components (loading: -0.124). The 279^{th} loading shows positive weighted area along the postcentral gyrus and inferior temporal gyrus. The other two components have areas of positive and negative loadings which do not correspond to specific functional areas. Additionally, the combined weight of the top 5% of the loadings is shown in Figure 4.2 (top right). The combined weighting results in a pattern of scattered areas of positive and negative loadings which do not correspond to easily identifiable anatomical or functional areas.

The loadings on the behavioural variables in the first mode correlate with the loadings on the CT variables. For example, low work fulfillment had the strongest loading across all parcellation methods and was associated with the strong negative loadings (aka decreases in cortical thickness) in the areas mentioned above. Conversely the negative behavioural loadings can be interpreted as an inverse correlation. For example, high sport participation is negatively correlated with CT decreases. This interpretation can be simplified as high sport participation is correlated with increased cortical thickness in the specified areas.

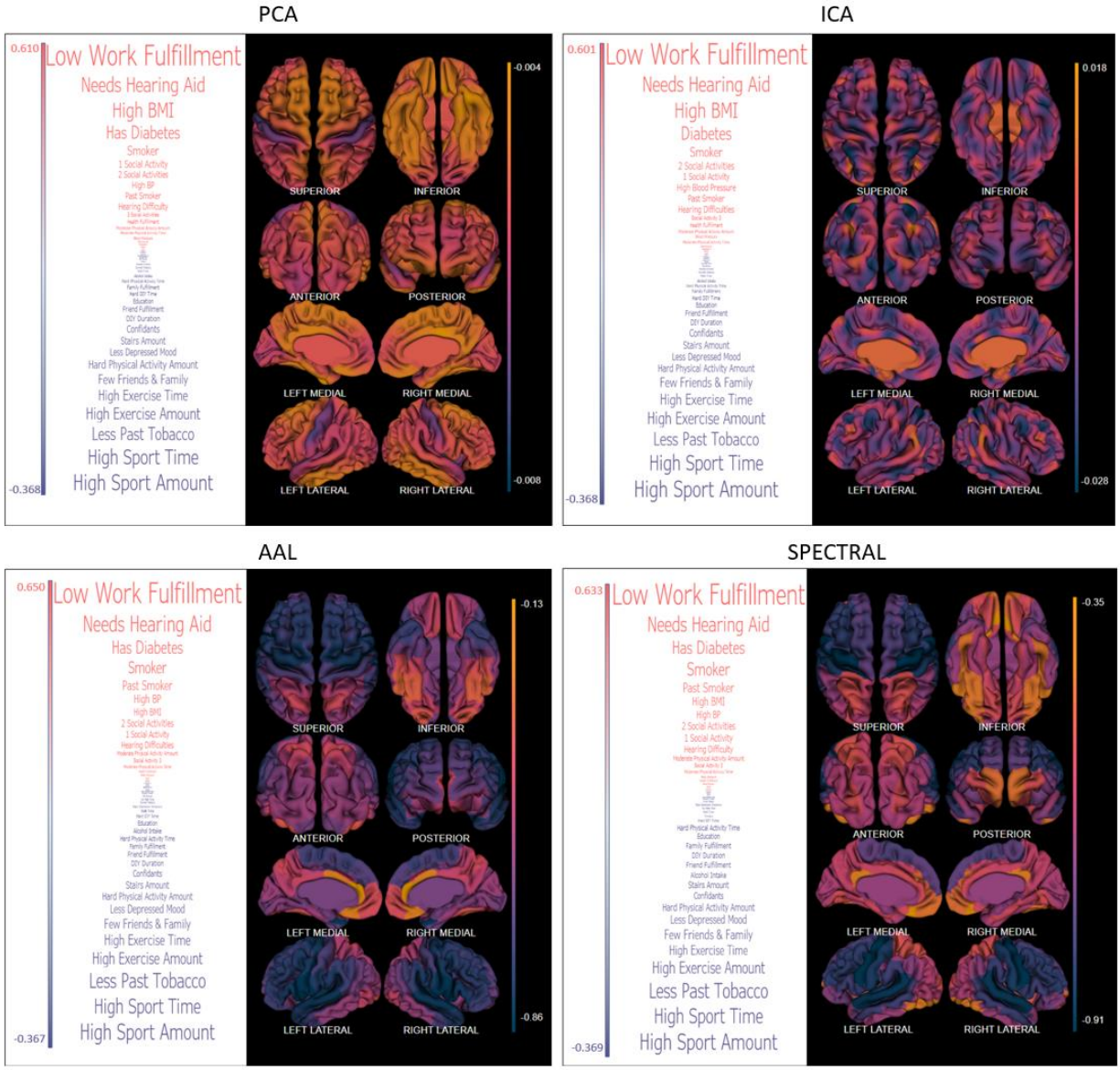

Figure 4.2. Behavioural and CT Loadings. A visualization of the loadings from the first CCA mode for each parcellation method. *Left:* List of behavioural variables weighted based on their loadings from the first CCA mode. *Right:* Visualization of the spectrally clustered CT value loadings from the first CCA mode. The midline CT values which were not included in the analysis are set to the mean value for visualization purposes.

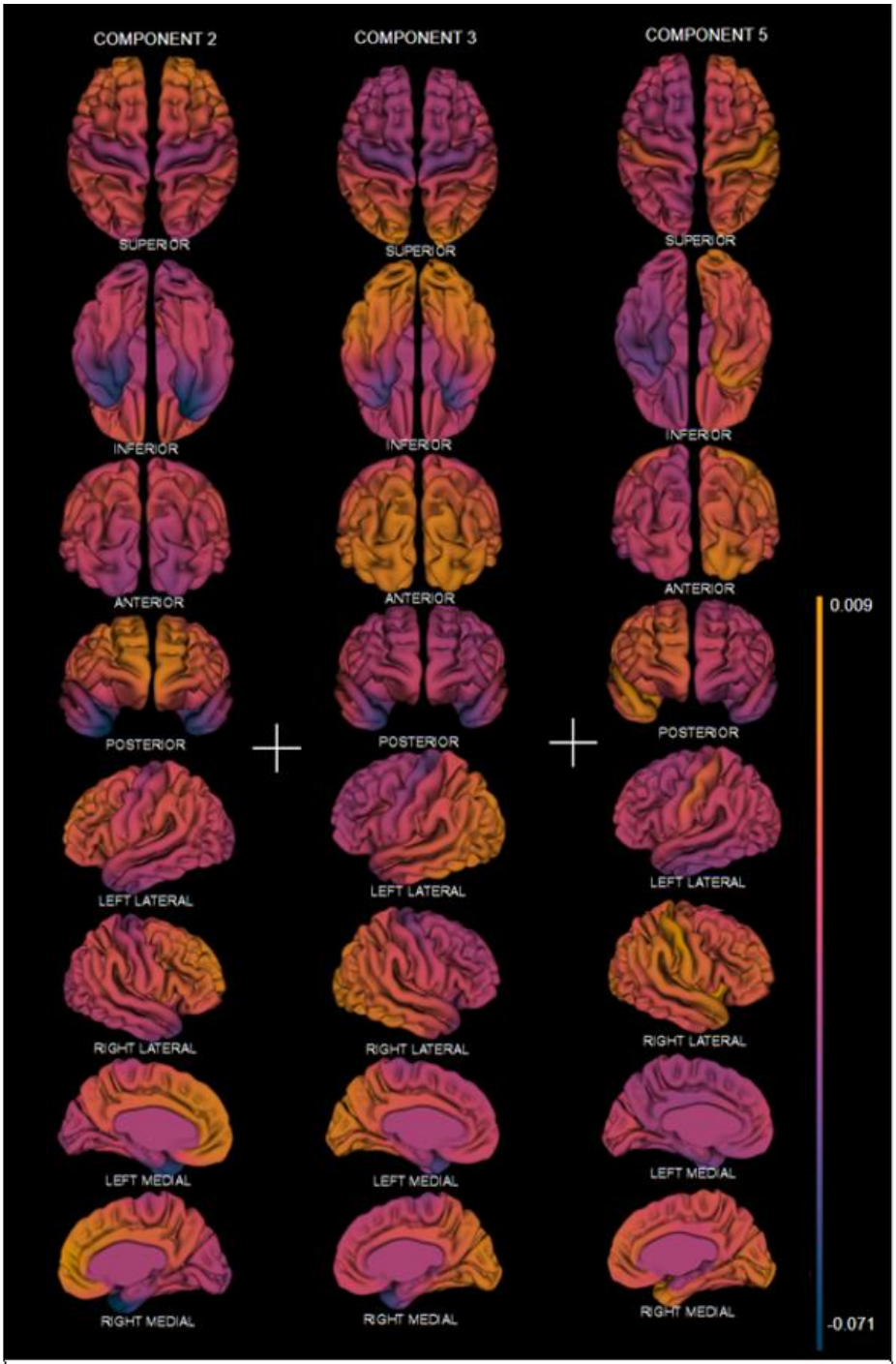

Figure 4.3. Top Principal Components. The top three principal components with the strongest loadings from the first canonical mode. The loadings from left to right are -0.334, 0.320, and -0.437.

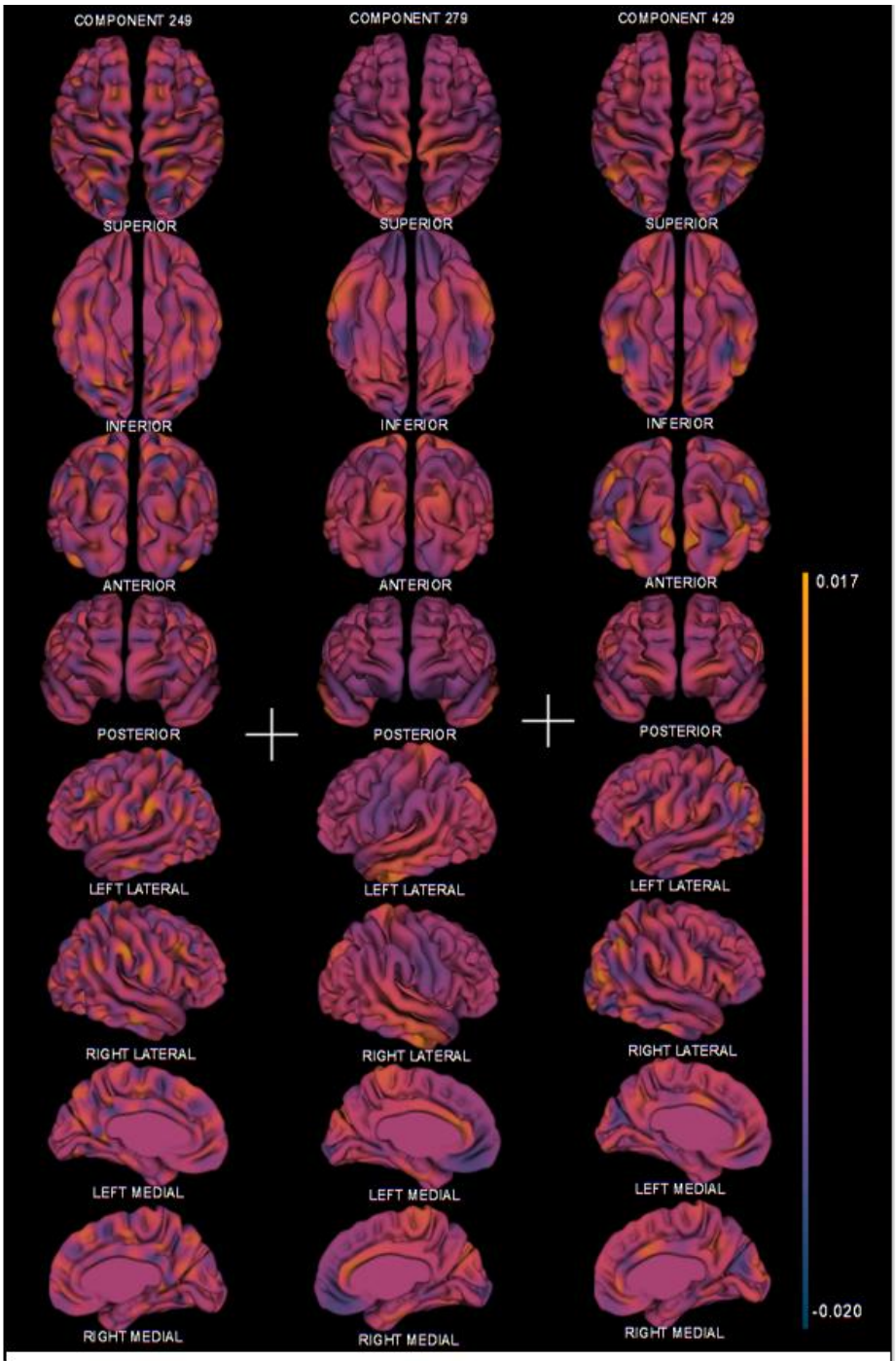

Figure 4.4. Top Independent Components. The top three independent components with the strongest loadings from the first canonical mode. The loadings from left to right are 0.124, -0.124, and -0.140.

4.3 Sampling

The evaluation of the 75% sample size canonical correlation results showed consistency across a smaller sample of population. The top 10 largest absolute value loadings for the behavioural matrix are shown in Figure 4.5. This figure demonstrates the stability of the loading values and their ordering over the random population subsamples for all parcellation methods.

Smaller subsamples were also created and the canonical correlation of the first mode of each was recorded. The canonical correlation for the first mode of CCA found by averaging the results from 100 random subsamples of the population is visualized in Figure 4.6. This is shown for the four parcellation methods: PCA, ICA, AAL clustering, and spectral clustering. The corresponding p-values for each sample size are shown in Figure 4.6 in the table to the right. As the sample size decreased the p-value decreased for CCA with all four parcellation methods. The CCA run with principal components and independent components reach significance levels at a sample consisting of 25% of the population.

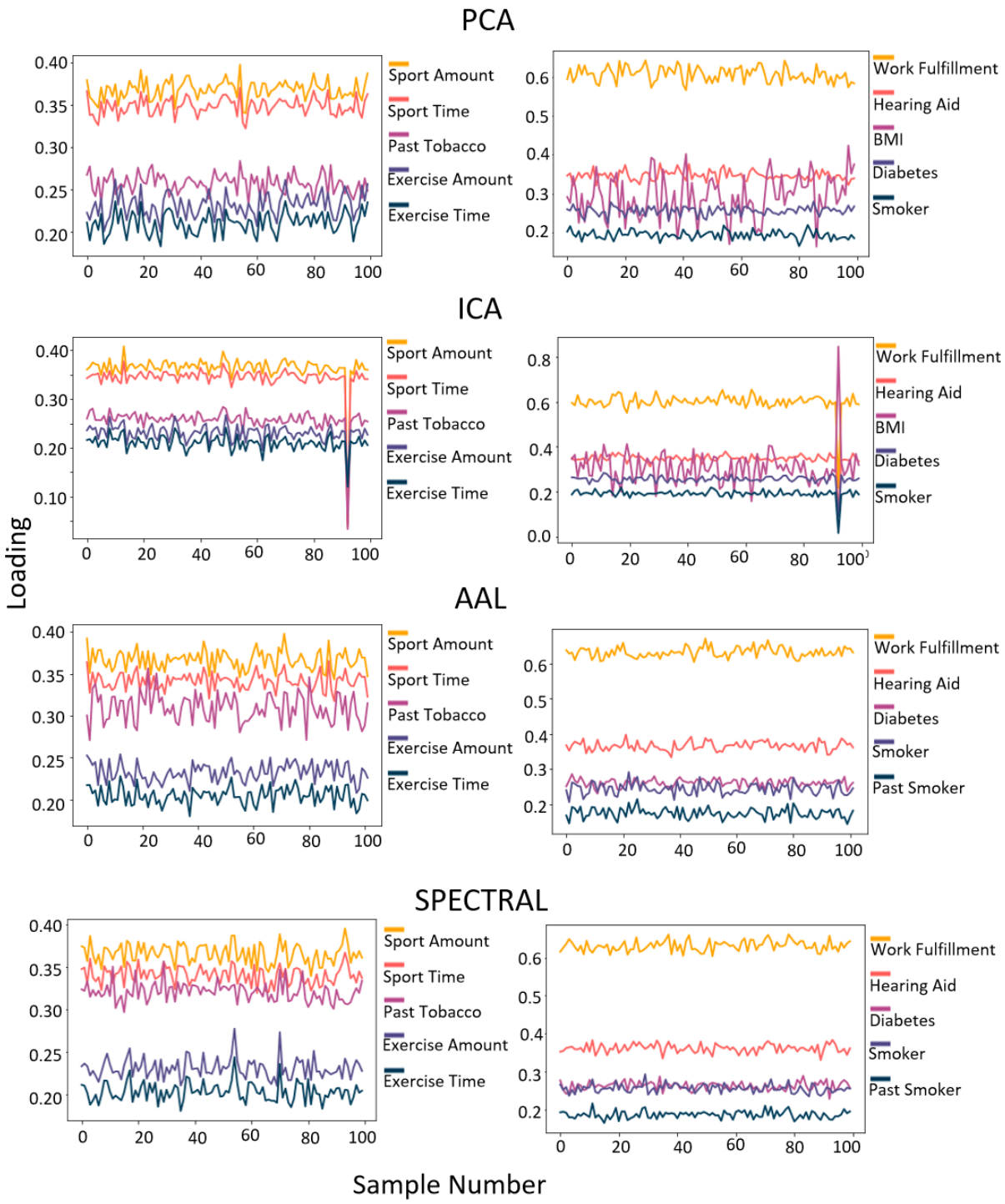

Figure 4.5. Canonical Loadings of Subsamples. Left: The 5 behavioural variables with the largest positive loading using a random sample of 75% of the participants. Right: The 5 behavioural variables with the largest negative loading using a random sample of 75% of the participants.

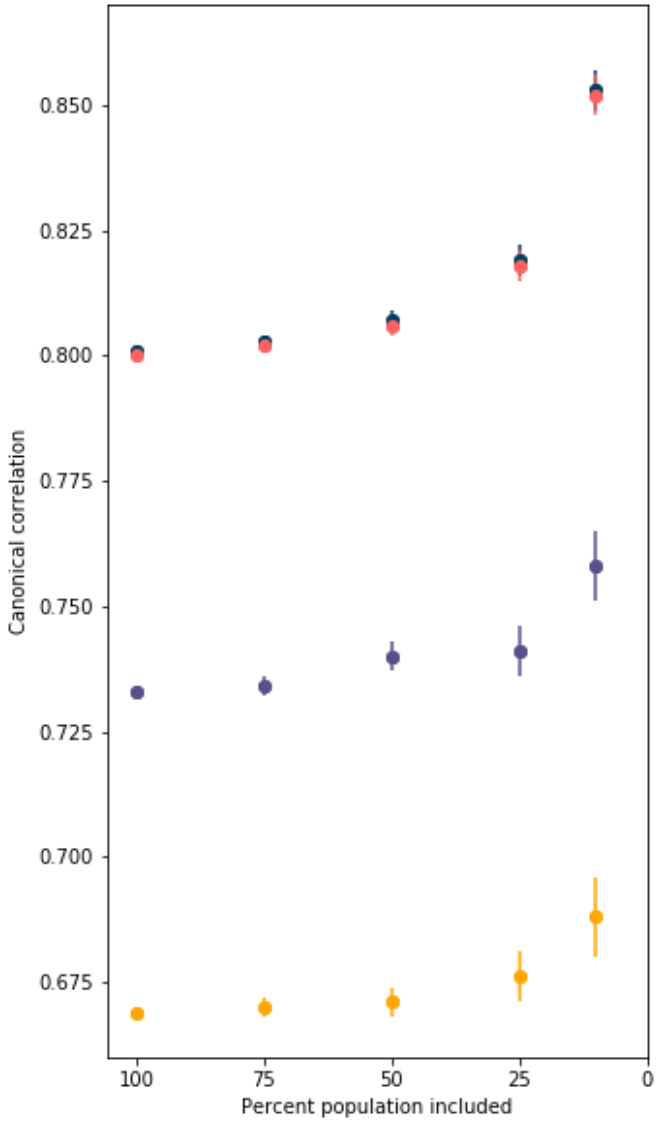

	100%	75%	50%	25%	10%
PCA	0.067	0.044	0.018	0.001	0
ICA	0.066	0.044	0.018	0.001	0
AAL	0.364	0.344	0.309	0.214	0.081
Spectral	0.232	0.204	0.159	0.075	0.008

Figure 4.6. Correlation of Reduced Samples. Left: The average canonical correlation of the first mode found using a subsample of the population. Above: The average P-values corresponding to the correlations shown on the left.

Chapter 5: Discussion

CCA has become an increasingly popular tool for neuroimaging studies - particularly those investigating relationships between human brain and behaviours. Despite this, little investigation has been done to evaluate how data processing decisions, and to a certain extent sample size considerations, impact CCA results. In this thesis, the results from CCA were compared using the same dataset parcellated using different methods. Additionally, the similarity of CCA results between subgroups of subjects randomly sampled from a large homogeneous data set were examined.

5.1 Brain and Behavioural Loadings

In this thesis, CCA was performed multiple times to capture relationships between brain and behavioural variables. None of the resulting modes from CCA produced significant results and thus making conclusions about these relationships based on the results would not be an accurate representation of the underlying ground truth. However, we can note that the areas on the brain with the strongest negative loadings generally correspond with areas which have previously been associated with risk factors for AD. This includes the temporal lobe, medial temporal pole, and frontal gyrus (Ashraf, 2019; Busovaca et al., 2016; Huang, 2020). Both the frontal gyrus and left precentral gyrus have been correlated with obesity-related and smoking-related variables (Brody et al., 2004; Herrmann et al., 2019). There has been no consensus about cortical thickness changes linked to social contact in older age, something which we represent partially by work satisfaction: the behavioural variable with the strongest loading. However, one study found that gray matter volume changes in the default mode network (medial prefrontal cortex and posterior cingulate cortex), have been linked to perceived loneliness and social isolation (Spreng et al., 2020). This study - which was also performed using data from the UK Biobank - claims lonely

older individuals display decreased gray matter in the central operculum, dorsolateral prefrontal cortex and increased GM in the inferior temporal gyrus, posterior superior temporal sulcus, and temporoparietal junction. The complexity in the relationships underlying the examined behavioural variables and their links with neurodegeneration cannot be overstated. Despite the lack of significant results from these initial analyses, this work provides important information about the nuances of utilizing CCA in complex neuroscientific research and demonstrates both the benefits and limitation of this methodology.

5.2 Parcellation Methods and CCA

As stated above, none of the parcellation methods resulted in significant CCA results, and as such the relationships between the sets of behavioural variables and brain regions found should be interpreted with caution. The resulting modes from PCA and ICA were more significant than those found using the AAL and spectral clustering. This suggests that these results may provide more information and are thus a preferable data reduction technique for use with CCA. The nature of PCA is such that it extracts the most discriminative features, however using PCA can lead to difficulty in interpreting the results. This is likely why CCA papers have a lot of variation in their choice of parcellation methods (H. T. Wang et al., 2020; Zhuang, Yang, & Cordes, 2020).

Other work has examined the effects of brain parcellation techniques for machine learning methods (Kalmady et al., 2019; Zang et al., 2021). Unlike machine learning methods, CCA identifies only linear relationships, however our finding that brain parcellation can greatly influence the end results corresponds with the findings from these papers. Additionally, work by Khundrakpam and colleagues suggests that increasing the spatial resolution of a cortical parcellation may improve predictive performance

(Khundrakpam et al., 2015). This should be taken into consideration when comparing results found using ICA and PCA (600 components) versus using the AAL atlas and spectral clustering (90 components).

5.3 Correlation Values and Subsampled Data

It has previously been suggested that interpretations of a given CCA mode are meaningless if the canonical correlations found are not statistically significant in a smaller validation subsample (Thorndike & Weiss, 1973). Our findings take this a step further and suggest that the canonical correlations of a given CCA mode are not a truthful measure of interpretability due to influences of sample size. As the sample size decreased, the loadings from the first mode remained consistent, however, the canonical correlation of the first mode increased. This demonstrates the discordance between the loadings and the correlation values, and thus the significance values. Although the canonical correlation between variates in a mode does measure the correlation between two sets of variables to some degree, the results show that the magnitude of the canonical correlation increased with the data dimensionality and should not be considered as a reliable measure without dataset context. Our results show that as the size of the random samples of participants decreased, the canonical correlation of the first mode increased. There was also more variation between the samples as the participant size decreased; shown through the increasing standard deviation values. These patterns occurred for all parcellation methods and suggests the canonical correlation of the modes from CCA is not an accurate measure of the correlation between the brain imaging data and behavioural data.

This supports similar findings by Yang et al. and has been established theoretically (Q. Yang et al., 2021). The properties of CCA ensure that the first mode found is the maximal correlation of linear combinations of

variables between the two input sets. Therefore, the canonical correlation of the first mode approaches one as the number of variables approaches the number of subjects resulting in a full-rank space (Q. Yang et al., 2021). Thus, the canonical correlation value should not be interpreted in isolation and must be considered in the context of dataset dimensionality and subject-to-variable ratio. However, previous studies have overlooked this limitation when interpreting and reporting results (Kottaram et al., 2019; Smith et al., 2015b; Zarnani et al., 2019). This should be considered when comparing between different studies, and the number of participants as well as the number of variables should always be taken in account.

5.4 Canonical Loadings of Subsampled Data

In addition to examining the canonical correlation of the first mode for subsamples of the data, the loadings for the behavioural and brain variables were compared. This comparison showed that subsamples had loadings which were ordered similar to those found using the entire population, however the values of the loadings themselves differed.

One paper examining loading stability in canonical correlates found that in scenarios where smaller samples of the dataset had different loadings, the relationships described by the full dataset were less reliable and the interpretations made from them were “hazardous” (Lambert & Durand, 1975). This paper suggests that interpretations which claim a direct influential relationship between two variables in the dataset are especially dubious. However, this study also notes that despite loading instability across samples, if similar variable ordering is present, interpretations can be warranted depending on the context. This corresponds to findings from previous work that canonical loadings may be subject to considerable variability between samples (Dattalo, 2014). The results found during our investigation support the cautious outlook on interpreting findings and

further confirm the importance of validation using subsampling methods. It is also important to note that the findings and recommendations from these two papers were made based on theoretical and behavioural studies and not in the context of neuroscientific or imaging research. Thus, the findings in this thesis provide valuable insight into the limitations and hazards of interpreting canonical loading values to represent truthful relationships between brain and behavioural variables.

5.5 Limitations

There are a few limitations of this work which should be considered. First, our assessment of the stability of CCA results was only focused on the first mode to avoid overly complicated analyses and because it is the most significant and most commonly reported result in CCA studies. Although it is expected that the same principles of CCA obtained from the first mode should also apply to other modes, confirmation is needed in future studies.

Additionally, this thesis only focused on classical CCA, however modified versions of CCA such as sparse CCA and kernel CCA have been used in neuroimaging studies. Sparse CCA has been suggested to reduce high-dimensional inputs by imposing the L1-norm penalty to induce sparsity on the canonical coefficients (Witten, Tibshirani, & Hastie, 2009). It has been used as an alternative to classical CCA to deal with high dimensional inputs which contain a lot of noise including voxel-wise brain data and brain connectivity data (Duda, Detre, Kim, Gee, & Avants, 2013; Jang et al., 2017; Kang, Kwak, Yoon, & Lee, 2018; Sintini et al., 2019) and genetic sequences (Du et al., 2017; Gossmann, Zille, Calhoun, & Wang, 2018; Grellmann et al., 2015; McMillan et al., 2014; Szefer, Lu, Nathoo, Beg, & Graham, 2017). A related version referred to as temporal constrained sparse CCA has also been used to investigate longitudinal gray matter density and genetic information in subjects with AD (Du et al., 2019). Kernel CCA has

been suggested to capture nonlinear relationships in the data by mapping the original feature space of the input through a predefined kernel function into a new feature space (Hardoon et al., 2004). It has been used to detect brain activation in response to functional MRI (fMRI) tasks (Hardoon, Mourão-Miranda, Brammer, & Shawe-Taylor, 2007; Z. Yang et al., 2018), and to investigate the nonlinear relationships between electroencephalography (EEG) and simultaneously collected fMRI and hemodynamic data (Murayama et al., 2010; B. Yang et al., 2018). Future work is needed to investigate whether modified versions of CCA behave differently in terms of neuroimaging applications.

As a consequence of its doubly multivariate nature, adding or removing a single variable in either one of the variable sets can lead to larger changes in the CCA solution (H. T. Wang et al., 2020; Witten, Tibshirani, & Hastie, 2009). Similarly, canonical loadings, and thus the relationships ascribed to them, may be sample-specific, and caution must be used when interpreting them (Dattalo, 2014). Overall, care must be taken in assessing reliability and robustness of results and caution must be used when interpreting CCA and comparing between studies. Further work would need to be done to determine the impact of each brain region and behavioural variable.

5.6 Future Work

Future work should consider the limitations discussed previously to expand upon this thesis work. An exploration of different versions of CCA, or CCA run with different parameters may provide further insight into the usefulness of this methodology for neuroimaging. Additionally, future work demonstrating the limitations and usefulness of CCA would benefit from performing analyses and comparing across multiple datasets.

Chapter 6: Conclusion

The study of AD and it's known risk factors is hampered by complex relationships between factors, heterogeneity in disease progression, and an overall limited understanding of AD etiology. This thesis aimed to address these limitations using an increasingly popular multivariate approach while simultaneously exploring the capabilities and limitations of the same approach.

The work done for this thesis demonstrated that although CCA is a promising multivariate approach which holds many advantages in exploring the relationship between the human brain and behavior, it cannot be used or interpreted without restriction. Importantly, canonical correlation values cannot be taken on their own as truthful measures of brain and behavioural relationships, and canonical loadings can be influenced by sample specific effects. This could have significant impact on the way future studies are conducted and older CCA studies are interpreted.

Chapter 7: References

Abell, J. G., Kivimäki, M., Dugravot, A., Tabak, A. G., Fayosse, A., Shipley, M., … Singh-Manoux, A. (2018). Association between systolic blood pressure and dementia in the Whitehall II cohort study: role of age, duration, and threshold used to define hypertension. *European Heart Journal*, *39*(33), 3119–3125. https://doi.org/10.1093/EURHEARTJ/EHY288

Ad-Dab'bagh, Y., Einarson, D., Lyttelton, O., Muehlboeck, J.-S., Mok, K., Ivanov, O., … Evans, A. C. (2006). The CIVET Image-Processing Environment: A Fully Automated Comprehensive Pipeline for Anatomical Neuroimaging Research B-References for tools called upon by CIVET: Figure 2: Example screen shots of the CIVET GUI Figure 1: Diagrammatic Representation of The. *IEEE Trans Med Imaging*, *17*(6), 95.

Adhikari, B. M., Hong, L. E., Sampath, H., Chiappelli, J., Jahanshad, N., Thompson, P. M., … Kochunov, P. (2019). Functional network connectivity impairments and core cognitive deficits in schizophrenia. *Human Brain Mapping*, *40*(16), 4593. https://doi.org/10.1002/HBM.24723

Ahmed, M. N., Yamany, S. M., Mohamed, N., Farag, A. A., & Moriarty, T. (2002). A modified fuzzy C-means algorithm for bias field estimation and segmentation of MRI data. *IEEE Transactions on Medical Imaging*, *21*(3), 193–199. https://doi.org/10.1109/42.996338

Aisen, P. S., Vellas, B., & Hampel, H. (2013). Moving towards early clinical trials for amyloid-targeted therapy in Alzheimer's disease. *Nature Reviews Drug Discovery 2013 12:4*, *12*(4), 324–324. https://doi.org/10.1038/nrd3842-c1

Albanese, E., Launer, L. J., Egger, M., Prince, M. J., Giannakopoulos, P., Wolters, F. J., & Egan, K. (2017). Body mass index in midlife and

dementia: Systematic review and meta-regression analysis of 589,649 men and women followed in longitudinal studies. *Alzheimer's & Dementia (Amsterdam, Netherlands)*, *8*, 165–178. https://doi.org/10.1016/J.DADM.2017.05.007

Alfaro-Almagro, F., Jenkinson, M., Bangerter, N. K., Andersson, J. L. R., Griffanti, L., Douaud, G., … Smith, S. M. (2018). Image processing and Quality Control for the first 10,000 brain imaging datasets from UK Biobank. *NeuroImage*, *166*, 400–424. https://doi.org/10.1016/J.NEUROIMAGE.2017.10.034

Almeida, O. P., Garrido, G. J., Lautenschlager, N. T., Hulse, G. K., Jamrozik, K., & Flicker, L. (2008). Smoking is associated with reduced cortical regional gray matter density in brain regions associated with incipient Alzheimer disease. *The American Journal of Geriatric Psychiatry : Official Journal of the American Association for Geriatric Psychiatry*, *16*(1), 92–98. https://doi.org/10.1097/JGP.0B013E318157CAD2

Alzheimer Society of Canada. (2016). Report summarys: Prevalence and monetary costs of dementia in Canada (2016): a report by the Alzheimer Society of Canada Alzheimer Society of Canada. *Health Promotion and Chronic Disease Prevention in Canada : Research, Policy and Practice*, *36*(10), 231. https://doi.org/10.24095/hpcdp.36.10.04

Amieva, H., Ouvrard, C., Meillon, C., Rullier, L., & Dartigues, J. F. (2018). Death, Depression, Disability, and Dementia Associated With Self-reported Hearing Problems: A 25-Year Study. *The Journals of Gerontology. Series A, Biological Sciences and Medical Sciences*, *73*(10), 1383–1389. https://doi.org/10.1093/GERONA/GLX250

Andersson, J. L. R., Jenkinson, M., & Smith, S. (2007a). *Non-linear optimisation FMRIB Technial Report TR07JA1*.

Andersson, J. L. R., Jenkinson, M., & Smith, S. (2007b). *Non-linear registration aka Spatial normalisation FMRIB Technial Report TR07JA2*.

Apostolova, L. G., Dinov, I. D., Dutton, R. A., Hayashi, K. M., Toga, A. W., Cummings, J. L., & Thompson, P. M. (2006). 3D comparison of hippocampal atrophy in amnestic mild cognitive impairment and Alzheimer's disease. *Brain : A Journal of Neurology*, *129*(Pt 11), 2867–2873. https://doi.org/10.1093/BRAIN/AWL274

Apostolova, L. G., Steiner, C. A., Akopyan, G. G., Dutton, R. A., Hayashi, K. M., Toga, A. W., … Thompson, P. M. (2007). Three-Dimensional Gray Matter Atrophy Mapping in Mild Cognitive Impairment and Mild Alzheimer Disease. *Archives of Neurology*, *64*(10), 1489–1495. https://doi.org/10.1001/ARCHNEUR.64.10.1489

Arbabshirani, M. R., Plis, S., Sui, J., & Calhoun, V. D. (2017). Single subject prediction of brain disorders in neuroimaging: Promises and pitfalls. *NeuroImage*, *145*(Pt B), 137–165. https://doi.org/10.1016/J.NEUROIMAGE.2016.02.079

Armstrong, N. M., An, Y., Doshi, J., Erus, G., Ferrucci, L., Davatzikos, C., … Resnick, S. M. (2019). Association of Midlife Hearing Impairment With Late-Life Temporal Lobe Volume Loss. *JAMA Otolaryngology–Head & Neck Surgery*, *145*(9), 794–802. https://doi.org/10.1001/JAMAOTO.2019.1610

Ashraf, G. M. (2019). Advances in Dementia Research. *Advances in Dementia Research*. https://doi.org/10.5772/INTECHOPEN.78252

Avants, B. B., Cook, P. A., Ungar, L., Gee, J. C., & Grossman, M. (2010). Dementia induces correlated reductions in white matter integrity and cortical thickness: A multivariate neuroimaging study with sparse canonical correlation analysis. *NeuroImage*, *50*(3), 1004–1016. https://doi.org/10.1016/J.NEUROIMAGE.2010.01.041

Bae, S., Harada, K., Lee, S., Harada, K., Makino, K., Chiba, I., … Shimada, H. (2020). The Effect of a Multicomponent Dual-Task Exercise on Cortical Thickness in Older Adults with Cognitive Decline: A Randomized

Controlled Trial. *Journal of Clinical Medicine 2020, Vol. 9, Page 1312*, *9*(5), 1312. https://doi.org/10.3390/JCM9051312

Barnes, D. E., & Yaffe, K. (2011, September 1). The projected effect of risk factor reduction on Alzheimer's disease prevalence. *The Lancet Neurology*, Vol. 10, pp. 819–828. https://doi.org/10.1016/S1474-4422(11)70072-2

Beauchet, O., Celle, S., Roche, F., Bartha, R., Montero-Odasso, M., Allali, G., & Annweiler, C. (2013). Blood pressure levels and brain volume reduction: a systematic review and meta-analysis. *Journal of Hypertension*, *31*(8), 1502–1516. https://doi.org/10.1097/HJH.0B013E32836184B5

Belaroussi, B., Milles, J., Carme, S., Zhu, Y. M., & Benoit-Cattin, H. (2006). Intensity non-uniformity correction in MRI: existing methods and their validation. *Medical Image Analysis*, *10*(2), 234–246. https://doi.org/10.1016/J.MEDIA.2005.09.004

Bhagwat, N., Pipitone, J., Voineskos, A. N., & Chakravarty, M. M. (2019). An artificial neural network model for clinical score prediction in Alzheimer disease using structural neuroimaging measures. *Journal of Psychiatry & Neuroscience : JPN*, *44*(4), 246. https://doi.org/10.1503/JPN.180016

Blacker, D., & Weuve, J. (2018). Brain Exercise and Brain Outcomes: Does Cognitive Activity Really Work to Maintain Your Brain? *JAMA Psychiatry*, *75*(7), 703–704. https://doi.org/10.1001/JAMAPSYCHIATRY.2018.0656

Bloch, F. (1946). Nuclear Induction. *Physical Review*, *70*(7–8), 460. https://doi.org/10.1103/PhysRev.70.460

Braak, H., & Braak, E. (1996). Evolution of the neuropathology of Alzheimer's disease. *Acta Neurologica Scandinavica*, *94*(S165), 3–12. https://doi.org/10.1111/J.1600-0404.1996.TB05866.X

Brody, A. L., Mandelkern, M. A., Jarvik, M. E., Lee, G. S., Smith, E. C., Huang, J. C., … London, E. D. (2004). Differences between smokers and

nonsmokers in regional gray matter volumes and densities. *Biological Psychiatry*, *55*(1), 77–84. https://doi.org/10.1016/S0006-3223(03)00610-3

Brooks, L. G., & Loewenstein, D. A. (2010). Assessing the progression of mild cognitive impairment to Alzheimer's disease: Current trends and future directions. *Alzheimer's Research and Therapy*, *2*(5), 1–9. https://doi.org/10.1186/ALZRT52/METRICS

Brundel, M., Van Den Heuvel, M., De Bresser, J., Kappelle, L. J., & Biessels, G. J. (2010). Cerebral cortical thickness in patients with type 2 diabetes. *Journal of the Neurological Sciences*, *299*(1–2), 126–130. https://doi.org/10.1016/J.JNS.2010.08.048

Busovaca, E., Zimmerman, M. E., Meier, I. B., Griffith, E. Y., Grieve, S. M., Korgaonkar, M. S., … Brickman, A. M. (2016). Is the Alzheimer's disease cortical thickness signature a biological marker for memory? *Brain Imaging and Behavior*, *10*(2), 517. https://doi.org/10.1007/S11682-015-9413-5

Carey, I. M., Anderson, H. R., Atkinson, R. W., Beevers, S. D., Cook, D. G., Strachan, D. P., … Kelly, F. J. (2018). Are noise and air pollution related to the incidence of dementia? A cohort study in London, England. *BMJ Open*, *8*(9), e022404. https://doi.org/10.1136/BMJOPEN-2018-022404

Chakravarty, M. M., Steadman, P., van Eede, M. C., Calcott, R. D., Gu, V., Shaw, P., … Lerch, J. P. (2013). Performing label-fusion-based segmentation using multiple automatically generated templates. *Human Brain Mapping*, *34*(10), 2635–2654. https://doi.org/10.1002/HBM.22092

Chatterjee, S., Peters, S. A. E., Woodward, M., Arango, S. M., Batty, G. D., Beckett, N., … Huxley, R. R. (2016). Type 2 Diabetes as a Risk Factor for Dementia in Women Compared With Men: A Pooled Analysis of 2.3 Million People Comprising More Than 100,000 Cases of Dementia. *Diabetes Care*, *39*(2), 300–307. https://doi.org/10.2337/DC15-1588

Chen, H., Kwong, J. C., Copes, R., Tu, K., Villeneuve, P. J., van Donkelaar, A., … Burnett, R. T. (2017). Living near major roads and the incidence of dementia, Parkinson's disease, and multiple sclerosis: a population-based cohort study. *The Lancet*, *389*(10070), 718–726. https://doi.org/10.1016/S0140-6736(16)32399-6/ATTACHMENT/E4B1D8DE-6088-4291-9D58-9BCFBD4FACEF/MMC1.PDF

Chenausky, K., Kernbach, J., Norton, A., & Schlaug, G. (2017). White Matter Integrity and Treatment-Based Change in Speech Performance in Minimally Verbal Children with Autism Spectrum Disorder. *Frontiers in Human Neuroscience*, *11*. https://doi.org/10.3389/FNHUM.2017.00175

Chenn, A., & Walsh, C. A. (2002). Regulation of cerebral cortical size by control of cell cycle exit in neural precursors. *Science (New York, N.Y.)*, *297*(5580), 365–369. https://doi.org/10.1126/SCIENCE.1074192

Cho, J., Sohn, J., Noh, J., Jang, H., Kim, W., Cho, S. K., … Kim, C. (2020). Association between exposure to polycyclic aromatic hydrocarbons and brain cortical thinning: The Environmental Pollution-Induced Neurological EFfects (EPINEF) study. *Science of The Total Environment*, *737*, 140097. https://doi.org/10.1016/J.SCITOTENV.2020.140097

Choi, D., Choi, S., & Park, S. M. (2018). Effect of smoking cessation on the risk of dementia: a longitudinal study. *Annals of Clinical and Translational Neurology*, *5*(10), 1192–1199. https://doi.org/10.1002/ACN3.633

Choi, U. S., Kawaguchi, H., Matsuoka, Y., Kober, T., & Kida, I. (2019). Brain tissue segmentation based on MP2RAGE multi-contrast images in 7 T MRI. *PLOS ONE*, *14*(2), e0210803. https://doi.org/10.1371/JOURNAL.PONE.0210803

Collins, D. L., Neelin, P., Peters, T. M., & Evans, A. C. (1994). Automatic 3D Intersubject Registration of MR Volumetric Data in Standardized

Talairach Space. *Journal of Computer Assisted Tomography*, *18*(2), 192–205. https://doi.org/10.1097/00004728-199403000-00005

Cremers, H. R., Wager, T. D., & Yarkoni, T. (2017). The relation between statistical power and inference in fMRI. *PLOS ONE*, *12*(11), e0184923. https://doi.org/10.1371/JOURNAL.PONE.0184923

Crous-Bou, M., Gascon, M., Gispert, J. D., Cirach, M., Sánchez-Benavides, G., Falcon, C., … Luis Molinuevo, J. (2020). Impact of urban environmental exposures on cognitive performance and brain structure of healthy individuals at risk for Alzheimer's dementia. *Environment International*, *138*, 105546. https://doi.org/10.1016/J.ENVINT.2020.105546

Currie, S., Hoggard, N., Craven, I. J., Hadjivassiliou, M., & Wilkinson, I. D. (2013). Understanding MRI: basic MR physics for physicians. *Postgraduate Medical Journal*, *89*(1050), 209–223. https://doi.org/10.1136/POSTGRADMEDJ-2012-131342

Dale, A. M., Fischl, B., & Sereno, M. I. (1999). Cortical surface-based analysis. I. Segmentation and surface reconstruction. *NeuroImage*, *9*(2), 179–194. https://doi.org/10.1006/NIMG.1998.0395

Dattalo, P. V. (2014). *A Demonstration of Canonical Correlation Analysis with Orthogonal Rotation to Facilitate Interpretation*. Retrieved from http://scholarscompass.vcu.edu/socialwork_pubs

Dementia A STRATEGY FOR CANADA. (n.d.).

Deoni, S. C. L. (2011). Correction of main and transmit magnetic field (B0 and B1) inhomogeneity effects in multicomponent-driven equilibrium single-pulse observation of T1 and T2. *Magnetic Resonance in Medicine*, *65*(4), 1021–1035. https://doi.org/10.1002/MRM.22685

Dickerson, B. C., Bakkour, A., Salat, D. H., Feczko, E., Pacheco, J., Greve, D. N., … Buckner, R. L. (2009). The Cortical Signature of Alzheimer's Disease: Regionally Specific Cortical Thinning Relates to Symptom

Severity in Very Mild to Mild AD Dementia and is Detectable in Asymptomatic Amyloid-Positive Individuals. *Cerebral Cortex*, *19*(3), 497–510. https://doi.org/10.1093/CERCOR/BHN113

Du, L., Liu, K., Yao, X., Risacher, S. L., Guo, L., Saykin, A. J., & Shen, L. (2019). DIAGNOSIS STATUS GUIDED BRAIN IMAGING GENETICS VIA INTEGRATED REGRESSION AND SPARSE CANONICAL CORRELATION ANALYSIS. *Proceedings. IEEE International Symposium on Biomedical Imaging*, *2019*, 356. https://doi.org/10.1109/ISBI.2019.8759489

Du, L., Liu, K., Yao, X., Yan, J., Risacher, S. L., Han, J., … Fargher, K. (2017). Pattern Discovery in Brain Imaging Genetics via SCCA Modeling with a Generic Non-convex Penalty. *Scientific Reports*, *7*(1). https://doi.org/10.1038/S41598-017-13930-Y

Duda, J. T., Detre, J. A., Kim, J., Gee, J. C., & Avants, B. B. (2013). Fusing functional signals by sparse canonical correlation analysis improves network reproducibility. *Medical Image Computing and Computer-Assisted Intervention : MICCAI ... International Conference on Medical Image Computing and Computer-Assisted Intervention*, *16*(Pt 3), 635. https://doi.org/10.1007/978-3-642-40760-4_79

Durazzo, T. C., Mattsson, N., & Weiner, M. W. (2014). Smoking and increased Alzheimer's disease risk: A review of potential mechanisms. *Alzheimer's & Dementia : The Journal of the Alzheimer's Association*, *10*(3 0), S122. https://doi.org/10.1016/J.JALZ.2014.04.009

Eckert, M. A., Cute, S. L., Vaden, K. I., Kuchinsky, S. E., & Dubno, J. R. (2012). Auditory cortex signs of age-related hearing loss. *JARO - Journal of the Association for Research in Otolaryngology*, *13*(5), 703–713. https://doi.org/10.1007/S10162-012-0332-5/FIGURES/3

Elobeid, A., Libard, S., Leino, M., Popova, S. N., & Alafuzoff, I. (2016). Altered Proteins in the Aging Brain. *Journal of Neuropathology and Experimental Neurology*, *75*(4), 316–325.

https://doi.org/10.1093/JNEN/NLW002

Eskildsen, S. F., Coupé, P., Fonov, V., Manjón, J. V., Leung, K. K., Guizard, N., … Collins, D. L. (2012). BEaST: brain extraction based on nonlocal segmentation technique. *NeuroImage*, *59*(3), 2362–2373. https://doi.org/10.1016/J.NEUROIMAGE.2011.09.012

Evans, I. E. M., Martyr, A., Collins, R., Brayne, C., & Clare, L. (2019). Social Isolation and Cognitive Function in Later Life: A Systematic Review and Meta-Analysis. *Journal of Alzheimer's Disease*, *70*(s1), S119–S144. https://doi.org/10.3233/JAD-180501

Evans, S., McRae-McKee, K., Hadjichrysanthou, C., Wong, M. M., Ames, D., Lopez, O., … Consortium, A. N. M. (2019). Alzheimer's disease progression and risk factors: A standardized comparison between six large data sets. *Alzheimer's & Dementia : Translational Research & Clinical Interventions*, *5*, 515. https://doi.org/10.1016/J.TRCI.2019.04.005

Fann, J. R., Ribe, A. R., Pedersen, H. S., Fenger-Grøn, M., Christensen, J., Benros, M. E., & Vestergaard, M. (2018). Long-term risk of dementia among people with traumatic brain injury in Denmark: a population-based observational cohort study. *The Lancet Psychiatry*, *5*(5), 424–431. https://doi.org/10.1016/S2215-0366(18)30065-8

Fischl, B., Sereno, M. I., & Dale, A. M. (1999). Cortical surface-based analysis. II: Inflation, flattening, and a surface-based coordinate system. *NeuroImage*, *9*(2), 195–207. https://doi.org/10.1006/NIMG.1998.0396

Fonken, L. K., Xu, X., Weil, Z. M., Chen, G., Sun, Q., Rajagopalan, S., & Nelson, R. J. (2011). Air pollution impairs cognition, provokes depressive-like behaviors and alters hippocampal cytokine expression and morphology. *Molecular Psychiatry*, *16*(10), 987–995. https://doi.org/10.1038/MP.2011.76

Frederiksen, K. S., Larsen, C. T., Hasselbalch, S. G., Christensen, A. N.,

Høgh, P., Wermuth, L., … Garde, E. (2018). A 16-Week Aerobic Exercise Intervention Does Not Affect Hippocampal Volume and Cortical Thickness in Mild to Moderate Alzheimer's Disease. *Frontiers in Aging Neuroscience*, *10*, 293. https://doi.org/10.3389/FNAGI.2018.00293/BIBTEX

Frisoni, G. B., Annapaola, A. E., Ae, P., Rasser, P. E., Matteo, A. E., Ae, B., & Thompson, P. M. (2009). *In vivo mapping of incremental cortical atrophy from incipient to overt Alzheimer's disease*. *J Neurol*(256), 916–924. https://doi.org/10.1007/s00415-009-5040-7

Friston, K. J., Ashburner, J., Frith, C. D., Poline, J. -B, Heather, J. D., & Frackowiak, R. S. J. (1995). Spatial registration and normalization of images. *Human Brain Mapping*, *3*(3), 165–189. https://doi.org/10.1002/HBM.460030303

García-García, I., Michaud, A., Dadar, M., Zeighami, Y., Neseliler, S., Collins, D. L., … Dagher, A. (2018). Neuroanatomical differences in obesity: meta-analytic findings and their validation in an independent dataset. *International Journal of Obesity 2018 43:5*, *43*(5), 943–951. https://doi.org/10.1038/s41366-018-0164-4

Gazdzinski, S., Durazzo, T. C., Studholme, C., Song, E., Banys, P., & Meyerhoff, D. J. (2005). Quantitative brain MRI in alcohol dependence: preliminary evidence for effects of concurrent chronic cigarette smoking on regional brain volumes. *Alcoholism, Clinical and Experimental Research*, *29*(8), 1484–1495. https://doi.org/10.1097/01.ALC.0000175018.72488.61

Gianaros, P. J., Greer, P. J., Ryan, C. M., & Jennings, J. R. (2006). Higher blood pressure predicts lower regional grey matter volume: Consequences on short-term information processing. *NeuroImage*, *31*(2), 754. https://doi.org/10.1016/J.NEUROIMAGE.2006.01.003

Gonzalez, C. E., Pacheco, J., Beason-Held, L. L., & Resnick, S. M. (2015).

Longitudinal changes in cortical thinning associated with hypertension. *Journal of Hypertension*, *33*(6), 1242. https://doi.org/10.1097/HJH.0000000000000531

Gossmann, A., Zille, P., Calhoun, V., & Wang, Y. P. (2018). FDR-Corrected Sparse Canonical Correlation Analysis With Applications to Imaging Genomics. *IEEE Transactions on Medical Imaging*, *37*(8), 1761–1774. https://doi.org/10.1109/TMI.2018.2815583

Grabner, G., Janke, A. L., Budge, M. M., Smith, D., Pruessner, J., & Collins, D. L. (2006). Symmetric atlasing and model based segmentation: An application to the hippocampus in older adults. *Lecture Notes in Computer Science (Including Subseries Lecture Notes in Artificial Intelligence and Lecture Notes in Bioinformatics)*, *4191 LNCS-II*, 58–66. https://doi.org/10.1007/11866763_8/COVER

Grellmann, C., Bitzer, S., Neumann, J., Westlye, L. T., Andreassen, O. A., Villringer, A., & Horstmann, A. (2015). Comparison of variants of canonical correlation analysis and partial least squares for combined analysis of MRI and genetic data. *NeuroImage*, *107*, 289–310. https://doi.org/10.1016/J.NEUROIMAGE.2014.12.025

Griffiths, T. D., Lad, M., Kumar, S., Holmes, E., McMurray, B., Maguire, E. A., … Sedley, W. (2020). How Can Hearing Loss Cause Dementia? *Neuron*, *108*(3), 401–412. https://doi.org/10.1016/J.NEURON.2020.08.003

Ha, J., Cho, Y. S., Kim, S. J., Cho, S. H., Kim, J. P., Jung, Y. H., … Kim, H. J. (2020). Hearing loss is associated with cortical thinning in cognitively normal older adults. *European Journal of Neurology*, *27*(6), 1003–1009. https://doi.org/10.1111/ENE.14195

Habeck, C., Gazes, Y., Razlighi, Q., & Stern, Y. (2020). Cortical thickness and its associations with age, total cognition and education across the adult lifespan. *PLOS ONE*, *15*(3), e0230298.

https://doi.org/10.1371/JOURNAL.PONE.0230298

Hansen, L. K., Larsen, J., Nielsen, F. Å., Strother, S. C., Rostrup, E., Savoy, R., … Paulson, O. B. (1999). Generalizable Patterns in Neuroimaging: How Many Principal Components? *NeuroImage*, *9*(5), 534–544. https://doi.org/10.1006/NIMG.1998.0425

Hardoon, D. R., Mourão-Miranda, J., Brammer, M., & Shawe-Taylor, J. (2007). Unsupervised analysis of fMRI data using kernel canonical correlation. *NeuroImage*, *37*(4), 1250–1259. https://doi.org/10.1016/J.NEUROIMAGE.2007.06.017

Hartikainen, P., Räsänen, J., Julkunen, V., Niskanen, E., Hallikainen, M., Kivipelto, M., … Soininen, H. (2012). Cortical Thickness in Frontotemporal Dementia, Mild Cognitive Impairment, and Alzheimer's Disease. *Journal of Alzheimer's Disease*, *30*(4), 857–874. https://doi.org/10.3233/JAD-2012-112060

Hayes, J. P., Logue, M. W., Sadeh, N., Spielberg, J. M., Verfaellie, M., Hayes, S. M., … Miller, M. W. (2017). Mild traumatic brain injury is associated with reduced cortical thickness in those at risk for Alzheimer's disease. *Brain*, *140*(3), 813. https://doi.org/10.1093/BRAIN/AWW344

Herrmann, M. J., Tesar, A. K., Beier, J., Berg, M., & Warrings, B. (2019). Grey matter alterations in obesity: A meta-analysis of whole-brain studies. *Obesity Reviews*, *20*(3), 464–471. https://doi.org/10.1111/OBR.12799

Hersi, M., Irvine, B., Gupta, P., Gomes, J., Birkett, N., & Krewski, D. (2017). Risk factors associated with the onset and progression of Alzheimer's disease: A systematic review of the evidence. *Neurotoxicology*, *61*, 143–187. https://doi.org/10.1016/J.NEURO.2017.03.006

Hotelling, H. (1936). Relations Between Two Sets of Variates. *Biometrika*, *28*(3–4), 321–377. https://doi.org/10.1093/biomet/28.3-4.321

Hou, Y., Dan, X., Babbar, M., Wei, Y., Hasselbalch, S. G., Croteau, D. L., &

Bohr, V. A. (2019). Ageing as a risk factor for neurodegenerative disease. *Nature Reviews Neurology 2019 15:10*, *15*(10), 565–581. https://doi.org/10.1038/s41582-019-0244-7

Hou, Z. (2006). A review on MR image intensity inhomogeneity correction. *International Journal of Biomedical Imaging*, *2006*. https://doi.org/10.1155/IJBI/2006/49515

Huang, X. (2020). Alzheimer's Disease: Drug Discovery. *Alzheimer's Disease: Drug Discovery*. https://doi.org/10.36255/EXONPUBLICATIONS.ALZHEIMERSDISEASE.2020

Huttenlocher, P. R. (1990). Morphometric study of human cerebral cortex development. *Neuropsychologia*, *28*(6), 517–527. https://doi.org/10.1016/0028-3932(90)90031-I

Irimia, A., & Van Horn, J. D. (2013). The structural, connectomic and network covariance of the human brain. *NeuroImage*, *66*, 489–499. https://doi.org/10.1016/J.NEUROIMAGE.2012.10.066

Irwin, K., Sexton, C., Daniel, T., Lawlor, B., & Naci, L. (2018). Healthy Aging and Dementia: Two Roads Diverging in Midlife? *Frontiers in Aging Neuroscience*, *10*(SEP). https://doi.org/10.3389/FNAGI.2018.00275

Jang, H., Kwon, H., Yang, J. J., Hong, J., Kim, Y., Kim, K. W., … Lee, J. M. (2017). Correlations between Gray Matter and White Matter Degeneration in Pure Alzheimer's Disease, Pure Subcortical Vascular Dementia, and Mixed Dementia. *Scientific Reports*, *7*(1). https://doi.org/10.1038/S41598-017-10074-X

Jenkinson, M., Bannister, P., Brady, M., & Smith, S. (2002). Improved optimization for the robust and accurate linear registration and motion correction of brain images. *NeuroImage*, *17*(2), 825–841. https://doi.org/10.1016/S1053-8119(02)91132-8

Jenkinson, M., & Smith, S. (2001). A global optimisation method for robust

affine registration of brain images. *Medical Image Analysis*, *5*(2), 143–156. https://doi.org/10.1016/S1361-8415(01)00036-6

Jonasson, L. S., Nyberg, L., Kramer, A. F., Lundquist, A., Riklund, K., & Boraxbekk, C. J. (2017). Aerobic Exercise Intervention, Cognitive Performance, and Brain Structure: Results from the Physical Influences on Brain in Aging (PHIBRA) Study. *Frontiers in Aging Neuroscience*, *8*(JAN). https://doi.org/10.3389/FNAGI.2016.00336

June, S. K., Singh, V., Jun, K. L., Lerch, J., Ad-Dab'bagh, Y., MacDonald, D., … Evans, A. C. (2005a). Automated 3-D extraction and evaluation of the inner and outer cortical surfaces using a Laplacian map and partial volume effect classification. *NeuroImage*, *27*(1), 210–221. https://doi.org/10.1016/J.NEUROIMAGE.2005.03.036

June, S. K., Singh, V., Jun, K. L., Lerch, J., Ad-Dab'bagh, Y., MacDonald, D., … Evans, A. C. (2005b). Automated 3-D extraction and evaluation of the inner and outer cortical surfaces using a Laplacian map and partial volume effect classification. *NeuroImage*, *27*(1), 210–221. https://doi.org/10.1016/J.NEUROIMAGE.2005.03.036

Jung, N. Y., Cho, H., Kim, Y. J., Kim, H. J., Lee, J. M., Park, S., … Seo, S. W. (2018). The impact of education on cortical thickness in amyloid-negative subcortical vascular dementia: Cognitive reserve hypothesis. *Alzheimer's Research and Therapy*, *10*(1), 1–9. https://doi.org/10.1186/S13195-018-0432-5/FIGURES/1

Kabani, N., Le Goualher, G., Macdonald, D., & Evans, A. C. (2001). *Measurement of Cortical Thickness Using an Automated 3-D Algorithm: A Validation Study*. https://doi.org/10.1006/nimg.2000.0652

Kalmady, S. V., Greiner, R., Agrawal, R., Shivakumar, V., Narayanaswamy, J. C., Brown, M. R. G., … Venkatasubramanian, G. (2019). Towards artificial intelligence in mental health by improving schizophrenia prediction with multiple brain parcellation ensemble-learning. *NPJ*

Schizophrenia, *5*(1). https://doi.org/10.1038/S41537-018-0070-8

Kang, K., Kwak, K., Yoon, U., & Lee, J. M. (2018). Lateral Ventricle Enlargement and Cortical Thinning in Idiopathic Normal-pressure Hydrocephalus Patients. *Scientific Reports*, *8*(1). https://doi.org/10.1038/S41598-018-31399-1

Karama, S., Ducharme, S., Corley, J., Chouinard-Decorte, F., Starr, J. M., Wardlaw, J. M., … Deary, I. J. (2015). Cigarette smoking and thinning of the brain's cortex. *Molecular Psychiatry*, *20*(6), 778–785. https://doi.org/10.1038/MP.2014.187

Kelly, M. E., Duff, H., Kelly, S., McHugh Power, J. E., Brennan, S., Lawlor, B. A., & Loughrey, D. G. (2017). The impact ofsocial activities, social networks, social support and social relationships on the cognitive functioning of healthy older adults: A systematic review. *Systematic Reviews*, *6*(1), 1–18. https://doi.org/10.1186/S13643-017-0632-2/TABLES/3

Khundrakpam, B. S., Tohka, J., Evans, A. C., Ball, W. S., Byars, A. W., Schapiro, M., … O'Neill, J. (2015). Prediction of brain maturity based on cortical thickness at different spatial resolutions. *NeuroImage*, *111*, 350–359. https://doi.org/10.1016/J.NEUROIMAGE.2015.02.046

Kim, J. P., Seo, S. W., Shin, H. Y., Ye, B. S., Yang, J. J., Kim, C., … Guallar, E. (2015). Effects of education on aging-related cortical thinning among cognitively normal individuals. *Neurology*, *85*(9), 806–812. https://doi.org/10.1212/WNL.0000000000001884

Korf, E. S. C., Scheltens, P., Barkhof, F., & De Leeuw, F. E. (2005). Blood pressure, white matter lesions and medial temporal lobe atrophy: closing the gap between vascular pathology and Alzheimer's disease? *Dementia and Geriatric Cognitive Disorders*, *20*(6), 331–337. https://doi.org/10.1159/000088464

Kottaram, A., Johnston, L. A., Cocchi, L., Ganella, E. P., Everall, I., Pantelis,

C., … Zalesky, A. (2019). Brain network dynamics in schizophrenia: Reduced dynamism of the default mode network. *Human Brain Mapping*, *40*(7), 2212. https://doi.org/10.1002/HBM.24519

Kovacs, G. G. (2018). Tauopathies. *Handbook of Clinical Neurology*, *145*, 355–368. https://doi.org/10.1016/B978-0-12-802395-2.00025-0

Kremen, W. S., Beck, A., Elman, J. A., Gustavson, D. E., Reynolds, C. A., Tu, X. M., … Franz, C. E. (2019). Influence of young adult cognitive ability and additional education on later-life cognition. *Proceedings of the National Academy of Sciences of the United States of America*, *116*(6), 2021–2026. https://doi.org/10.1073/PNAS.1811537116

Kuo, Y. L., Kutch, J. J., & Fisher, B. E. (2019). Relationship between Interhemispheric Inhibition and Dexterous Hand Performance in Musicians and Non-musicians. *Scientific Reports 2019 9:1*, *9*(1), 1–10. https://doi.org/10.1038/s41598-019-47959-y

Lambert, Z. V., & Durand, R. M. (1975). Some Precautions in Using Canonical Analysis: *Https://Doi.Org/10.1177/002224377501200411*, *12*(4), 468–475. https://doi.org/10.1177/002224377501200411

Lane, C. A., Barnes, J., Nicholas, J. M., Sudre, C. H., Cash, D. M., Parker, T. D., … Schott, J. M. (2019). Associations between blood pressure across adulthood and late-life brain structure and pathology in the neuroscience substudy of the 1946 British birth cohort (Insight 46): an epidemiological study. *The Lancet Neurology*, *18*(10), 942–952. https://doi.org/10.1016/S1474-4422(19)30228-5/ATTACHMENT/63AF7626-43A5-423B-A289-0B2A4B3FC239/MMC1.PDF

Lee, J. S., Shin, H. Y., Kim, H. J., Jang, Y. K., Jung, N. Y., Lee, J., … Seo, S. W. (2016). Combined effects of physical exercise and education on age-related cortical thinning in cognitively normal individuals. *Scientific Reports 2016 6:1*, *6*(1), 1–9. https://doi.org/10.1038/srep24284

Lerch, J. P., & Evans, A. C. (2005). Cortical thickness analysis examined

through power analysis and a population simulation. *NeuroImage*, *24*(1), 163–173. https://doi.org/10.1016/J.NEUROIMAGE.2004.07.045

Lerch, J. P., Pruessner, J. C., Zijdenbos, A., Hampel, H., Teipel, S. J., & Evans, A. C. (2005). Focal Decline of Cortical Thickness in Alzheimer's Disease Identified by Computational Neuroanatomy. *Cerebral Cortex*, *15*(7), 995–1001. https://doi.org/10.1093/CERCOR/BHH200

Lerch, J. P., Van Der Kouwe, A. J. W., Raznahan, A., Paus, T., Johansen-Berg, H., Miller, K. L., … Sotiropoulos, S. N. (2017). Studying neuroanatomy using MRI. *Nature Neuroscience 2017 20:3*, *20*(3), 314–326. https://doi.org/10.1038/nn.4501

Leritz, E. C., Salat, D. H., Williams, V. J., Schnyer, D. M., Rudolph, J. L., Lipsitz, L., … Milberg, W. P. (2011). *Thickness of the human cerebral cortex is associated with metrics of cerebrovascular health in a normative sample of community dwelling older adults*. https://doi.org/10.1016/j.neuroimage.2010.10.050

Li, Q., Zhao, Y., Chen, Z., Long, J., Dai, J., Huang, X., … Gong, Q. (2019). Meta-analysis of cortical thickness abnormalities in medication-free patients with major depressive disorder. *Neuropsychopharmacology 2019 45:4*, *45*(4), 703–712. https://doi.org/10.1038/s41386-019-0563-9

Li, Y., Wang, Y., Wu, G., Shi, F., Zhou, L., Lin, W., & Shen, D. (2012). Discriminant analysis of longitudinal cortical thickness changes in Alzheimer's disease using dynamic and network features. *Neurobiology of Aging*, *33*(2), 427.e15-427.e30. https://doi.org/10.1016/J.NEUROBIOLAGING.2010.11.008

Liu, Y., Julkunen, V., Paajanen, T., Westman, E., Wahlund, L. O., Aitken, A., … Soininen, H. (2012). Education increases reserve against Alzheimer's disease-Evidence from structural MRI analysis. *Neuroradiology*, *54*(9), 929–938. https://doi.org/10.1007/S00234-012-1005-0/FIGURES/3

Livingston, G., Huntley, J., Sommerlad, A., Ames, D., Ballard, C., Banerjee, S., … Mukadam, N. (2020). Dementia prevention, intervention, and care: 2020 report of the Lancet Commission. *The Lancet*, *396*(10248), 413–446. https://doi.org/10.1016/S0140-6736(20)30367-6/ATTACHMENT/CEE43A30-904B-4A45-A4E5-AFE48804398D/MMC1.PDF

Livingston, G., Sommerlad, A., Orgeta, V., Costafreda, S. G., Huntley, J., Ames, D., … Mukadam, N. (2017, December 16). Dementia prevention, intervention, and care. *The Lancet*, Vol. 390, pp. 2673–2734. https://doi.org/10.1016/S0140-6736(17)31363-6

Long, Z., Huang, J., Li, B., Li, Z., Li, Z., Chen, H., & Jing, B. (2018). A Comparative Atlas-Based Recognition of Mild Cognitive Impairment With Voxel-Based Morphometry. *Frontiers in Neuroscience*, *12*, 916. https://doi.org/10.3389/FNINS.2018.00916

Loughrey, D. G., Kelly, M. E., Kelley, G. A., Brennan, S., & Lawlor, B. A. (2018). Association of Age-Related Hearing Loss With Cognitive Function, Cognitive Impairment, and Dementia: A Systematic Review and Meta-analysis. *JAMA Otolaryngology–Head & Neck Surgery*, *144*(2), 115–126. https://doi.org/10.1001/JAMAOTO.2017.2513

Lowe, V. J., Wiste, H. J., Senjem, M. L., Weigand, S. D., Therneau, T. M., Boeve, B. F., … Jack, C. R. (2018). Widespread brain tau and its association with ageing, Braak stage and Alzheimer's dementia. *Brain*, *141*(1), 271. https://doi.org/10.1093/BRAIN/AWX320

Luchsinger, J. A., & Gustafson, D. R. (2009). Adiposity and Alzheimer's disease. *Current Opinion in Clinical Nutrition and Metabolic Care*, *12*(1), 15–21. https://doi.org/10.1097/MCO.0B013E32831C8C71

Lyttelton, O., Boucher, M., Robbins, S., & Evans, A. (2007). An unbiased iterative group registration template for cortical surface analysis. *NeuroImage*, *34*(4), 1535–1544. https://doi.org/10.1016/J.NEUROIMAGE.2006.10.041

MacDonald, D., Kabani, N., Avis, D., & Evans, A. C. (2000). Automated 3-D extraction of inner and outer surfaces of cerebral cortex from MRI. *NeuroImage*, *12*(3), 340–356. https://doi.org/10.1006/NIMG.1999.0534

Macklin, K. (2021). On the Frontlines of the Alzheimer's Crisis:: Advocacy Organizations in Delaware and Nationwide Urge Public Health Intervention to Curb Staggering Disease Trends. *Delaware Journal of Public Health*, *7*(4), 20. https://doi.org/10.32481/DJPH.2021.09.005

Maharani, A., Dawes, P., Nazroo, J., Tampubolon, G., Pendleton, N., Bertelsen, G., … von Hanno, T. (2018). Longitudinal Relationship Between Hearing Aid Use and Cognitive Function in Older Americans. *Journal of the American Geriatrics Society*, *66*(6), 1130–1136. https://doi.org/10.1111/JGS.15363

Maintz, J. B. A., & Viergever, M. A. (1998). A survey of medical image registration. *Medical Image Analysis*, *2*(1), 1–36. https://doi.org/10.1016/S1361-8415(01)80026-8

Marek, S., Tervo-Clemmens, B., Calabro, F. J., Montez, D. F., Kay, B. P., Hatoum, A. S., … Dosenbach, N. U. F. (2022). Reproducible brain-wide association studies require thousands of individuals. *Nature 2022 603:7902*, *603*(7902), 654–660. https://doi.org/10.1038/s41586-022-04492-9

Martin, A., O'Connor, S., & Jackson, C. (2020). A scoping review of gaps and priorities in dementia care in Europe. *Dementia*, *19*(7), 2135–2151. https://doi.org/10.1177/1471301218816250

McGrath, E. R., Beiser, A. S., DeCarli, C., Plourde, K. L., Vasan, R. S., Greenberg, S. M., & Seshadri, S. (2017). Blood pressure from mid- to late life and risk of incident dementia. *Neurology*, *89*(24), 2447–2454. https://doi.org/10.1212/WNL.0000000000004741

McMillan, C. T., Toledo, J. B., Avants, B. B., Cook, P. A., Wood, E. M., Suh, E., … Grossman, M. (2014). Genetic & Neuronanatomic Associations in

Sporadic Frontotemporal Lobar Degeneration. *Neurobiology of Aging*, *35*(6), 1473. https://doi.org/10.1016/J.NEUROBIOLAGING.2013.11.029

McRobbie, D. W., Moore, E. A., Graves, M. J., & Prince, M. R. (2006). MRI from picture to proton. *MRI from Picture to Proton*, 1–397. https://doi.org/10.1017/CBO9780511545405

Mehta, A., Tom, S., Crane, P., Bennett, D., Izard, S., De Jager, P., & Schneider, J. (2022). Education, Early Life Socioeconomic Status, and Later Life Alzheimer's Disease-Related Neuropathological Lesions (S20.008). *Neurology*, *98*(18 Supplement).

Milene, V., Philippe, B., & Frédéric, C. (2015). Can insulin signaling pathways be targeted to transport Aß out of the brain? *Frontiers in Aging Neuroscience*, *7*(MAY), 114. https://doi.org/10.3389/FNAGI.2015.00114/BIBTEX

Mohamed, A. Z., Nestor, P. J., Cumming, P., & Nasrallah, F. A. (2022). Traumatic brain injury fast-forwards Alzheimer's pathology: evidence from amyloid positron emission tomorgraphy imaging. *Journal of Neurology*, *269*(2), 873–884. https://doi.org/10.1007/S00415-021-10669-5/TABLES/3

Mortamais, M., Ash, J. A., Harrison, J., Kaye, J., Kramer, J., Randolph, C., … Ritchie, K. (2017). Detecting cognitive changes in preclinical Alzheimer's disease: A review of its feasibility. *Alzheimer's & Dementia : The Journal of the Alzheimer's Association*, *13*(4), 468–492. https://doi.org/10.1016/J.JALZ.2016.06.2365

Mountcastle, V. B. (1997). The columnar organization of the neocortex. *Brain : A Journal of Neurology*, *120 (Pt 4)*(4), 701–722. https://doi.org/10.1093/BRAIN/120.4.701

Murayama, Y., Bießmann, F., Meinecke, F. C., Müller, K. R., Augath, M., Oeltermann, A., & Logothetis, N. K. (2010). Relationship between neural and hemodynamic signals during spontaneous activity studied with

temporal kernel CCA. *Magnetic Resonance Imaging*, *28*(8), 1095–1103. https://doi.org/10.1016/J.MRI.2009.12.016

Murray, M. E., Graff-Radford, N. R., Ross, O. A., Petersen, R. C., Duara, R., & Dickson, D. W. (2011). Neuropathologically defined subtypes of Alzheimer's disease with distinct clinical characteristics: a retrospective study. *The Lancet Neurology*, *10*(9), 785–796. https://doi.org/10.1016/S1474-4422(11)70156-9

Mwangi, B., Tian, T. S., & Soares, J. C. (2014). A review of feature reduction techniques in neuroimaging. *Neuroinformatics*, *12*(2), 229. https://doi.org/10.1007/S12021-013-9204-3

Neuschwander, P., Hänggi, J., Zekveld, A. A., & Meyer, M. (2019). Cortical thickness of left Heschl's gyrus correlates with hearing acuity in adults – A surface-based morphometry study. *Hearing Research*, *384*, 107823. https://doi.org/10.1016/J.HEARES.2019.107823

Noh, Y., Jeon, S., Lee, J. M., Seo, S. W., Kim, G. H., Cho, H., … Na, D. L. (2014). Anatomical heterogeneity of Alzheimer disease. *Neurology*, *83*(21), 1936–1944. https://doi.org/10.1212/WNL.0000000000001003

Nordström, A., & Nordström, P. (2018). Traumatic brain injury and the risk of dementia diagnosis: A nationwide cohort study. *PLoS Medicine*, *15*(1). https://doi.org/10.1371/JOURNAL.PMED.1002496

Okamura, N., Harada, R., Furumoto, S., Arai, H., Yanai, K., & Kudo, Y. (2014). Tau PET Imaging in Alzheimer's Disease. *Current Neurology and Neuroscience Reports*, *14*(11), 1–7. https://doi.org/10.1007/S11910-014-0500-6/TABLES/2

Oliveira, F. P. M., & Tavares, J. M. R. S. (2014). Medical image registration: a review. *Computer Methods in Biomechanics and Biomedical Engineering*, *17*(2), 73–93. https://doi.org/10.1080/10255842.2012.670855

Oudin, A., Forsberg, B., Adolfsson, A. N., Lind, N., Modig, L., Nordin, M., …

Nilsson, L. G. (2016). Traffic-related air pollution and dementia incidence in Northern Sweden: A longitudinal study. *Environmental Health Perspectives*, *124*(3), 306–312. https://doi.org/10.1289/EHP.1408322

Oudin, A., Segersson, D., Adolfsson, R., & Forsberg, B. (2018). Association between air pollution from residential wood burning and dementia incidence in a longitudinal study in Northern Sweden. *PLOS ONE*, *13*(6), e0198283. https://doi.org/10.1371/JOURNAL.PONE.0198283

Pan, X., Luo, Y., & Roberts, A. R. (2018). Secondhand Smoke and Women's Cognitive Function in China. *American Journal of Epidemiology*, *187*(5), 911–918. https://doi.org/10.1093/AJE/KWX377

Park, J. Y., Na, H. K., Kim, S., Kim, H., Kim, H. J., Seo, S. W., … Seong, J. K. (2017). Robust Identification of Alzheimer's Disease subtypes based on cortical atrophy patterns. *Scientific Reports 2017 7:1*, *7*(1), 1–14. https://doi.org/10.1038/srep43270

Pedregosa, F., Varoquaux, G., Gramfort, A., Michel, V., Thirion, B., Grisel, O., … Duchesnay, E. (2011). Scikit-learn: Machine Learning in {P}ython. *Journal of Machine Learning Research*, *12*, 2825–2830.

Peelle, J. E., Troiani, V., Grossman, M., & Wingfield, A. (2011). Hearing Loss in Older Adults Affects Neural Systems Supporting Speech Comprehension. *Journal of Neuroscience*, *31*(35), 12638–12643. https://doi.org/10.1523/JNEUROSCI.2559-11.2011

Petersen, J. D., Wehberg, S., Packness, A., Svensson, N. H., Hyldig, N., Raunsgaard, S., … Waldorff, F. B. (2021). Association of Socioeconomic Status With Dementia Diagnosis Among Older Adults in Denmark. *JAMA Network Open*, *4*(5), e2110432–e2110432. https://doi.org/10.1001/JAMANETWORKOPEN.2021.10432

Petersen, R. C. (2004). Mild cognitive impairment as a diagnostic entity. *Journal of Internal Medicine*, *256*(3), 183–194. https://doi.org/10.1111/J.1365-2796.2004.01388.X

Pillai, J. A., Mcevoy, L. K., Hagler, D. J., Holland, D., Dale, A. M., Salmon, D. P., … Fennema-Notestine, C. (2012). Higher Education is Not Associated with Greater Cortical Thickness in Brain Areas Related to Literacy or Intelligence in Normal Aging or Mild Cognitive Impairment. *Journal of Clinical and Experimental Neuropsychology*, *34*(9), 925. https://doi.org/10.1080/13803395.2012.702733

Pipitone, J., Park, M. T. M., Winterburn, J., Lett, T. A., Lerch, J. P., Pruessner, J. C., … Chakravarty, M. M. (2014). Multi-atlas segmentation of the whole hippocampus and subfields using multiple automatically generated templates. *NeuroImage*, *101*, 494–512. https://doi.org/10.1016/J.NEUROIMAGE.2014.04.054

Power, M. C., Adar, S. D., Yanosky, J. D., & Weuve, J. (2016). Exposure to air pollution as a potential contributor to cognitive function, cognitive decline, brain imaging, and dementia: A systematic review of epidemiologic research. *NeuroToxicology*, *56*, 235–253. https://doi.org/10.1016/J.NEURO.2016.06.004

Prestia, A., Drago, V., Rasser, P. E., Bonetti, M., Thompson, P. M., & Frisoni, G. B. (2010). Cortical Changes in Incipient Alzheimer's Disease. *Journal of Alzheimer's Disease*, *22*(4), 1339–1349. https://doi.org/10.3233/JAD-2010-101191

Prince, M., Albanese, E., Guerchet, M., & Prina, M. (2014). *World Alzheimer Report 2014: Dementia and risk reduction: An analysis of protective and modifiable risk factors*. Retrieved from https://kclpure.kcl.ac.uk/portal/en/publications/world-alzheimer-report-2014(4604f34c-5db5-487e-87c9-e3f52c86f7f4).html

Profant, O., Škoch, A., Balogová, Z., Tintěra, J., Hlinka, J., & Syka, J. (2014). Diffusion tensor imaging and MR morphometry of the central auditory pathway and auditory cortex in aging. *Neuroscience*, *260*, 87–97. https://doi.org/10.1016/J.NEUROSCIENCE.2013.12.010

Purcell, E. M., Torrey, H. C., & Pound, R. V. (1946). Resonance absorption by nuclear magnetic moments in a solid [7]. *Physical Review*, *69*(1–2), 37–38. https://doi.org/10.1103/PHYSREV.69.37/FIGURE/1/THUMB

Rakic, P. (1988). Specification of cerebral cortical areas. *Science (New York, N.Y.)*, *241*(4862), 170–176. https://doi.org/10.1126/SCIENCE.3291116

Rankin, K. P., Gorno-Tempini, M. L., Allison, S. C., Stanley, C. M., Glenn, S., Weiner, M. W., & Miller, B. L. (2006). Structural anatomy of empathy in neurodegenerative disease. *Brain*, *129*(11), 2945–2956. https://doi.org/10.1093/BRAIN/AWL254

Rast, P., Kennedy, K. M., Rodrigue, K. M., Robinson, P. R. A. W., Gross, A. L., Mclaren, D. G., … Willis, S. L. (2018). APOEε4 Genotype and Hypertension Modify 8-year Cortical Thinning: Five Occasion Evidence from the Seattle Longitudinal Study. *Cerebral Cortex*, *28*(6), 1934–1945. https://doi.org/10.1093/CERCOR/BHX099

Ray, J., Popli, G., & Fell, G. (2018). Association of Cognition and Age-Related Hearing Impairment in the English Longitudinal Study of Ageing. *JAMA Otolaryngology-- Head & Neck Surgery*, *144*(10), 876–882. https://doi.org/10.1001/JAMAOTO.2018.1656

Raz, N., & Rodrigue, K. M. (2006). Differential aging of the brain: Patterns, cognitive correlates and modifiers. *Neuroscience and Biobehavioral Reviews*, *30*(6), 730. https://doi.org/10.1016/J.NEUBIOREV.2006.07.001

Raznahan, A., Shaw, P. W., Lerch, J. P., Clasen, L. S., Greenstein, D., Berman, R., … Giedd, J. N. (2014). Longitudinal four-dimensional mapping of subcortical anatomy in human development. *Proceedings of the National Academy of Sciences of the United States of America*, *111*(4), 1592–1597. https://doi.org/10.1073/PNAS.1316911111/SUPPL_FILE/SM02.MP4

Reiter, K., Nielson, K. A., Smith, T. J., Weiss, L. R., Alfini, A. J., & Carson

Smith, J. (2015). Improved Cardiorespiratory Fitness Is Associated with Increased Cortical Thickness in Mild Cognitive Impairment. *Journal of the International Neuropsychological Society*, *21*(10), 757–767. https://doi.org/10.1017/S135561771500079X

Ritchie, K., Ritchie, C. W., Jaffe, K., Skoog, I., & Scarmeas, N. (2015). Is late-onset Alzheimer's disease really a disease of midlife? *Alzheimer's & Dementia : Translational Research & Clinical Interventions*, *1*(2), 122. https://doi.org/10.1016/J.TRCI.2015.06.004

Rostowsky, K. A., & Irimia, A. (2021). Acute cognitive impairment after traumatic brain injury predicts the occurrence of brain atrophy patterns similar to those observed in Alzheimer's disease. *GeroScience 2021 43:4*, *43*(4), 2015–2039. https://doi.org/10.1007/S11357-021-00355-9

Russ, T. C., Stamatakis, E., Hamer, M., Starr, J. M., Kivimäki, M., & Batty, G. D. (2013). Socioeconomic status as a risk factor for dementia death: individual participant meta-analysis of 86 508 men and women from the UK. *The British Journal of Psychiatry*, *203*(1), 10. https://doi.org/10.1192/BJP.BP.112.119479

Sabia, S., Dugravot, A., Dartigues, J. F., Abell, J., Elbaz, A., Kivimäki, M., & Singh-Manoux, A. (2017). Physical activity, cognitive decline, and risk of dementia: 28 year follow-up of Whitehall II cohort study. *BMJ (Clinical Research Ed.)*, *357*. https://doi.org/10.1136/BMJ.J2709

Saito, T., Murata, C., Saito, M., Takeda, T., & Kondo, K. (2018). Influence of social relationship domains and their combinations on incident dementia: a prospective cohort study. *J Epidemiol Community Health*, *72*(1), 7–12. https://doi.org/10.1136/JECH-2017-209811

Salat, D. H., Buckner, R. L., Snyder, A. Z., Greve, D. N., Desikan, R. S. R., Busa, E., … Fischl, B. (2004). Thinning of the Cerebral Cortex in Aging. *Cerebral Cortex*, *14*(7), 721–730. https://doi.org/10.1093/CERCOR/BHH032

Schüz, A., & Palm, G. (1989). Density of neurons and synapses in the cerebral cortex of the mouse. *The Journal of Comparative Neurology*, *286*(4), 442–455. https://doi.org/10.1002/CNE.902860404

Schwarzinger, M., Pollock, B. G., Hasan, O. S. M., Dufouil, C., Rehm, J., Baillot, S., … Luchini, S. (2018). Contribution of alcohol use disorders to the burden of dementia in France 2008–13: a nationwide retrospective cohort study. *The Lancet Public Health*, *3*(3), e124–e132. https://doi.org/10.1016/S2468-2667(18)30022-7/ATTACHMENT/099AD4A0-E69F-4B26-95A7-866365B523F0/MMC1.PDF

Ségonne, F., Dale, A. M., Busa, E., Glessner, M., Salat, D., Hahn, H. K., & Fischl, B. (2004). A hybrid approach to the skull stripping problem in MRI. *NeuroImage*, *22*(3), 1060–1075. https://doi.org/10.1016/J.NEUROIMAGE.2004.03.032

Seo, S. W., Ahn, J., Yoon, U., Im, K., Lee, J. M., Tae Kim, S., … Na, D. L. (2010). Cortical Thinning in Vascular Mild Cognitive Impairment and Vascular Dementia of Subcortical Type. *Journal of Neuroimaging*, *20*(1), 37–45. https://doi.org/10.1111/J.1552-6569.2008.00293.X

Sharifian, N., Zaheed, A. B., Morris, E. P., Sol, K., Manly, J. J., Schupf, N., … Zahodne, L. B. (2022). Social network characteristics moderate associations between cortical thickness and cognitive functioning in older adults. *Alzheimer's & Dementia*, *18*(2), 339–347. https://doi.org/10.1002/ALZ.12383

Sherif, T., Rioux, P., Rousseau, M. E., Kassis, N., Beck, N., Adalat, R., … Evans, A. C. (2014). CBRAIN: a web-based, distributed computing platform for collaborative neuroimaging research. *Frontiers in Neuroinformatics*, *8*(MAY). https://doi.org/10.3389/FNINF.2014.00054

Shi, L., Cheng, Y., Xu, Y., Shen, Z., Lu, Y., Zhou, C., … Xu, X. (2019). Effects of hypertension on cerebral cortical thickness alterations in patients with type 2 diabetes. *Diabetes Research and Clinical Practice*,

157, 107872. https://doi.org/10.1016/J.DIABRES.2019.107872

Singh-Manoux, A., Dugravot, A., Fournier, A., Abell, J., Ebmeier, K., Kivimäki, M., & Sabia, S. (2017). Trajectories of Depressive Symptoms Before Diagnosis of Dementia: A 28-Year Follow-up Study. *JAMA Psychiatry*, *74*(7), 712–718. https://doi.org/10.1001/JAMAPSYCHIATRY.2017.0660

Singh, V., Chertkow, H., Lerch, J. P., Evans, A. C., Dorr, A. E., & Kabani, N. J. (2006). Spatial patterns of cortical thinning in mild cognitive impairment and Alzheimer's disease. *Brain*, *129*(11), 2885–2893. https://doi.org/10.1093/BRAIN/AWL256

Sintini, I., Schwarz, C. G., Senjem, M. L., Reid, R. I., Botha, H., Ali, F., … Whitwell, J. L. (2019). Multimodal neuroimaging relationships in progressive supranuclear palsy. *Parkinsonism & Related Disorders*, *66*, 56. https://doi.org/10.1016/J.PARKRELDIS.2019.07.001

Sirivelu, M. P., MohanKumar, S. M. J., Wagner, J. G., Harkema, J. R., & MohanKumar, P. S. (2006). Activation of the stress axis and neurochemical alterations in specific brain areas by concentrated ambient particle exposure with concomitant allergic airway disease. *Environmental Health Perspectives*, *114*(6), 870–874. https://doi.org/10.1289/EHP.8619

Sled, J. G., Zijdenbos, A. P., & Evans, A. C. (1998). A nonparametric method for automatic correction of intensity nonuniformity in mri data. *IEEE Transactions on Medical Imaging*, *17*(1), 87–97. https://doi.org/10.1109/42.668698

Smith, S. M. (2002). Fast robust automated brain extraction. *Human Brain Mapping*, *17*(3), 143. https://doi.org/10.1002/HBM.10062

Smith, S. M., Alfaro-Almagro, F., & Miller, K. L. (n.d.). *UK Biobank Brain Imaging Documentation UK Biobank Brain Imaging Documentation Contributors to UK Biobank Brain Imaging*. Retrieved from

http://www.ukbiobank.ac.uk

Smith, S. M., Nichols, T. E., Vidaurre, D., Winkler, A. M., Behrens, T. E. J., Glasser, M. F., … Miller, K. L. (2015a). A positive-negative mode of population covariation links brain connectivity, demographics and behavior. *Nature Neuroscience*, *18*(11), 1565. https://doi.org/10.1038/NN.4125

Smith, S. M., Nichols, T. E., Vidaurre, D., Winkler, A. M., Behrens, T. E. J., Glasser, M. F., … Miller, K. L. (2015b, November 1). A positive-negative mode of population covariation links brain connectivity, demographics and behavior. *Nature Neuroscience*, Vol. 18, pp. 1565–1567. https://doi.org/10.1038/nn.4125

Solé-Padullés, C., Bartrés-Faz, D., Junqué, C., Vendrell, P., Rami, L., Clemente, I. C., … Molinuevo, J. L. (2009). Brain structure and function related to cognitive reserve variables in normal aging, mild cognitive impairment and Alzheimer's disease. *Neurobiology of Aging*, *30*(7), 1114–1124. https://doi.org/10.1016/J.NEUROBIOLAGING.2007.10.008

Sommerlad, A., Sabia, S., Singh-Manoux, A., Lewis, G., & Livingston, G. (2019). Association of social contact with dementia and cognition: 28-year follow-up of the Whitehall II cohort study. *PLOS Medicine*, *16*(8), e1002862. https://doi.org/10.1371/JOURNAL.PMED.1002862

Spreng, R. N., Dimas, E., Mwilambwe-Tshilobo, L., Dagher, A., Koellinger, P., Nave, G., … Bzdok, D. (2020). The default network of the human brain is associated with perceived social isolation. *Nature Communications 2020 11:1*, *11*(1), 1–11. https://doi.org/10.1038/s41467-020-20039-w

Steffener, J. (2021). Education and age-related differences in cortical thickness and volume across the lifespan. *Neurobiology of Aging*, *102*, 102–110. https://doi.org/10.1016/J.NEUROBIOLAGING.2020.10.034

Strike, L. T., Hansell, N. K., Couvy-Duchesne, B., Thompson, P. M., De

Zubicaray, G. I., McMahon, K. L., & Wright, M. J. (2019). Genetic Complexity of Cortical Structure: Differences in Genetic and Environmental Factors Influencing Cortical Surface Area and Thickness. *Cerebral Cortex*, *29*(3), 952–962. https://doi.org/10.1093/CERCOR/BHY002

Sudlow, C., Gallacher, J., Allen, N., Beral, V., Burton, P., Danesh, J., … Collins, R. (2015). UK Biobank: An Open Access Resource for Identifying the Causes of a Wide Range of Complex Diseases of Middle and Old Age. *PLOS Medicine*, *12*(3), e1001779. https://doi.org/10.1371/JOURNAL.PMED.1001779

Suh, J. S., Schneider, M. A., Minuzzi, L., MacQueen, G. M., Strother, S. C., Kennedy, S. H., & Frey, B. N. (2019). Cortical thickness in major depressive disorder: A systematic review and meta-analysis. *Progress in Neuro-Psychopharmacology and Biological Psychiatry*, *88*, 287–302. https://doi.org/10.1016/J.PNPBP.2018.08.008

Swan, G. E., & Lessov-Schlaggar, C. N. (2007). The effects of tobacco smoke and nicotine on cognition and the brain. *Neuropsychology Review*, *17*(3), 259–273. https://doi.org/10.1007/S11065-007-9035-9

Szefer, E., Lu, D., Nathoo, F., Beg, M. F., & Graham, J. (2017). Multivariate association between single-nucleotide polymorphisms in Alzgene linkage regions and structural changes in the brain: discovery, refinement and validation. *Statistical Applications in Genetics and Molecular Biology*, *16*(5–6), 349. https://doi.org/10.1515/SAGMB-2016-0077

Thambisetty, M., Wan, J., Carass, A., An, Y., Prince, J. L., & Resnick, S. M. (2010). Longitudinal changes in cortical thickness associated with normal aging. *NeuroImage*, *52*(4), 1215–1223. https://doi.org/10.1016/J.NEUROIMAGE.2010.04.258

Thompson, P. M., Hayashi, K. M., De Zubicaray, G., Janke, A. L., Rose, S. E., Semple, J., … Toga, A. W. (2003). Dynamics of Gray Matter Loss in

Alzheimer's Disease. *Journal of Neuroscience*, *23*(3), 994–1005. https://doi.org/10.1523/JNEUROSCI.23-03-00994.2003

Thorndike, R. M., & Weiss, D. J. (1973). A study of the stability of canonical correlations and canonical components. *Educational and Psychological Measurement*, *33*(1), 123–134. https://doi.org/10.1177/001316447303300113

Tian, Y., Zalesky, A., Bousman, C., Everall, I., & Pantelis, C. (2019). Insula Functional Connectivity in Schizophrenia: Subregions, Gradients, and Symptoms. *Biological Psychiatry: Cognitive Neuroscience and Neuroimaging*, *4*(4), 399–408. https://doi.org/10.1016/J.BPSC.2018.12.003

Toga, A. W., & Thompson, P. M. (2001). Maps of the brain. *The Anatomical Record*, *265*(2), 37–53. https://doi.org/10.1002/AR.1057

Tohka, J., Zijdenbos, A., & Evans, A. (2004). Fast and robust parameter estimation for statistical partial volume models in brain MRI. *NeuroImage*, *23*(1), 84–97. https://doi.org/10.1016/J.NEUROIMAGE.2004.05.007

Topiwala, A., Allan, C. L., Valkanova, V., Zsoldos, E., Filippini, N., Sexton, C., … Ebmeier, K. P. (2017). Moderate alcohol consumption as risk factor for adverse brain outcomes and cognitive decline: longitudinal cohort study. *BMJ*, *357*(16), 1190–1192. https://doi.org/10.1136/BMJ.J2353

Tsvetanov, K. A., Henson, R. N. A., Tyler, L. K., Razi, A., Geerligs, L., Ham, T. E., & Rowe, J. B. (2016). Extrinsic and Intrinsic Brain Network Connectivity Maintains Cognition across the Lifespan Despite Accelerated Decay of Regional Brain Activation. *Journal of Neuroscience*, *36*(11), 3115–3126. https://doi.org/10.1523/JNEUROSCI.2733-15.2016

Tustison, N. J., Avants, B. B., Cook, P. A., Zheng, Y., Egan, A., Yushkevich, P. A., & Gee, J. C. (2010). N4ITK: Improved N3 Bias Correction. *IEEE Transactions on Medical Imaging*, *29*(6), 1310.

https://doi.org/10.1109/TMI.2010.2046908

Tzourio-Mazoyer, N., Landeau, B., Papathanassiou, D., Crivello, F., Etard, O., Delcroix, N., … Joliot, M. (2002). Automated anatomical labeling of activations in SPM using a macroscopic anatomical parcellation of the MNI MRI single-subject brain. *NeuroImage*, *15*(1), 273–289. https://doi.org/10.1006/NIMG.2001.0978

Uurtio, V., Monteiro, J. M., Kandola, J., Shawe-Taylor, J., Fernandez-Reyes, D., & Rousu, J. (2017). A Tutorial on Canonical Correlation Methods. *ACM Computing Surveys (CSUR)*, *50*(6), 1–33. https://doi.org/10.1145/3136624

van der Kouwe, A. J. W., Benner, T., Salat, D. H., & Fischl, B. (2008). Brain morphometry with multiecho MPRAGE. *NeuroImage*, *40*(2), 559–569. https://doi.org/10.1016/J.NEUROIMAGE.2007.12.025

Van Leemput, K., Maes, F., Vandermeulen, D., & Suetens, P. (2003). A unifying framework for partial volume segmentation of brain MR images. *IEEE Transactions on Medical Imaging*, *22*(1), 105–119. https://doi.org/10.1109/TMI.2002.806587

Verbaten, M. N. (2009). Chronic effects of low to moderate alcohol consumption on structural and functional properties of the brain: beneficial or not? *Human Psychopharmacology: Clinical and Experimental*, *24*(3), 199–205. https://doi.org/10.1002/HUP.1022

Veronese, N., Facchini, S., Stubbs, B., Luchini, C., Solmi, M., Manzato, E., … Fontana, L. (2017). Weight loss is associated with improvements in cognitive function among overweight and obese people: A systematic review and meta-analysis. *Neuroscience and Biobehavioral Reviews*, *72*, 87–94. https://doi.org/10.1016/J.NEUBIOREV.2016.11.017

Vuorinen, M., Kåreholt, I., Julkunen, V., Spulber, G., Niskanen, E., Paajanen, T., … Solomon, A. (2013). Changes in vascular factors 28 years from midlife and late-life cortical thickness. *Neurobiology of Aging*, *34*(1),

100–109. https://doi.org/10.1016/J.NEUROBIOLAGING.2012.07.014

Wang, H. T., Smallwood, J., Mourao-Miranda, J., Xia, C. H., Satterthwaite, T. D., Bassett, D. S., & Bzdok, D. (2020). Finding the needle in a high-dimensional haystack: Canonical correlation analysis for neuroscientists. *NeuroImage*, *216*, 116745. https://doi.org/10.1016/J.NEUROIMAGE.2020.116745

Wang, M. L., Wei, X. E., Yu, M. M., Li, W. Bin, Li, P. Y., & Li, W. Bin. (2017). Self-reported traumatic brain injury and in vivo measure of AD-vulnerable cortical thickness and AD-related biomarkers in the ADNI cohort. *Neuroscience Letters*, *655*, 115–120. https://doi.org/10.1016/J.NEULET.2017.06.055

Witten, D. M., Tibshirani, R., & Hastie, T. (2009). A penalized matrix decomposition, with applications to sparse principal components and canonical correlation analysis. *Biostatistics (Oxford, England)*, *10*(3), 515–534. https://doi.org/10.1093/BIOSTATISTICS/KXP008

World Health Organization. (2021). Dementia. Retrieved April 4, 2022, from https://www.who.int/news-room/fact-sheets/detail/dementia

Wyss-Coray, T. (2016). Ageing, neurodegeneration and brain rejuvenation. *Nature*, *539*(7628), 180–186. https://doi.org/10.1038/NATURE20411

Yaffe, K. (2007). Metabolic syndrome and cognitive disorders: Is the sum greater than its parts? *Alzheimer Disease and Associated Disorders*, *21*(2), 167–171. https://doi.org/10.1097/WAD.0B013E318065BFD6

Yang, B., Cao, J., Zhou, T., Dong, L., Zou, L., & Xiang, J. (2018). Exploration of Neural Activity under Cognitive Reappraisal Using Simultaneous EEG-fMRI Data and Kernel Canonical Correlation Analysis. *Computational and Mathematical Methods in Medicine*, *2018*. https://doi.org/10.1155/2018/3018356

Yang, Q., Zhang, X., Song, Y., Liu, F., Qin, W., Yu, C., & Liang, M. (2021). Stability test of canonical correlation analysis for studying brain-behavior

relationships: The effects of subject-to-variable ratios and correlation strengths. *Human Brain Mapping*, *42*(8), 2374–2392. https://doi.org/10.1002/HBM.25373

Yang, Z., Zhuang, X., Sreenivasan, K., Mishra, V., Curran, T., Byrd, R., … Cordes, D. (2018). 3D Spatially-Adaptive Canonical Correlation Analysis: Local and Global Methods. *NeuroImage*, *169*, 240. https://doi.org/10.1016/J.NEUROIMAGE.2017.12.025

Zang, J., Huang, Y., Kong, L., Lei, B., Ke, P., Li, H., … Wu, K. (2021). Effects of Brain Atlases and Machine Learning Methods on the Discrimination of Schizophrenia Patients: A Multimodal MRI Study. *Frontiers in Neuroscience*, *15*. https://doi.org/10.3389/FNINS.2021.697168/FULL

Zarnani, K., Nichols, T. E., Alfaro-Almagro, F., Fagerlund, B., Lauritzen, M., Rostrup, E., & Smith, S. M. (2019). Discovering markers of healthy aging: a prospective study in a Danish male birth cohort. *Aging*, *11*(16), 5943–5974. https://doi.org/10.18632/AGING.102151

Zhang, B., Lin, L., Liu, L., Shen, X., & Wu, S. (2022). Concordance of Alzheimer's Disease Subtypes Produced from Different Representative Morphological Measures: A Comparative Study. *Brain Sciences*, *12*(2). https://doi.org/10.3390/BRAINSCI12020187

Zhang, B., Lin, L., Wu, S., & Al-masqari, Z. H. M. A. (2021). Multiple Subtypes of Alzheimer's Disease Base on Brain Atrophy Pattern. *Brain Sciences*, *11*(2), 1–15. https://doi.org/10.3390/BRAINSCI11020278

Zhang, Y., Brady, M., & Smith, S. (2001). Segmentation of brain MR images through a hidden Markov random field model and the expectation-maximization algorithm. *IEEE Transactions on Medical Imaging*, *20*(1), 45–57. https://doi.org/10.1109/42.906424

Zhuang, X., Yang, Z., & Cordes, D. (2020). A technical review of canonical correlation analysis for neuroscience applications. *Human Brain Mapping*, *41*(13), 3807–3833. https://doi.org/10.1002/HBM.25090

Zhuang, X., Yang, Z., Curran, T., Byrd, R., Nandy, R., & Cordes, D. (2017). A family of locally constrained CCA models for detecting activation patterns in fMRI. *NeuroImage*, *149*, 63–84. https://doi.org/10.1016/J.NEUROIMAGE.2016.12.081

Zijdenbos, A. P., Forghani, R., & Evans, A. C. (2002). Automatic "pipeline" analysis of 3-D MRI data for clinical trials: Application to multiple sclerosis. *IEEE Transactions on Medical Imaging*, *21*(10), 1280–1291. https://doi.org/10.1109/TMI.2002.806283

Zorlu, N., Cropley, V. L., Zorlu, P. K., Delibas, D. H., Adibelli, Z. H., Baskin, E. P., … Pantelis, C. (2017). Effects of cigarette smoking on cortical thickness in major depressive disorder. *Journal of Psychiatric Research*, *84*, 1–8. https://doi.org/10.1016/J.JPSYCHIRES.2016.09.009

Zotcheva, E., Bergh, S., Selbæk, G., Krokstad, S., Håberg, A. K., Strand, B. H., & Ernstsen, L. (2018). Midlife Physical Activity, Psychological Distress, and Dementia Risk: The HUNT Study. *Journal of Alzheimer's Disease : JAD*, *66*(2), 825–833. https://doi.org/10.3233/JAD-180768